Fornybar Norge

Pore pressure and concrete dams

Authors:
Thomas Konow, Å-Energi Hydropower
Bjørn Nilsen, NTNU
Simon Bjønness, Dr.techn.Olav Olsen

DR. TECHN. OLAV OLSEN ARTELIA GROUP

REVISIONS

Rev.	Dato	Sign.	Contr.	Appr.
00	13.03.25	Thomas Konow, Bjørn Nilsen, Simon Bjønness and Olav Guddal	Thomas Konow, Bjørn Nilsen and Simon Bjønness	Simon Bjønness
01	12.12.25	Thomas Konow, Bjørn Nilsen, Simon Bjønness and Olav Guddal	Thomas Konow, Bjørn Nilsen, and Simon Bjønness	Simon Bjønness

CHANGE LOG

Rev.	Reference	Description
00	-	For Review by DSHP, dam owners, NVE, KTH and others
01		Final report

PROJECT INFORMATION

Client:	Fornybar Norge/DSHP
Client contact person:	Name: Torgeir Johnson Email: torgeir.johnson@fornybarnorge.no

SUMMARY AND MAIN FINDINGS

The purpose of this report has been to evaluate pore pressure assumptions for concrete dams in the Norwegian dam safety regulations (Energidepartementet, 2009). The assumptions for "Pore Pressure" in the Norwegian regulations, distinguish between the uplift pressures for the following calculations:

- **Dam stability**: This applies for stability of the dam body and includes the contact zone between concrete and rock foundation. Design considerations for Gravity dams are given in the NVE guidelines for concrete dams (NVE, 2005) in the following chapters:
    - Gravity dams - chapter 2.2.1, "Internal pore pressure and drainage"
    - Buttress dams - chapter 2.6.1, under sub-chapter "Overturning where cracks will not cause increased pore pressure with uplift".
- **Rock foundation;** This applies for the foundation stability of the rock foundation under the dam. Design considerations are given in the NVE guidelines for concrete dams , (NVE, 2005), chapter 3.7, "Foundation".

An important basis for the report has been a case study of five buttress dams with a total of 87 piezometers installed in the foundations to monitor pore pressure.

The definition of pore pressure in the Norwegian regulations can be misinterpreted regarding buttress dams . Therefore, this report has focus on aspects regarding buttress dams.

The main findings in the report are summarised below. However, reference is also made to Chapter 7 "Conclusions" in which a more detailed overview is given.

Buttress dams and pore pressure (including the contact zone of the rock foundation):

Piezometer measurements documented in this report show the following:

- Drainage directly downstream the buttress slab eliminates pore pressure under the buttresses. For very wide buttresses, a gallery (or box drain) between the upstream slab and the buttress supports will give sufficient drainage.
    - No pore pressure was detected by the 71 piezometers installed in the dams with slender buttress supports or very wide buttress supports with an upstream gallery/box drain (dam B, C1, C2 and D).
    - "Very wide" buttress supports refer to cases C1, C2 and D that have about 6 m wide buttress supports with upstream drainage gallery/box drain.
- In the case study of dam A in this report there are no box drains. Measurements from one piezometer in dam A, may indicate that a reduced pore pressure can occur, under the upstream part of a very wide buttress(>5-6 m wide). Out of the 87 piezometers evaluated in this report, this is the only sensor that measure a pore pressure that correlates with variations in the upstream water level.

In general, pore pressure can only propagate if there is an open crack in the dam or the contact zone between concrete and rock, i.e. there is no bond in the crack. This is only possible if the pore pressure is greater than the bond, which will lead to hydraulic fracturing (and/or hydraulic jacking). As the tensile strength in uplift joints or the bedrock contact zone are weaker than in the solid concrete

structure, installing rock bolts and/or reinforcement bars will reduce the possibility of hydraulic fracturing.

Rock foundation:

1. Calculations of the stability of the foundation, should be based on a geologic evaluation of the rock mass.
2. Stereographic projection (see figure below) and rock mass classification according to the RMR system have been found to be best suited for geological characterization of dam foundations
3. "Joint water pressure" causing uplift in the foundation is the main concern when evaluating foundation stability. Uplift can occur when joints are oriented parallel or sub-parallel to the surface. There is no "pore pressure" in sound Norwegian rock of good quality.
4. Increasing depth of the rock fracture also reduces the adverse effects of uplift, i.e. the shallower fractures are those of most concern.
5. Drainage curtains are the most efficient way to control pore pressures. It is important to note that drainage holes in a drain curtain will need to be checked and cleaned/flushed at regular intervals, as the holes can become clogged by fines and minerals from the bedrock.

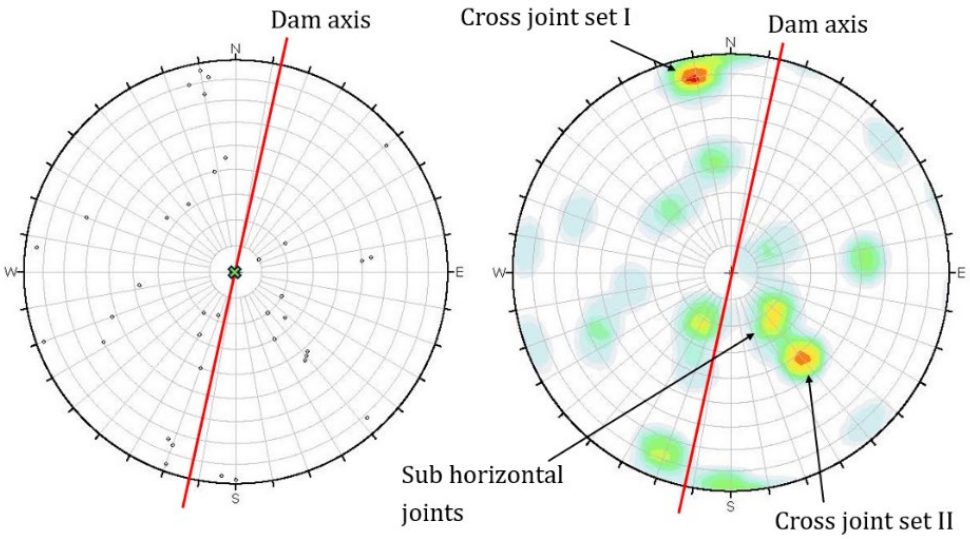

Figure 1. Illustration of stereographic presentation.. Indication of the dam-axis is important, as the orientation of joints relative to the dam axis is important to identify critical joints.

Instrumentation:

- The Norwegian regulations have no general requirements for instrumentation to measure pore pressure for dams founded on rock of good quality.
- If piezometers are considered, the installation should be based on a geologic evaluation of the foundation. The placement, inclination and depth of the borehole and chamber for measuring of pore pressure must be carefully selected from a geological mapping. Random instrumentation of rock foundation is of little value.
- Measurement of pore pressure does not increase the dam safety but can be used to verify that

the dam's actual behaviour corresponds to the assumptions made during design. Given the potential of errors associated with sensors, structural safety should in general not rely on instrumentation.

The Norwegian regulations:

- The assumptions for pore pressure in the regulations and guidelines are considered to be a good basis for design, and the regulations are in line with general international practice. However, there is a need for better specifications of the design pore pressure for buttress dams in the Norwegian regulations.
- We recommend that the terms defined in the regulations should be used by NVE, consultants and dam owners (i.e. light buttress dam and heavy buttress dam). Using terms not defined in the regulations can result in misunderstandings that potentially can have large consequences. .

The general design practice for pore pressure assumptions is given in chapter 2.

Table 1. General design practice in Norway for pore pressure distribution according to different dam types.

Gravity dam:	**Drained Gravity dam.**	**Slab buttress dam:**
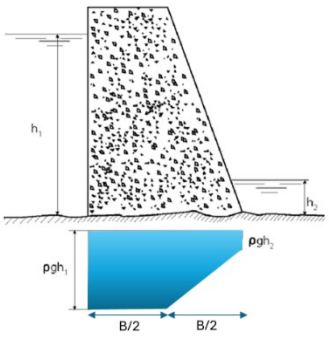	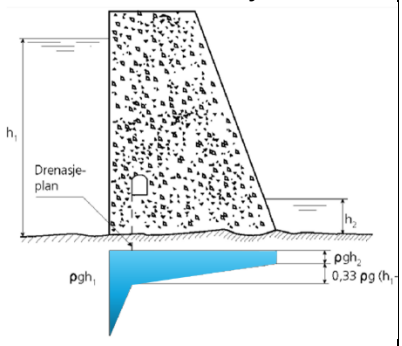	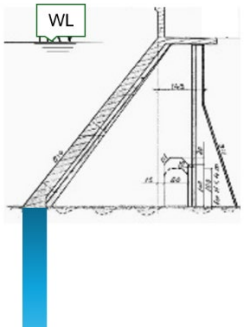
Linearly decreasing pore pressure is assumed in areas with compressive stress in the foundation, and full pore pressure in areas with no compressive stress. Example shows pressure distribution in ALS, with compressive stress only in the downstream part.	Reduced pore pressure can be assumed when the dam is drained. However, full pore pressure should be considered in all parts of the cross-section where there are no calculated compressive stresses.	Stability requirements are given as a safety factor. As this method does not depend on the location of the resultant, it is possible that there is no compressive stress under the upstream slab, which in turn can result in a crack and full pore pressure (as for Gravity dams). Therefore, full pore pressure is assumed under the upstream slab.

TABLE OF CONTENS

Summary and main findings 2

Table of Contens 5

1 Introduction 8

1.1 Objective 8

1.2 Background 8

1.3 Dam types 9

1.3.1 Gravity dams 9

1.3.2 Buttress dams 11

1.3.3 Arch dams 13

1.4 Definitions and acronyms 14

2 Pore Pressure – Theory and principles 16

2.1 Assumptions for pore pressure in Norway 16

2.1.1 Safety requirements and pore pressure 16

2.1.2 Gravity Dams 17

2.1.3 Gravity Dams with drainage 19

2.1.4 Dry laid masonry dams 21

2.1.5 Buttress dams 22

2.1.6 Rock foundation 23

2.2 Theory: Structural stability 24

2.2.1 Pore pressure and gravity dams 26

2.2.2 Pore pressure and buttress dams 26

2.3 Theory: Rock foundations 28

2.3.1 Joint water pressure 28

2.3.2 Effect of rock stresses 30

2.3.3 Hydraulic jacking 32

2.3.4 Hydraulic fracturing 33

2.4 Measures to reduce uplift pore pressure 35

2.4.1 Drainage 35

2.4.2 Foundation treatment and Grout curtain 39

2.5 Practice in other countries 41

2.5.1 Europe 41

2.5.2 Sweden – Buttress dams 43

2.5.3 USA (FERC) 44

3 Instrumentation and Monitoring 47

3.1 Purpose of monitoring of dams 47

3.2 NVE requirements 47

3.3 Experience with pore pressure measurements 48

3.3.1 Installation of piezometers 48

3.3.2 Sources of error 49

4 Engineering Geology and Rock Mechanics 50

4.1 Permeability of rocks and rock masses 50

4.2 Key fracture parameters 53

4.3 Engineering geological mapping 55
4.4 Rock mass classification 60
4.5 Mechanical properties of rock and rock mass 63
4.6 In-situ monitoring 66
5 Literature study 68
5.1 Literature search based on Databases 68
5.1.1 NTNU databases 68
5.1.2 ISRM-database 70
5.2 Buttress dams - Cases 71
5.2.1 UK, Hydraulic structures, 4th edition (P. Novak, 2007) 71
5.2.2 Brazil; Itaipú Buttress dam 72
5.2.3 Sweden; Storfinnforsen buttress dam 74
5.3 Other cases/other references 77
5.3.1 Malpasset dam 77
5.3.2 ICOLD European Working Group on Uplift Pressure 78
5.3.3 Study carried out by EPRI (USA) 79
6 Case studies of selected Norwegian dams 80
6.1 Dam A 85
6.1.1 General overview of the dam 85
6.1.2 Description of the bedrock 88
6.1.3 Measurements of pore pressure 93
6.1.4 Assessment of results 106
6.2 Dam B 108
6.2.1 General overview of the dam 108
6.2.2 Description of the bedrock 110
6.2.3 Measurements of pore pressure 116
6.2.4 Assessment of results 119
6.3 Dam C1 and C2 121
6.3.1 General overview of the dam 121
6.3.2 Description of the bedrock 124
6.3.3 Measurements of pore pressure 130
6.3.4 Assessment of results 132
6.4 Dam D 133
6.4.1 General overview of the dam 133
6.4.2 Description of the bedrock 136
6.4.3 Measurements of pore pressure 140
6.4.4 Assessment of results 141
7 Conclusions 142
7.1 Pore pressure and design considerations 142
7.1.1 Dam stability and pore pressure 142
7.1.2 Rock foundation and Pore pressure (Foundation stability) 143
7.2 Engineering Geological Mapping 144
7.3 Instrumentation 146
7.3.1 Experience gained from this report 146
7.3.2 Sampling and data storage 146

7.3.3 Experience from the cases in this report 147
7.4 The Norwegian regulations 148
8 References 150

1 INTRODUCTION

1.1 Objective

The purpose of this report is to examine how data from installed pore pressure sensors at five Norwegian dam sites correspond with the requirements for pore pressure beneath concrete dams in NVE's regulatory framework. The contact zone between concrete and rock, as well as the foundation beneath the dam, has been assessed.

1.2 Background

Pore pressure is normally a significant design load for gravity dams, but for slab buttress dams, it has been common practice to use a greatly reduced pore pressure. NVE's regulations provide clear assumptions for pore pressure for gravity dams, given in the NVE Guidelines for concrete dams (NVE, 2005), chapter 2.1. Pore pressure assumptions for buttress dams are indicated in the same guidelines chapter 2.6.1 under the heading "Overturning where cracks will not cause increased pore pressure with uplift" which applies for Buttress dams.

Design considerations are given in the NVE guidelines for concrete dams, NVE (2005), chapter 3.7, where the assumptions should be based on a qualified assessment of the rock foundation.

1.3 Dam types

Load transfer and pore pressure is dependent on the dam type in question. Definition of dam types are therefore important to understand assumptions for pore pressure.

The following dam types are of particular interest to this report (ICOLD, 1994) (NVE, 2005) (SNL, 2023):

- **Gravity dams**, including the following main types:
  - Concrete gravity dams
  - Masonry dams
- **Buttress dams,** including the following main types:
  - Slab buttress dams (or deck dam)
  - Multiple-arch dams
  - Solid head buttress dams

In addition, concrete dams also include arch dams, which are not relevant for this report, but mentioned for completeness.

Details of the different dam types are given below. (Barton, 1988) (ICOLD, 1994)

1.3.1 Gravity dams

This dam type includes concrete dams and masonry dams where the dam structure depends on its own weight to be stable and withstand the water pressure.

Massive concrete dams are normally "triangular" where the water side is approximately vertical, and the bottom width is 0.7 to 0.9 times the height. Internationally, it has become increasingly common to use rolled concrete or RCC (Roller Compacted Concrete) in the construction of gravity dams, but currently there are no RCC dams in Norway.

In the case of massive concrete dams, the pore pressure will normally constitute a significant load when checking stability. However, some dams are designed with drainage and sometimes also a drainage gallery towards the upstream side, so that a reduced pore pressure can be assumed.

Masonry dams are a type of gravity dam where the entire cross-section is made up of stone. In terms of construction, there are two types (i) dry laid masonry dams (dams made up of stone blocks without any mortar in the joints) and (ii) dams here the stones are placed in mortar throughout the dam body. The later has mortar in all joints throughout the entire cross-section and the dam body is therefore not drained so that the pore pressure is assumed to be similar to that in concrete gravity dams. Dry laid masonry dams, on the other hand, have good drainage throughout the dam body, where sealing on the upstream side is normally either grouted joints, concrete slabs or impermeable loose materials (moraine, clay or peat). In the case of dry laid masonry dams, a reduced pore pressure is normally assumed.

Figure 2. Concrete gravity dam (photo: T.Konow).

Figure 3. Dry laid masonry dam(photo. T.Konow)

1.3.2 Buttress dams

Buttress dams include the following main dam types:

- Slab buttress dams
- Solid head buttress dams
- Multiple arch dam

The dam consists of:

i. An upstream slab, arch or buttress-head that also acts as the water sealing.
ii. Support on the downstream side (buttress support). This is usually a vertical wall that support the upstream side.

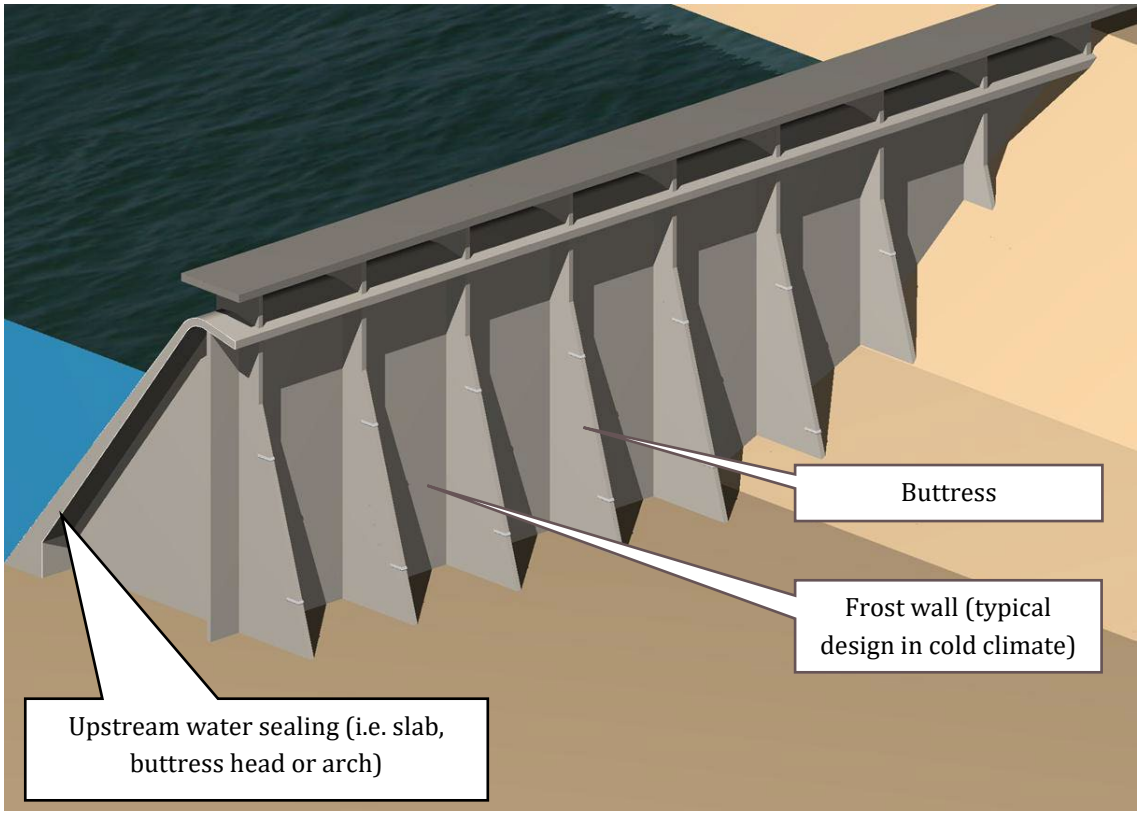

Figure 4. Illustration of the main elements in a buttress dam.

Multiple Arch dams and Slab Buttress dams have a watertight upstream slab supported by a series of supports on the downstream side. The upstream slab is inclined and contributes to the stability of the dam. The force from the water pressure is transferred to the foundation through the buttress supports. Traditional Slab Buttress dams normally have supports at a fixed spacing of 5 m along the dam axis. For Multiple Arch dams, the distance between the supports is much greater.

Solid Head Buttress dams consist of several free-standing buttresses, where each individual buttress is stable without contribution from the adjacent buttress. Each buttress has a buttress head on the upstream side. The Buttress heads form continuous watertight sealing along the dam. Buttress Head dams normally have a more vertical upstream side, so that the weight of each buttress contributes to the stability of the dam (and not the water pressure as in the case of Multiple Arch dams and Slab

Buttress dams).

Reduced pore pressure is one of the advantages of buttress dams, as the area between the buttress supports is freely drained. Reduced pore pressure contributes to a better stability, allowing the weight of the dam to be reduced. This provides savings in construction cost as the volume of concrete in the dam can be reduced, compared to a gravity dam.

The Norwegian regulations (Energidepartementet, 2009) chapter § 5-11, refer to the following buttress dam types:

- Light Buttress Dams and Slab Buttress Dams (i.e. traditional Slab Buttress Dams e.g. dam A in chapter 6.1)
- Heavy Buttress Dams (i.e. Solid Head Buttress dams, or rehabilitated Slab Buttress Dams e.g. dam B, C and D in chapter 6)

According to the regulations, only Heavy Buttress Dams are allowed to be built in consequence class 3 and 4. In the later years, several Slab Buttress Dams in consequence class 3 and 4 have been rehabilitated, and after rehabilitation they are defined as "Heavy Buttress Dams". Dam B, C and D described in Chapter 6.2 to 6.4 are examples of Slab Buttress dams that have been rehabilitated into Heavy Buttress Dams approved for class 3 and 4. However as the dams still have a slab as a water tight upstream seal, they are still considered to be slab buttress dams

In Norway, there are about 290 slab buttress dams, and this represent about 10 % of the dams in Norway. The "Norwegian" slab buttress dams typically have a height between 10 m and 20 m, however the highest are around 30 m high. Buttress dams are labour intensive dams, and this dam type was competitive in Norway until the 1980's, when the general level of wages increased.

The buttress dam is not a dominant dam type. Internationally, the solid head buttress dams and multiple arch dams have typically been designed for heights between 20 to 200 meters, however the dominant height is around 50 meters.

Figure 5. Solid head buttress dam, Dam Svartediket (photo: T.Konow).

Figure 6. Buttress dam: Upstream side of a multiple arch dam (Photo: National Park Service, US)

Figure 7. Slab buttress dam. Dam Svartevatn (photo: NVE/Karen Marie Straume)

1.3.3 Arch dams

Arch dams are built as an arc in a narrow valley so that the water pressure is transferred to the abutments. Arch dams do not rely on weight to achieve stability, and they can be built with a much slimmer cross-section than a gravity dam.

Pore pressure distribution should be evaluated for each specific dam, and the design should consider treatment, injection and drainage of the rock foundation and abutments.

This report does not consider pore pressure under arch dams, as there are no general design requirements in Norway. However, the same general physical laws apply for any foundation, and several of the case studies refer to arch dams.

1.4 Definitions and acronyms

The bullet points below describe the most relevant definitions and acronyms used in this document. The list is structured alphabetically.

- **ALS (Accident Limit State):** A design criterion describing the state at which a structure experiences damage due to accidental or rare events, beyond which functionality is compromised.
- **B (Width of the Transition Zone):** The width of the transition zone between the dam body and the foundation, measured from the downstream toe to the upstream heel.
- **Box Drainage:** Horizontal drainage placed directly on the rock foundation to facilitate drainage in the contact zone between concrete and bedrock.
- **Cross joints:** Rock joints crossing the main structural direction (e.g. Schistosity or foliation).
- **Drainage curtain**: Bore holes at constant spacing in the bedrock along the dam axis. Generally, the holes are vertical and the top of the hole ends in an inspection gallery at the box drain (se chapter 2.4.1).
- **Dam axis:** An axis following the length of the dam**.**
- **DMR (Dam Mass Rating):** A rock mass classification system for assessing the quality and stability of dam foundations (Romana, 2003).
- **DQC (Data Quality Cycle):** The framework for ensuring the quality of measurement data across various phases, including planning, installation, operation, and data analysis (Ljunggren, et al., 2023).
- **DSHP (Nor: "Damsikkerhet i et helhetlig perspektiv"):** A project organized by Renewable Norway aimed at advancing dam safety from a socially optimal perspective, through knowledge and innovation.
- **EPRI (Electric Power Research Institute):** A California-based institute specializing in electric power research.
- **FERC (Federal Energy Regulatory Commission):** One of the primary regulatory authorities for dams in the USA.
- **Foliation:** The main structure in anisotropic rocks like micaschist and phyllite.
- **Fully Grouted Method:** A method for installing piezometers where the borehole is entirely filled with a homogeneous grout mixture. This enables the installation of multiple piezometers within the same borehole.
- **GSI (Geological Strength Index):** A system for rock mass characterization developed mainly to meet the need for input in numerical analysis.
- **ISRM:** International Society for Rock Mechanics.
- **Limit Value:** As per the Norwegian dam safety regulations (§ 7-4), a limit value is a threshold that triggers emergency preparedness. It requires sensors with continuous monitoring and predefined threshold values that activate alarms when exceeded. See also "Threshold Value."
- **NBG ("Norsk Bergmekanikkgruppe"):** Norwegian Rock mechanics Group.
- **NGF ("Norsk Geoteknisk Forening"):** Norwegian Geotechnical Association.
- **NGI ("Norges Geotekniske Institutt"):** Norwegian Geotechnical Institute.
- **NGU ("Norges Geologiske Undersøkelse"):** Geological Survey of Norway.
- **NVE ("Norges vassdrags- og energidirektorat"):** Norwegian Water Resources and Energy Directorate.
- **Uplift (Nor: "oppdrift"/"opptrykk"):** The pressure exerted by water beneath a concrete dam. Referred to as "uplift" in the NVE guidelines.

- **Piezometer:** An instrument used to measure pore pressure in soil or rock.
- **Pore Pressure:** The pressure of water in the voids (pores) in soil or between rock particles. This term also includes joint water pressure and uplift in the context of dam safety, as it is widely recognized in the industry.
- **Q-System:** A classification system for evaluating the rock mass quality and rock support requirement of underground structures (Barton, Lien, and Lunde, 1974; NGI, 2015).
- **Response Time:** The time it takes for a piezometer to react to a change in pore pressure.
- **RMR (Rock Mass Rating):** A rock mass classification system developed by Bieniawski (1973) for assessing rock stability.
- **RQD (Rock Quality Designation):** A measure of the degree of jointing based on rock cores obtained from a borehole (Deere et al., 1967).
- **SF (Safety Factor):** The ratio between the resisting forces and the driving forces affecting dam stability.
- **Joint Water Pressure (Nor:" Sprekkevannstrykk"):** Water pressure in rock fractures. Unlike pore pressure, which is typically evenly distributed, joint water pressure is concentrated in fractures with significantly higher permeability. If fractures are oriented approximately parallel to the foundation surface, water pressure can result in uplift.
- **Threshold Value:** A level indicating a change at the dam that requires follow-up but does not impact immediate structural safety. A threshold value may trigger closer investigation or adjustments of the monitoring. Monitoring does not require continuous measurement but can be assessed periodically. See also "Limit Value."
- **UCS (Uniaxial Compressive Strength):** A measure of the strength of a rock sample, defined as the compressive strength of a cylindrical sample in a uniaxial compression test with no lateral pressure.
- **ULS (Ultimate Limit State):** A design criterion describing the maximum load a structure can withstand before failure.
- **USACE (US Army Corps of Engineers):** A U.S. military division and one of the largest dam owners in the country.
- **USBR (US Bureau of Reclamation):** A federal agency and one of the largest dam owners in the USA.

2 PORE PRESSURE – THEORY AND PRINCIPLES

The assumptions for "pore pressure" in the Norwegian regulations distinguish between uplift pressures for (i) Structural stability and (ii) Foundation stability as summarized here:

- **Structural stability:** This is the "pore pressure" assumed for stability analyses (i) of the dam body or (ii) the transitions between the dam and the foundation.
    - Design considerations for gravity dams are given in the NVE guidelines for concrete dams (NVE, 2005), chapter 2.2.1.
    - Design considerations for buttress dams are given in the NVE guidelines for concrete dams (NVE, 2005), chapter 2.6.1 under the heading "Overturning where cracks will not cause increased pore pressure with uplift".
- **Foundation stability including the rock foundation;** This is "joint water pressure" found in the cracks within the rock. This is the water pressure which can cause uplift if the cracks are oriented parallel to the surface.
    - Design considerations are given in the NVE guidelines for concrete dams, NVE (2005), chapter 3.7.

In this report, the term "pore pressure" also includes "joint water pressure" and "uplift pressure", as "pore pressure" is an established term within the dam sector in Norway. Pore pressure is defined as the unit weight of water times the depth beneath the piezometric surface (meters of water column) at the point in question.

2.1 Assumptions for pore pressure in Norway

2.1.1 Safety requirements and pore pressure

There are different safety requirements for gravity dams and buttress dams. Gravity dams include concrete gravity dams and masonry dams. The main differences are assumptions for pore pressure distribution and safety limits for overturning. This is summarised in the below table.

Table 2-1. Design requirements for Norwegian dams.

Safety requirements for Norwegian dams	Overturning		Sliding	
	Gravity dam Resultant[1]	Buttress dam SF[2]	Gravity dam SF[2]	Buttress dam SF[2]
Ultimate limit state (ULS)	1/3B[3]	1.4	1.5	1.4
Accident limit stat (ALS)	1/6B[3]	1.3	1.1	1.1

[1] Resultant: Safety requirement is defined as the distance from point of action of the resultant force to the downstream toe of the dam.
[2] SF = See definition in chapter Definitions and acronyms 1.4
[3] B = See definition in chapter 1.4

Risk of pore pressure build-up is the key factor for understanding the different safety requirements.

Gravity dams: The safety against overturning is calculated by finding the point of action of the resultant force. The location of the resultant gives the compressive stress distribution along the foundation, and thereby the pore pressure distribution can be identified. In general, it is assumed to be full pore pressure in parts of the foundation with no compressive stress, while the pore pressure is linearly decreasing towards the downstream toe in the areas with compressive stress in the foundation (see figure below).

Buttress dams: These dams are freely drained on the downstream side of the upstream slab, and dangerous pore pressure build-up cannot occur in the structure. Location of the resultant is therefore not critical for this dam type, and calculation of pore pressure distribution is not required. This is also assumed to be the reason that a lower safety factor for sliding can be applied for this dam type.

2.1.2 Gravity Dams

Pore pressure is one of the major forces acting on a concrete gravity dam, when computing the dam stability.

Assumptions of pore pressure for gravity dams are given in (NVE, 2005), chapter 2.2.1, where the following apply:

1. Full upstream pore pressure should be assumed in all parts of the cross-section where there are no calculated compressive stresses.
2. In parts of the dam with calculated compressive stresses, the pore pressure is considered to decrease linearly towards the downstream toe the structure.

Cohesion or adhesion/bond in the cross-section is generally not included. However, cohesion can be included if it is documented, but this is very difficult. In practice, cohesion isn't included.

In parts with no compressive stress the calculations assume no tensile stresses. Adhesion is not considered in the cross-section and thereby, full upstream pore pressure can develop. This is a conservative approach, as adhesion will not be broken unless the tensile stress is greater than the tensile bond. This will in fact not occur before the cross section starts to move, that is, when the resultant is close to the downstream dam toe.

The safety requirements in ULS mean that there is compressive stress throughout the foundation, and thereby a linearly decreasing pore pressure. In ALS, the point of action of the resultant force should be at least B/6 upstream, which implies that there is no compressive stress in the upstream half of the foundation. In this part of the foundation, a full pore pressure is assumed. Pore pressure distribution is illustrated in the figures below.

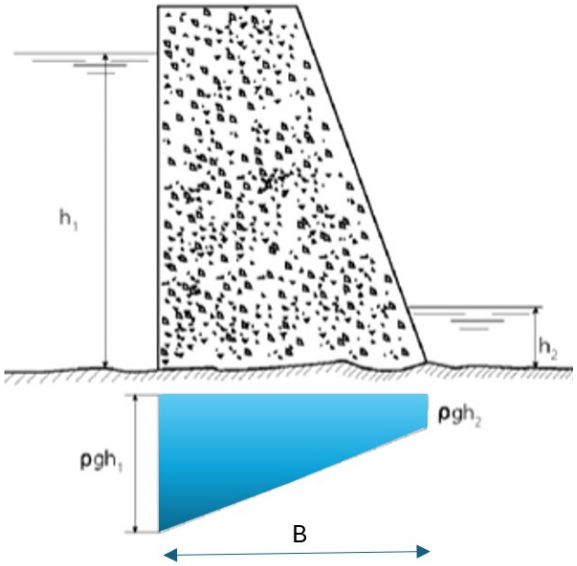

Figure 8. ULS: Pore pressure distribution assumed for gravity dams with compressive stresses through-out the cross-section, from (NVE, 2005).

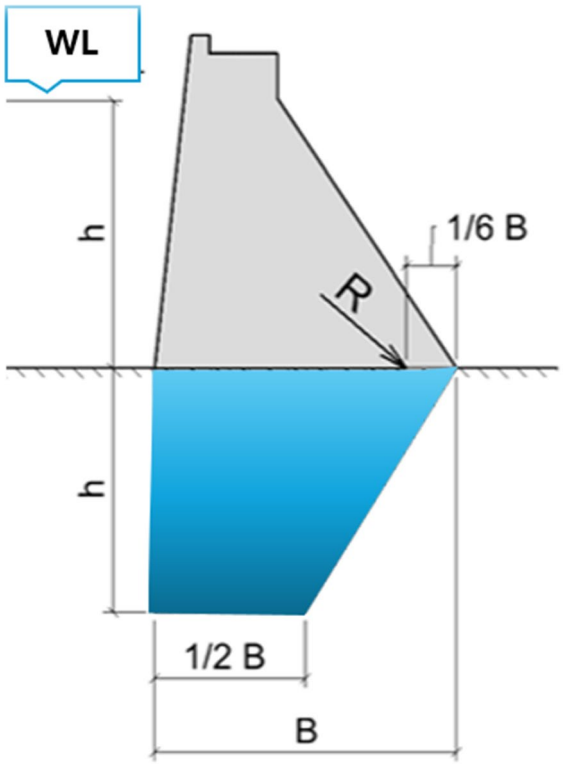

Figure 9. ALS: Pore pressure with compressive stresses in the downstream half of the cross-section, i.e. the resultant is placed B/6 from the downstream toe. This assumption implies an open crack with no bond in the foundation with no compressive stresses (upstream B/2 of the foundation).

2.1.3 Gravity Dams with drainage

According to the guidelines, chapter 2.2.1, gravity dams with drainage can assume the following pore pressure:

Ultimate Limit State (ULS)

- The full upstream pore pressure should be considered in all parts of the cross-section where there are no calculated compressive stresses.
- The pore pressure in the drainage plane is calculated using the formula:
  - $p_{dren} = p_2 + k(p_1 - p_2)$
  - Where
    - p_2 is the pore pressure in the downstream toe
    - p_1 is the pore pressure in the upstream heel
    - k is a drain-factor assumed to be 0.33, unless other values can be documented (se figure below).

Accident Limit State (ALS)

- The dam should be checked for pore pressure load cases as for dams without drainage as an Accident Limit State.

The requirements for ALS imply that design loads in ULS should be checked according to the general rules for gravity dams without drainage, and thereby the following requirements apply:

Table 2-2. Design requirements for gravity dams with drainage

Safety requirements for Gravity dams with drainage	**Pore pressure**	**Loads**	**Overturning**	**Sliding**
			Resultant Point of action[4]	**SF[5]**
Ultimate limit state (ULS)	Drained (k=0.33)	Design flood Ice Pressure	>B/3[6]	1.5
Accident limit stat (ALS)	Drained (k=0.33)	PMF Earh Quake	>B/6[6]	1.1
	No drainage (k=0)	Design flood Ice Pressure	>B/6[6]	1.1

The following figure illustrates pore pressure for a gravity dam with drainage.

[4] Safety requirement is defined as the distance from point of action of the resultant force to the downstream toe of the dam.
[5] SF = Se chapter 1.4
[6] B = Se chapter 1.4

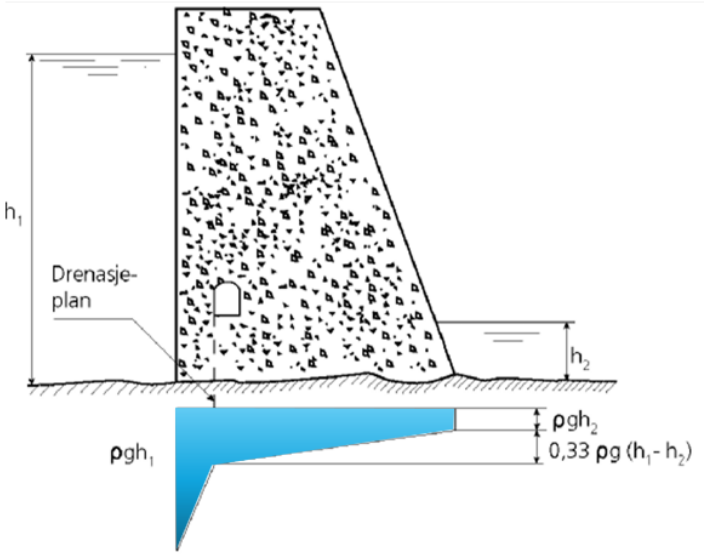

Figure 10. Pore pressure distribution for a gravity dam with drainage from (NVE, 2005).

The additional check of stability with no drainage only applies for concrete gravity dams with drainage and is not used for dray laid masonry dams or buttress dams.

2.1.4 Dry laid masonry dams

Dray laid masonry dams are a gravity dams built with loose stone blocks throughout the entire cross-section, as described in chapter 1.3.1.

Dry laid masonry dams are drained throughout the dam body, where the sealing is on the upstream side and is generally either grouted joints, a cast concrete slab or impermeable loose material (moraine, clay or peat).

Dry laid Masonry dams (dams) are assumed to be drained, with a drain-factor, $k = 0.33$, and where the point of drainage is equal to $0.25*h_1$, ie. 0.25 times the water pressure at the upstream heel, according to the NVE Guideline for Masonry dams (NVE, 2011),

The pore pressure distribution is not dependent of the point of action of the resultant and the dam structure is assumed to be drained even in parts of the foundation with no compressive stress (applies to ALS). This compares to the assumptions for buttress dams, as both structures are freely drained downstream the upstream watertight seal. Possible leakage through the seal will therefore not lead to increased pore pressure throughout the structure. This is also the reason there is no required check for stability without drainages, as the case is for concrete gravity dams "with drainage".

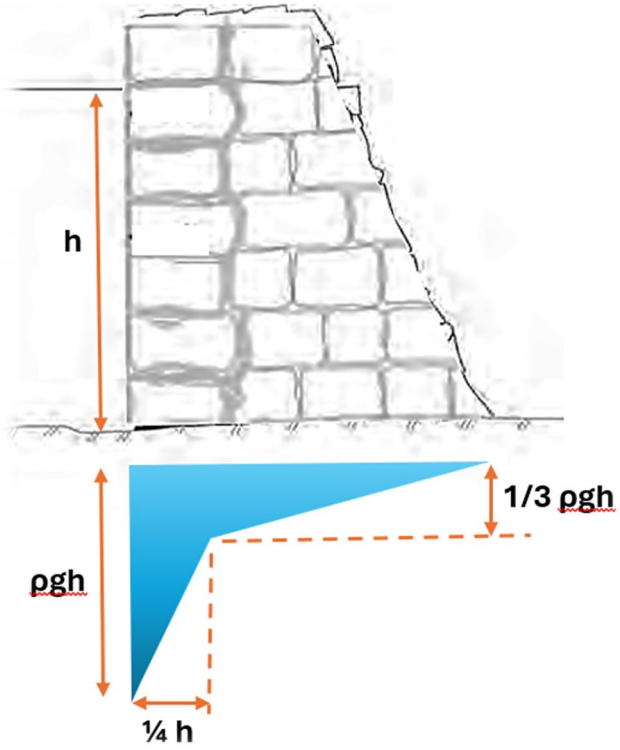

Figure 11. Pore pressure distribution for dry laid masonry dams. The pore pressure distribution is not dependent on the point of action of the resultant and the dam structure is assumed to be drained even in parts of the foundation with no compressive stress (applies to ALS).

2.1.5 Buttress dams

Reduced pore pressure is one of the advantages of buttress dams, as the area between the buttresses can be considered drained. The reduced pore pressure load results in better stability so that the weight of the dam can be reduced.

Requirements for slab buttress dams are given in the NVE Guidelines for Concrete dams (NVE, 2005) Chapter 2.6.1, under the paragraph "Overturning where cracks will not cause increased pore pressure with uplift". This definition implies that slab buttress dams and other buttress dams should be considered in the same way.

According to traditional practice in Norway, slab buttress dams have been assumed to have full pore pressure under the slab, and no pore pressure downstream the slab and under the buttresses. This is coinciding with the text in (NVE, 2005).

As shown in Chapter 3.1.1, stability for overturning of buttress dams is defined by safety factor, and not the location of the resultant force. As a result "no compressive stresses" can occur under the upstream slab of the dam. A crack with full pore pressure can thereby occur under the upstream slab and full pore pressure will be the most correct simplified assumed. This is illustrated to the left in the below figure.

In some cases, the pore pressure has been assumed to be linearly decreasing over a distance equal to two times the slab thickness, which gives the same total pore pressure force. These pore pressure assumptions are illustrated in the figure below.

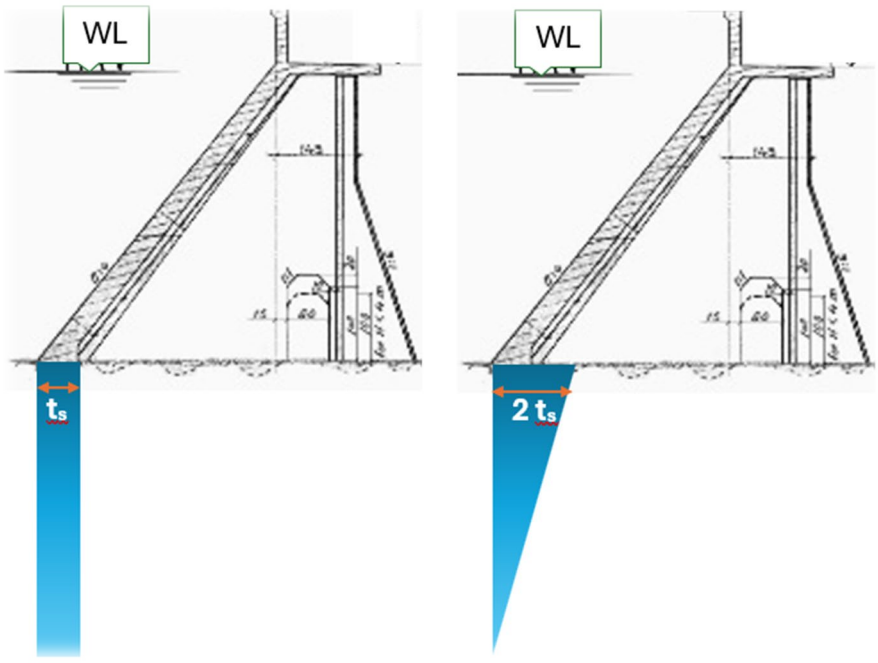

Figure 12. Assumed pore pressure distribution for slab buttress dams (t_s = slab thickness).

2.1.6 Rock foundation

As mentioned earlier in this chapter, the Norwegian regulations distinguish between:

(i) Pore pressure in the dam body as described in in chapter 2.1
(ii) Joint water pressure in cracks within the rock foundation.

Dangerous pore pressure in rock foundations is generally located in cracks that are oriented parallel to the surface and thereby cause uplift.

As rock foundations are not homogeneous, a general assumption for pore pressure in the foundation is not possible. The design assumptions must therefore be based on an evaluation and assessment of the rock foundation.

Description for evaluation of the rock foundation is given in the NVE Guidelines for Concrete Dams (NVE, 2005), chapter 3.7. This is summarized here:

- If there is doubt about the integrity of the foundation, a simple stability assessment should be carried out. The result will determine whether it is necessary to proceed with supplementary investigations and stability calculations.
- Where seepage through the foundation can influence the dam safety in terms of pore pressure buildup, erosion, ice formation, etc., seepage tests should be performed.
- For new structures, the design of the dam must be adapted to the ground conditions. During reassessment, it may be relevant to recheck previous calculations, or in the absence of calculations, to conduct a geological survey of the foundation with calculations if there is doubt about stability.

2.2 Theory: Structural stability

The general theory for pore pressure distribution in the Norwegian regulations is based on a very rough simplification and is assumed to be on the conservative side. The theory assumes seepage lines according to geotechnical theory, and these assumptions is transferred to construct pore pressure distribution in the dam structure and between the dam and the foundation. This is the same theory as used for soil or poor rock foundation.

Pore pressure distribution in rock mass is described in chapter 4.

For structural stability, pore pressure is assumed to be the product of the seepage effects where the water moves through the voids of the structure, driven by the higher water pressure in the reservoir. The seepage effects can be described by the flow net theory, where the following apply:

- The material should be homogeneous and isotropic, thus the hydraulic conductivity is equal in all the directions $K_j = K_x = K_y$.
- The voids of the material should be filled with water hence saturated (constant flow).
- Darcy´s law, $Q = K_j$ regarding flow in porous material and steady-flow condition (does not change with time) should both be applicable, where:

  K_j is the hydraulic conductivity, [m/s]
  i is the hydraulic or pressure gradient, [m/m]

The flow nets can be described mathematically by using the Laplace equation for two-dimension flow analysis. If the above-mentioned principles apply. The equation is characterised by the following two orthogonal sets of curves which simulate the flow of water through material:

- The equipotential lines
- The flow lines

The figure below illustrates seepage through a foundation (R. S. Olsen, 2016). Differential pore pressure is defined as ΔH. Water flow is along seepage lines and equal potential lines define contours of equal elevation pore pressure. In this example there are 8.3 equal potential elevation contours and 4 flow lines defining this flow net (i.e. 4 flow zones). A pore pressure loss equal to ΔH/8.3 occurs as seepage along a flow line pass each equal potential line.

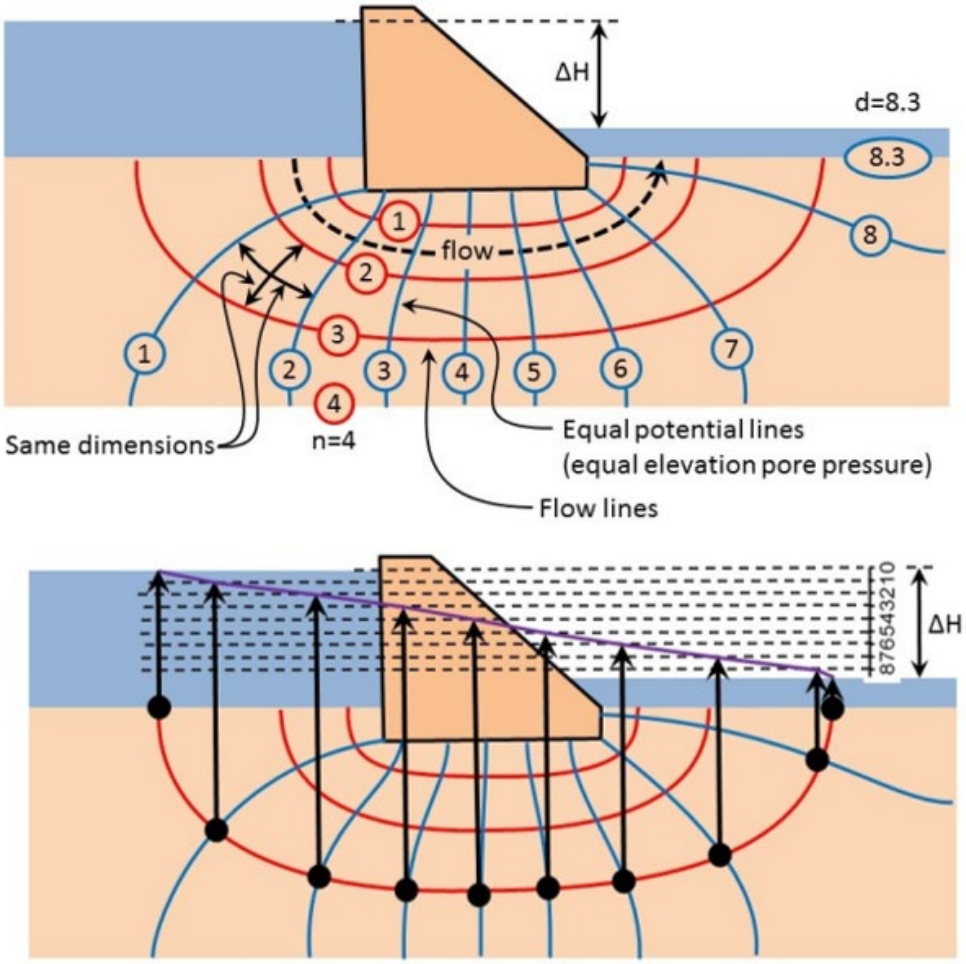

Figure 13. Simple flow net construction (above) and corresponding pore pressure along a flow line (below) (R. S. Olsen, 2016). Pore pressure along flow line no. 3 is shown as a purple lien in the lower figure.

The headwater along any equipotential line can be calculated according to the Bernoulli Equation. By assuming that the kinetic energy along a joint is small ($v = 0\ m/s$) then the Bernoulli Equation can be simplified to calculate the water pressure.

$$P_w = \rho_w \cdot g \cdot (h - z) \qquad (2.3)$$

where,

P_w is the resulting water pressure, [kPa]
ρ_w is the density of water, [kg/m3]
g is the gravity acceleration, [m/s2]
h is the headwater or water energy measured at the equipotentional line, [m]
z is the headwater elevation, [m]

This is the basic theory for assumptions of pore pressure in the dam structure and between the dam and the foundation.

The above figures illustrate pore pressure under a gravity dam with compressive stress in the foundation.

2.2.1 Pore pressure and gravity dams

The monitoring of uplift pressures within the body of concrete dams is rare. It is carried out only in exceptional cases and very little information on this subject is available in technical literature. According to (ICOLD, 2004), meaningful data on uplift pressures within the dam body was only available for five dams. In these five cases measured pressures varied widely, from about 5% up to about 50% of reservoir head. These limited findings, support the usual practice of giving primary attention to uplift at the concrete-foundation interface and in the foundation (ICOLD, 2004).

Destabilising pore pressure can only occur if there is an open crack, i.e. there is no bond in the lift joint or contact zone between the foundation and the concrete structure. In general, this can only occur if the pore pressure is greater than the bond and results in hydraulic fracturing (and/or hydraulic jacking). As the tensile strength in lift joint or the contact zone to the bedrock, is weaker than in the solid concrete structure, installing rock bolts and/or reinforcement bars will reduce the possibility of hydraulic fracturing in these joints.

2.2.2 Pore pressure and buttress dams

By using the same theory of flowlines under a buttress dams, flowlines can be constructed, as illustrated in the figures below. These match the pore pressure distribution assumed by the Norwegian Regulations (see previous chapter).

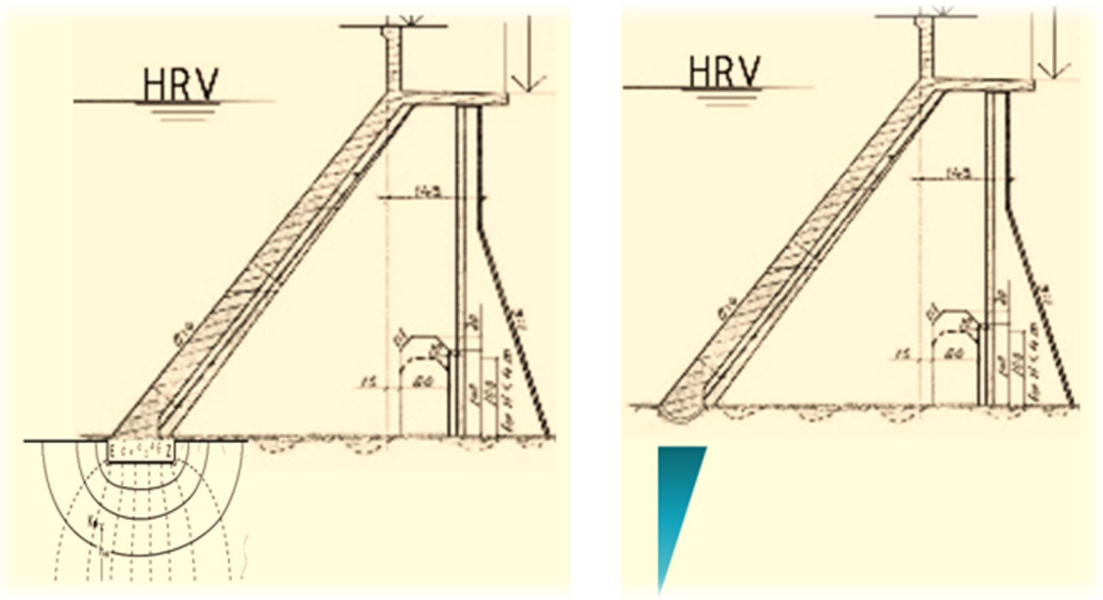

Figure 14. Flowlines under the upstream slab (left) and the resulting pore pressure (right).

As shown in chapter 2.1.5, stability against overturning of buttress dams is defined by a safety factor, and not the location of the resultant force. As a result “no compressive stresses” can occur under the upstream face of the dam. A crack with full water pressure can thereby occur under the upstream face and full pore pressure can occur. This is illustrated in the figure below.

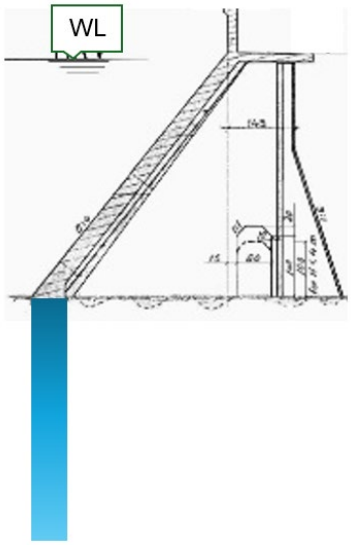

Figure 15. Theoretic pore pressure distribution with an open crack under the upstream face.

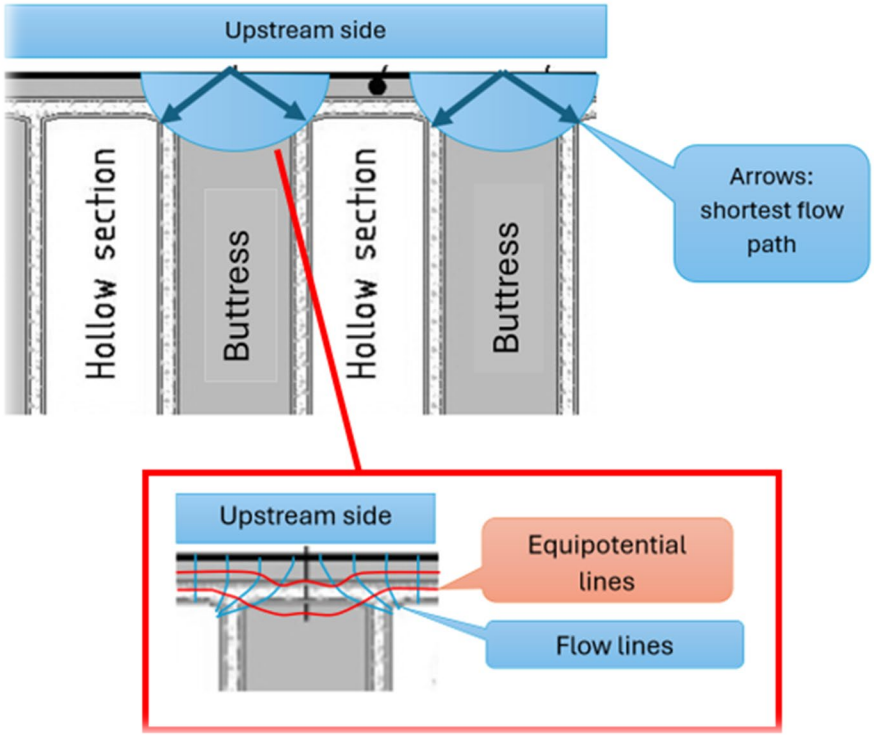

Figure 16. Illustration of flow lines through the upstream slab and buttresses. According to the theory, seepage will flow the shortest way to the downstream side, and there will be no pore pressure under the buttresses.

The (ICOLD, 2004), refer to the report; "San Giacomo Dam: Results derived from the improvement of the uplift monitoring". This report describes a comprehensive monitoring of uplift pressures in the concrete of a buttress dam. Seven automatic piezometers were installed in the dam. No uplift pressures were measured by piezometers placed at a distance of a few metres from the upstream face, confirming the widespread opinion that an effective hydraulic connection with the reservoir load can rarely be established in a sound concrete.

2.3 Theory: Rock foundations

The basic rock engineering aspects of this issue are discussed in Chapter 4 of this report, "Engineering Geology and Rock Mechanics ". In this chapter, the special aspects related to water pressure build-up at dam foundations will be discussed in more detail.

As discussed in chapter 2.1 the general theory for pore pressure distribution is valid in homogeneous materials, but not in heterogeneous foundations with discontinuities such as joints and fractures in the bedrock, which will normally result in nonlinear distribution of the uplift pressure.

The discontinuities can be any defect that separates the rock mass and is characterized by zero or very small tensile strength and therefore may easily deform and displace.

2.3.1 Joint water pressure

The key joint parameters are described in Chapter 4.3 of this report. In the following the potential of joints and fractures to build-up of unfavourable uplift pore pressure in the rock foundation and potential failure planes will be discussed.

The most common assumption regarding pressure build-up for dam foundation is that the aperture (opening) remains constant along the joint, which results in a linear distributed uplift pressure beneath the dam according to the figure below.

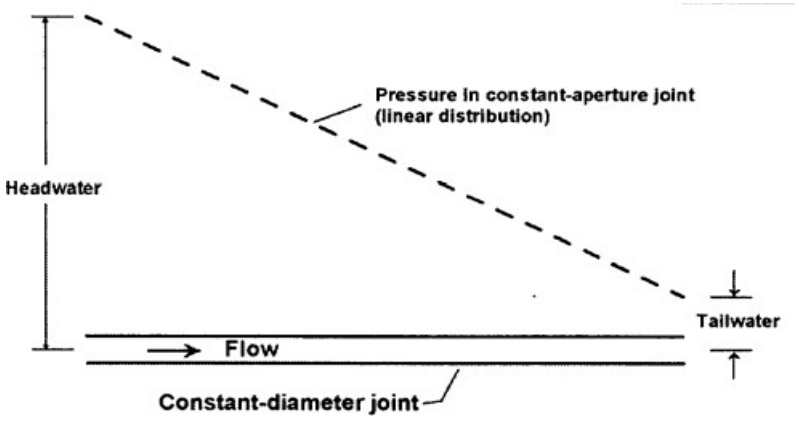

Figure 17. Linearly distributed pressure from the heel to the toe of a dam (USACE/ERDC, 2002)

A joint with varying aperture will in theory result in a nonlinear uplift distribution. Consequently, the joint can be modelled with a large aperture starting from the heel and a smaller aperture in the toe of the dam and the effect simulated as shown in the figure below. This is the same effect assumed for structural stability in areas without compressive stresses, as described in chapter 2, Figure 9. However, in the case of structural stability, the downstream part of the pipe is closed so that a full pore pressure can develop in the upstream part where there is no compressive stress.

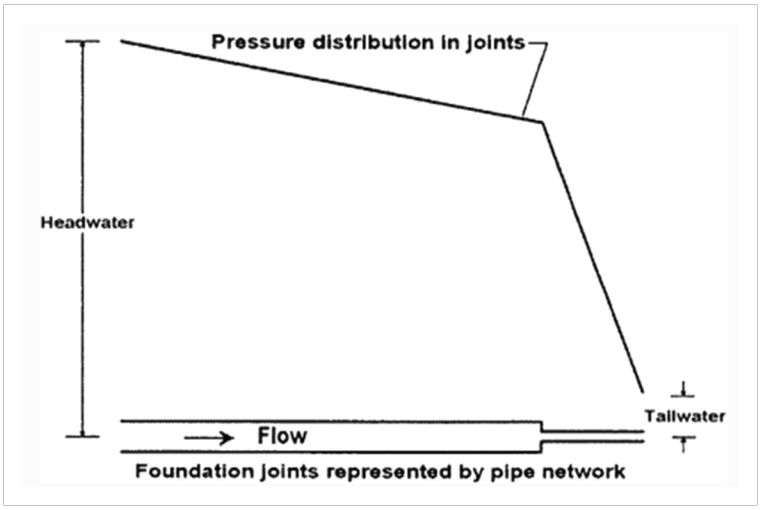

Figure 18. Nonlinearly distributed pressure by a two-pipe network (USACE/ERDC, 2002)

The degree of interconnection between the joints and their length can change the distribution of the uplift pressure, as shown in the figures below.

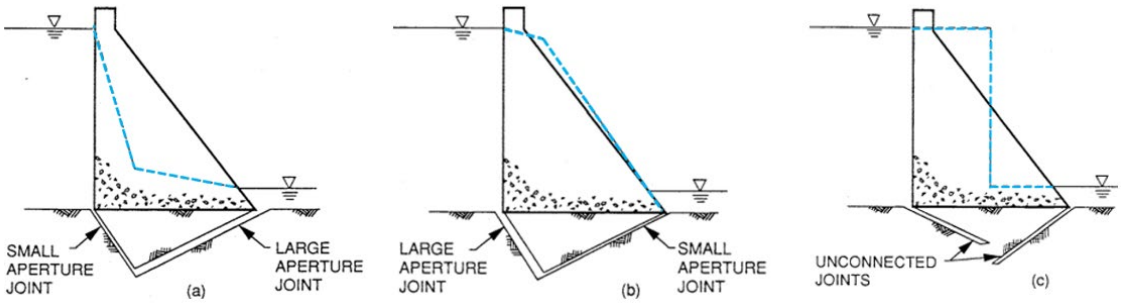

Figure 19. Influence of joint aperture and interconnectivity on uplift. (EPRI, 1992). The pore pressure is illustrated with dotted blue line.

Interconnection between joints in a dam foundation also may have effects analogous with the common assumption regarding worst-case condition for rock slopes (heavy, prolonged rainfall), where the distribution of joint water pressure is assumed to be triangular as illustrated in Figure 19 (a). Experience from a large number of rock slopes however indicates that the real, in-situ water pressure is much smaller than what should be caused by the triangular distribution. This has been found to be due mainly to the fact that most fractures do not convey water in the entire fracture plane, and that considerable amounts of water may escape along secondary, intersecting fractures as illustrated in Figure 19 (b). Similar effects may influence on joint water pressure also at dam foundations, resulting in considerable exaggeration of joint water pressure if configuration like in Figure 2-8 is used in calculation.

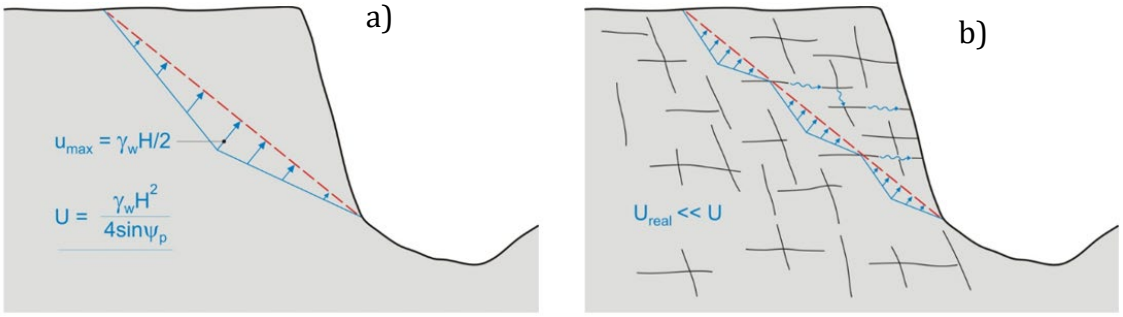

Figure 20. Alternative configurations of joint water pressure along potential sliding plane in rock slope; (a) Triangular distribution along continuous joint (water enters at the top and is fully drained at the toe after having reached a maximum pressure corresponding to the hydrostatic at approx. 50 % of the slope height), b) Reduced, more realistic distribution due to water drainage through secondary (minor) joints, From (Nilsen, 2016).

2.3.2 Effect of rock stresses

Across valleys where dams are located the rock stress distribution is normally as sketched in Figure 21, with the major principal stress (σ_1) oriented along the slope of the valley, the minor principal stress (σ_3) perpendicularly to the surface of the slope and the intermediate principal stress (σ_2) along the direction of the valley. This may cause fractures parallel with the surface (horizontal at the valley bottom, more inclined further up in the valley; commonly referred to as exfoliation joints) to be much less confined, and more vulnerable to hydraulic jacking (see below) than fractures perpendicularly to the surface (vertical at the valley bottom).

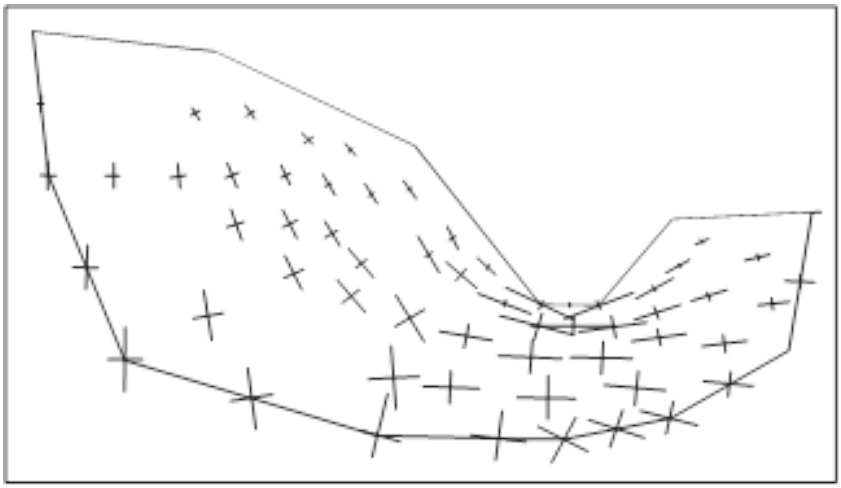

Figure 21. Magnitudes and directions of the major and minor principal stresses in a valley as computed by finite element analysis. The lengths and directions of the crosses indicate the magnitudes and directions of the major and minor principal stresses.

Under a dam, the pressure on the rock foundation may vary with a higher pressure acting at the downstream toe. High rock stress has the effect of compressing the joint fracture walls and thus reducing permeability. This effect is highly dependent on the rock properties and the magnitude of load transfer from the dam structure on to the foundation. This implies that the dam height is an important factor, as a high dams will have larger load transfer to the foundation.

The loads transferred from a dam structure will be higher at the downstream toe as the water pressure on the upstream face results in an overturning force. This effect may result in decreased

permeability towards the downstream toe. Change in aperture in the direction of flow may cause uplift pressure to follow a curved rather than a linear distribution. The figure below shows the analogy extended to nonlinear pressure distribution for a tapered joint, for which the aperture changes continuously from the heel to the toe. This is probably a more realistic approach where the aperture at the heel gradually decreases until the toe of the dam (USACE/ERDC, 2002) .

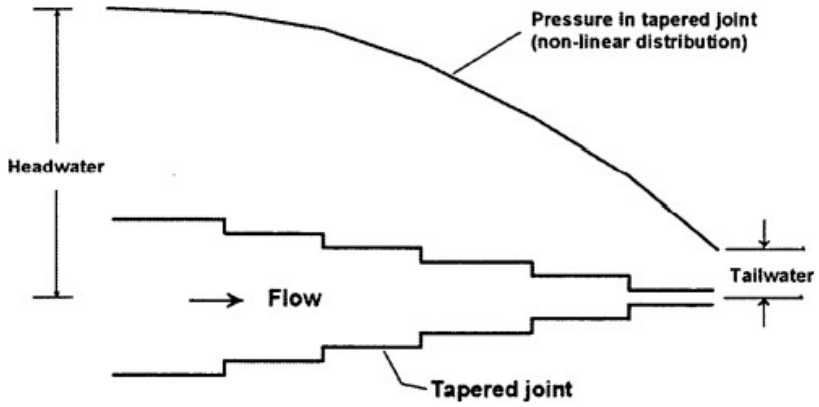

Figure 22. Nonlinearly distributed pressure by a tapered joint (EPRI, 1992).

The effect illustrated in the above figure may be dependent on the loads transferred from the dam structure. The effect will therefore be more visible for higher dams and can also be seen with different water levels in the dam, as shown in the figure below. This implies that the pore pressure can be of greater concern for high dams compared to than lower dams with less load and thereby less deformations in the foundation and a linear pore pressure distribution.

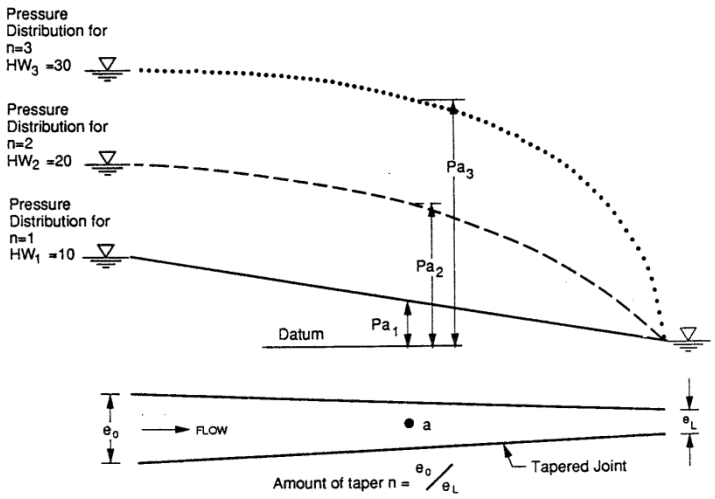

Figure 23. Uplift distribution in a deformable rock joint with increasing headwater and thereby increasing rock stress (EPRI, 1992).

Based on the monitoring data from some dams and the results of the theoretical analysis it appeared that only small aperture joints deform sufficiently to give rise to non-linear uplift response. Large aperture joints will probably not deform enough under the stress changes caused by headwater

variations to create noticeable non-linearity.

It also appeared that grouting may stiffen joints sufficiently to prevent tapering of joints and the resulting non-linear uplift. None of the dams included in the study mentioned, which had extensive consolidation grouting showed non-linear uplift. Dams which would be expected to have non-linear uplift would consequently be those with tight, ungrouted joints and large variations in reservoir level (ICOLD, 2004).

2.3.3 Hydraulic jacking

Hydraulic jacking occurs when the water pressure in an existing joint exceeds the normal rock stress acting on that joint.

In-situ testing based on hydraulic jacking is most used as a "pilot-test" for evaluating the tightness of the rock mass when exposed to high pressure water or gas. Main emphasis in such cases is on jacking of unfavourably oriented joints and the main principle of the test is to increase the water pressure gradually in test sections between two packers in a borehole (or between the bottom of the borehole and one packer), and to record the water flow as a function of pressure as shown in Figure 24.

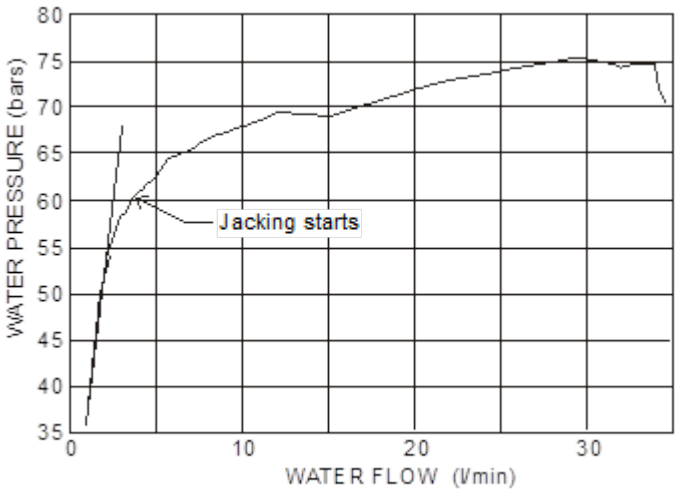

Figure 24. Example of result from hydraulic jacking test (from Nilsen & Palmstrøm, 2000).

Hydraulic jacking in a dam foundation will cause deformation/widening of rock joints and cause the water flow to increase considerably, as illustrated in Figure 24. It will also cause uplift and may contribute significantly to instability of the dam foundation. It is therefore important to fully understand the mechanisms behind hydraulic jacking.

2.3.4 Hydraulic fracturing

Hydraulic fracturing occurs when new joints are created by water pressure in originally intact, solid rock. The basic principle of a hydraulic fracturing test is to isolate a section of a drill hole and gradually increase the pressure of water which is pumped into the hole to obtain fracturing of the surrounding rock. By recording water pressure and flow, the principal stress situation may be evaluated. Hydraulic fracturing is the only rock stress determination technique that is successfully applied to deep drill holes.

An idealised hydraulic fracturing record is shown in the figure below. The water pressure at the moment of fracturing is termed the "fracture initiation pressure" (p_f) or breakdown pressure. After injecting a water volume sufficient to propagate a fracture length about three times the drill hole diameter injection is stopped, and the hydraulic system is sealed or "shut-in" at a pressure referred to as the "instantaneous shut-in pressure" (p_s). Additional re-pressurisation cycles are used to determine the "fracture reopening pressure" (p_r) and additional measurements of the shut-in pressure (p_s).

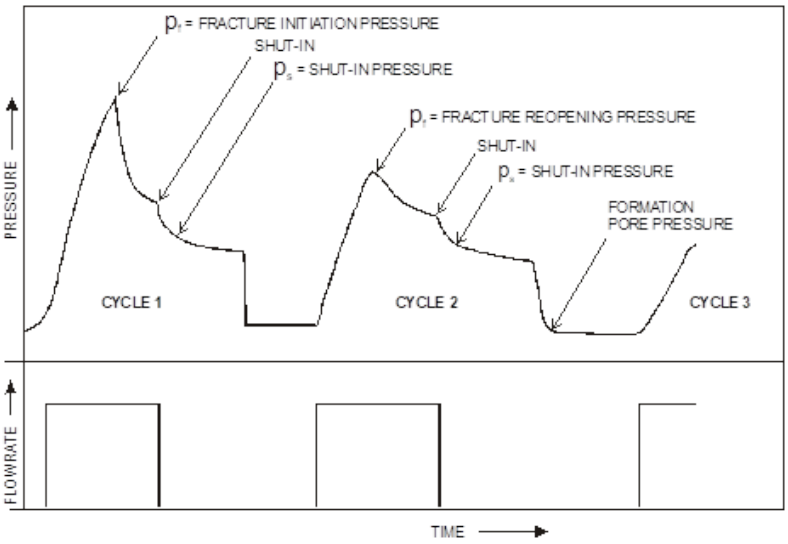

Figure 25. Idealised hydraulic fracturing pressure record (from ISRM, 1987).

To be able to calculate stresses, the drill hole direction has to be parallel with a principal stress direction. Usually, this assumption is considered valid for vertical holes drilled from a horizontal surface. In such cases, the vertical stress is calculated from the overburden weight, and when the plane of hydrofracturing is nearly parallel to the drill hole axis, the following expressions may be used to obtain the horizontal stresses (ISRM, 1987):

Minimum horizontal stress, $\sigma_{min} = p_s$

Maximum horizontal stress for initial pressurisation cycle, $\sigma_{max} = T + 3p_s - p_f - p_0$

Maximum horizontal stress for subsequent pressurisation cycles, $\sigma_{max} = 3p_s - p_r - p_0$

Tensile strength of the rock = T

Initial pore water pressure = p_0

Hydraulic fracturing in rock engineering is relevant mainly in connection with rock stress estimation

for optimisation of the location of the transition zones/concrete plugs in unlined high-pressure tunnels and is not very relevant for dam foundations, although a few rare cases of suspected hydraulic fractures at hydropower project have been observed in concrete dams with water pressure higher than 100 m.

The 186 m high Zillergound dam in Austria is one example where hydraulic fracturing was suspected (P. Obernhuber, 2009). Here a crack formed at an upstream water pressure of 16 bar just above the base joint, as shown in the figure below. Fracture mechanical studies of the concrete material showed that initial cracks up to a length of about 1 m remain stable up to a difference between water pressure and vertical stress of about 10 bar.

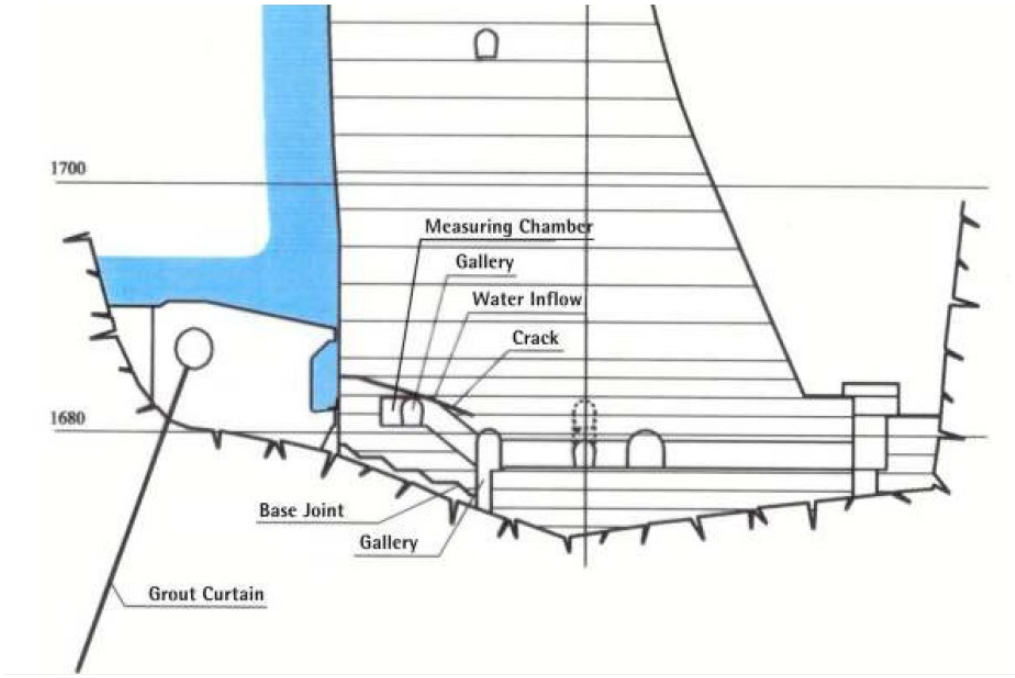

Figure 26. Cross section of the crack at the Zillergound dam. (P. Obernhuber, 2009)

2.4 Measures to reduce uplift pore pressure

The following measures are generally applied to reduce and control the pore pressure in or under a dam structure:

- Drainage
- Foundation treatment (Grout curtain)
- Cut-off walls (Not common for rock foundations)

According to (EPRI, 1992), a well-designed foundation treatment and drainage will limit the adverse effects of geology. Case studies given, show that drains are the most effective method of reducing uplift. According to the same report, the cases also show that a curtain grouting can reduce the quantity of flow, but several of the cases showed that a grout curtain did not control the uplift flow. All the examples, however, had only a single row of grout curtain, which represents an older practice. Modern practice using two or three rows of grout curtains provides substantially better sealing performance than older single-row systems, and available evidence indicates that current grouting methods achieve higher and more consistent efficiency.

Implementation of drainage and/or grout curtain should be based on a geological survey and an assessment of the engineering geological conditions. The need for foundation treatment is also dependent on the dam height and water pressure. For higher dams, a grout curtain is often combined with a downstream a drainage curtain in the foundation.

2.4.1 Drainage

The experience from the piezometers in this report show that box drains on the rock surface will ensure that no pore pressure develop in the downstream buttress support. The drains in these dams are easy to access and inspect.

According to (ICOLD, 2004), drainage is the single most effective mean of reducing uplift pressure.

According to (EPRI, 1992), there are two basic types of drains:

1. Drainage curtain of vertical drilled holes in the rock foundation
2. Box drains (or contact drains). This type of drain is normally placed on the rock foundation along the dam axis.

Examples of different drainage are shown in the figures below.

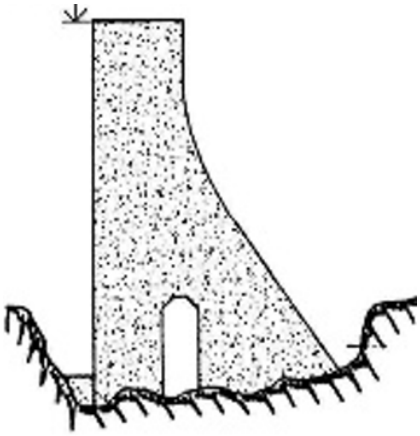

Figure 27. Example of a combined box drain and inspection gallery.

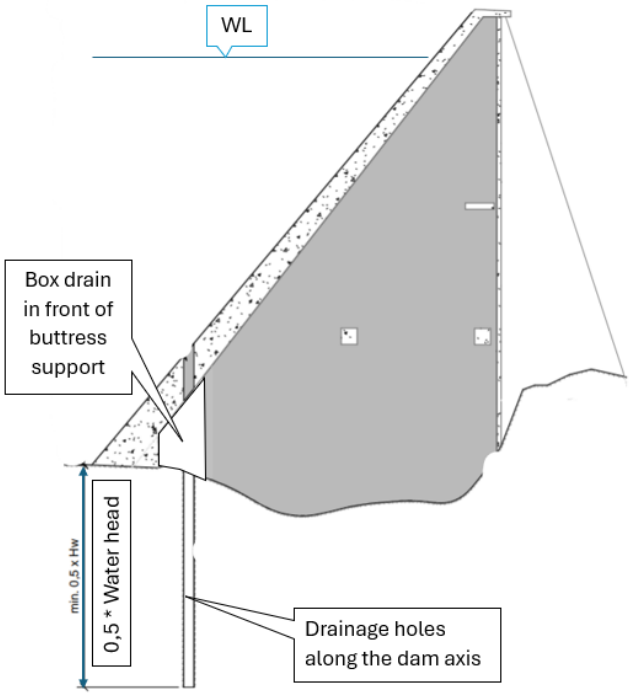

Figure 28. Drainage arrangement, dam D. The dam has a drainage curtain where the drainage holes are placed in a box drain in front of the buttress support.

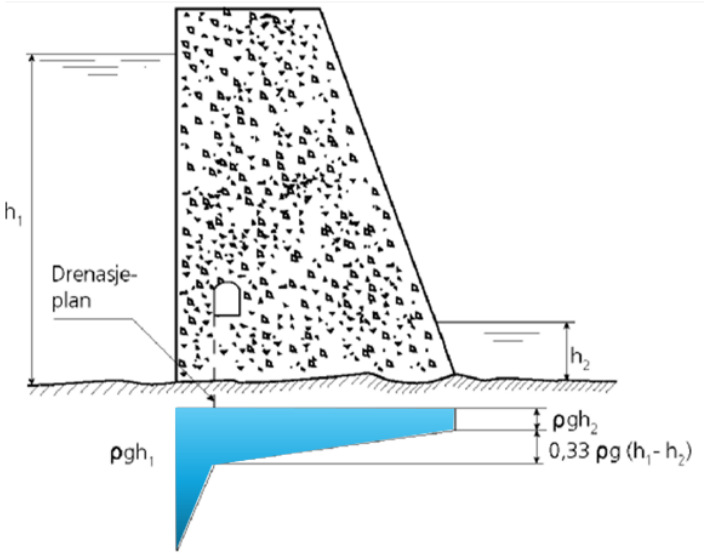

Figure 29. Illustration of drainage curtain where the drainage holes are drained in an inspection gallery inside the dam (NVE, 2005).

According to several studies, i.e. (EPRI, 1992) and (ICOLD, 2004), drainage curtain is the most common type of drainage. A Study from the Swiss Committee on Dams (ICOLD, 2004), show that the drains are effective with a clear break directly behind the drainage line (se figure below).

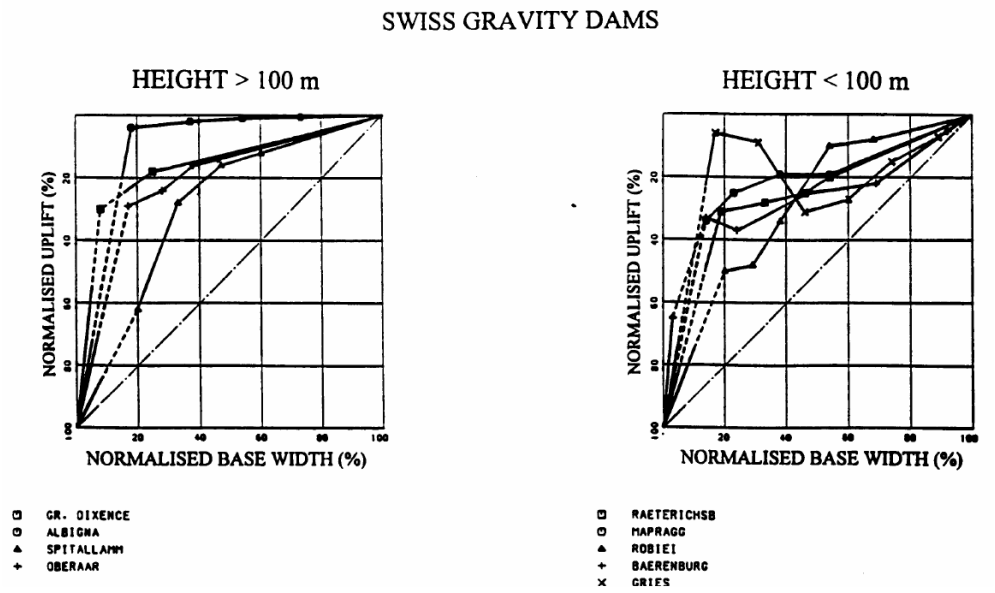

Figure 30. Measured effect of drainage on the pore pressure (ICOLD, 2004).

In Norway, the application of a drainage curtain is not very common and can be explained by the general god quality of rock. According to (NVE, 2005) the following recommendations apply to drainage of foundations:

- If drainage of the foundation and dam is used to reduce the uplift, drainage holes are drilled in the rock foundation with an outlet in an inspection gallery in the dam structure. It is assumed that leakage water from each individual drainage hole is visible in the inspection tunnel and that the water drains are frost-free and are freely drained (without pumping).

The inspection tunnel should be above the normal downstream water level.

- The drainage holes are drilled downstream of the grouting curtain and no closer to the upstream side than 1 m plus 5% of the dam height.
- Drainage holes should have a minimum diameter of 100 mm with a centre distance of no more than 3 m, drilled to a depth corresponding to at least 50% of the water pressure.

It is important to note that drainage holes in a drain curtain will need to be checked and cleaned/flushed at regular intervals, as the holes can be clogged by fines and minerals form the bedrock.

Longitudinal box drains are often found in older gravity dams to drain the concrete-rock interface area (ICOLD, 2004). They were often constructed by laying a line of half-round culverts or on the rock foundation just before the first lift of concrete was poured. The drains were connected to tailwater for the release of the collected leakage water. In gravity dams, the box drains can often be difficult to access and clean and the effect can thereby be reduced over time.

2.4.2 Foundation treatment and Grout curtain

Foundation treatment is any action taken to improve the quality of the foundation rock mass. Foundations are treated to improve the strength and uniformity of the rock mass and to control seepage under the dam.

Foundation grouting has becoming more standardised and normal over the years. As shown in the cases in this report, the 3 oldest dams built prior to 1970's do not have a grout curtain, while the last dam built in the 1980's has a grout curtain (se figure below). Dams built prior to the 1930 generally do not have a grout curtain (EPRI, 1992).

The grout curtain is normally installed in the bedrock foundation below the upstream part of the dam and its main purpose is to reduce the water seepage through the bedrock. A grout curtain is constructed by drilling deep holes in the foundation parallel to the dam axis below the heel of the dam. The hole spacing and hole depth are dependent on the geology of the rock mass. The extent of grouting is decided on site and dependent on tests of rock permeability during grouting.

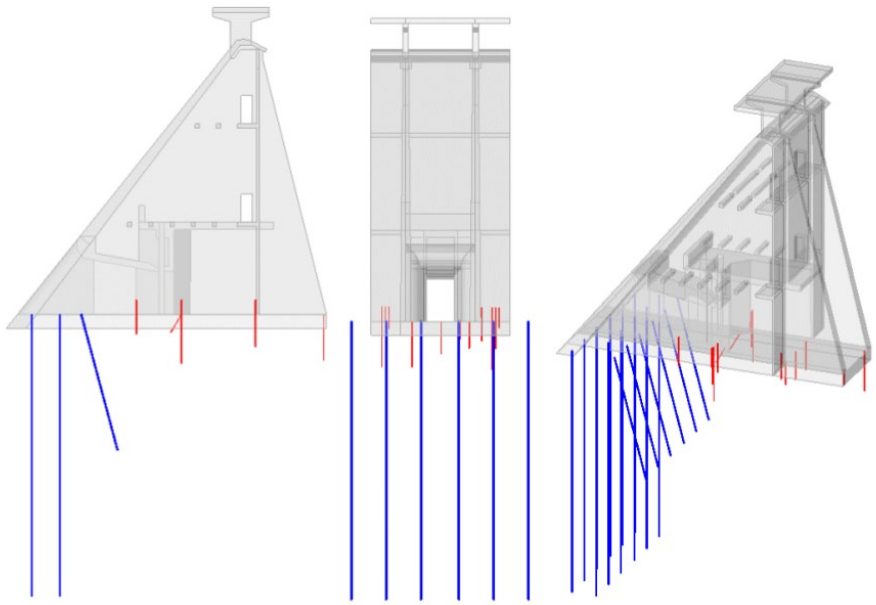

Figure 31. Grout curtain with 3 rows of drill holes parallel to the dam axis (dam A). Left: section with the upstream side to the left. Middle: front view of the midsection. Right: 3D illustration of the grout curtain and the dam section.

As indicated in Figure 31, grout holes are often drilled with two different purposes:

- Sealing the contact between concrete and the bedrock surface, and fractures in the upper part of the bedrock (red lines in Figure 31).
- Sealing fractures in the bedrock from the bedrock surface to a greater depth.

Even when extensive grouting is done, a 100 % effective sealing of all rock fractures is rarely achieved. This is mainly because of the complexity, inhomogeneity and unpredictability of rock fractures, and the lack of ability of grout to penetrate into the tightest fractures. Details on the significance of fracture character are discussed in chapters 4.1 "Permeability of rocks and rock masses " 4.2 "Key fracture parameters" and 4.6 "In-situ monitoring".

When the foundation consist of weak rock or soils, an aprons or a soil blankets can be an efficient solution to reduce seepage, as shown in the figure below.

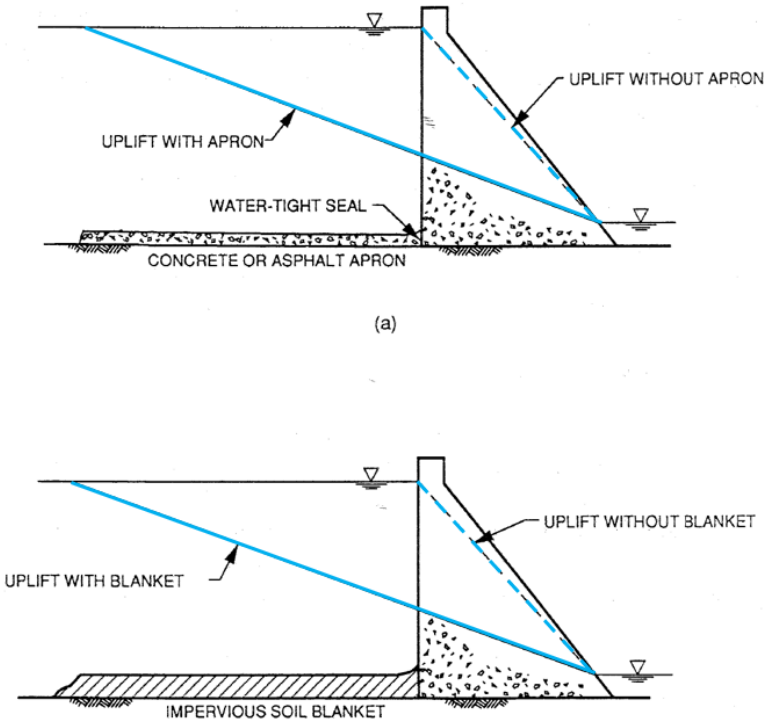

Figure 32. Example of apron or soil blankets. Pore pressure is reduced by increasing the flow path through the foundation.

2.5 Practice in other countries

2.5.1 Europe

This chapter is based on the report from the ICOLD European Working Group titled "Uplift Pressures under Concrete Dams - Final Report" from 2004 (ICOLD, 2004). The report is also described in this report, Chapter 5.3.2.

The group started up in 1995 with the aim of examining aspects related to regulatory rules and normal practice for design, construction and operation of dams throughout Europe.

The working group behind the report, "Uplift Pressures under Concrete Dams", included experts from different countries and made the information easily accessible. The report includes a summary of the regulatory rules and design practice from several European countries as summarised in the table below.

Explanation of the columns in the table:

- **Design practice:** Identifies if the assumptions are given as regulatory rules (RR) or normal design practice (NP).
- **Uplift similar to NVE guidelines**: Indicates whether the pore pressure assumptions for Concrete Gravity Dams and Buttress Dams are comparable to the requirements in the NVE Guidelines (NVE, 2005), as described in chapter 2.1.

Table 2-3. Summary of assumptions for pore pressure in design. General reference (ICOLD, 2004) unless otherwise is noted.

Country	Design practice[7]	Uplift similar to NVE guidelines[8]		Comments Reference is (ICOLD, 2004) unless otherwise is noted.
		Gravity dam	Buttress dam	
Italy	RR	Yes	(Yes)	Gravity Dam: • Similar assumptions for pore pressure distribution as in Norway. • Effect of drains and grout curtain can be included. Buttress Dam: Assumed pore pressure depends on the width ratio (Buttress head/Buttress support) • Ratio > 2; Fully drained downstream the head/slab. • Ratio < 2; Pore pressure as for a gravity dam. NB: The requirements are only valid for design of new buttress dams. Theoretical stability of existing buttress dams are based on observations of behaviour and experience with the dam during operation.
Spain	RR	(Yes)	-	The info about pore pressure assumptions is unclear.

[7] RR = Regulatory requirement, NP = Normal design practice
[8] Assumptions for Pore pressure are given in chapter 2.1

Country	Design practice[7]	Uplift similar to NVE guidelines[8]		Comments Reference is (ICOLD, 2004) unless otherwise is noted.
		Gravity dam	Buttress dam	
Portugal	RR	-	-	The info about pore pressure assumptions is unclear. The effect of drains can be included.
Germany	RR	Yes	-	Gravity Dam: • Similar assumptions for pore pressure distribution as in Norway. Effect of drains and grout curtain can be included.
Norway	RR	Yes	Yes	
Finland	RR	Yes	-	Gravity Dam: • Similar assumptions for pore pressure distribution as in Norway. • The info about effect of drains is unclear.
UK	NP	(Yes)	Yes	Gravity Dams: • Upstream pore pressure = 0,66-1,0 of headwater Buttress Dams: • Reference (P. Novak, 2007), see chapter 7.2.1
France	NP	Yes	-	Gravity Dam: • Similar assumptions for pore pressure distribution as in Norway. • Effect of drains and grout curtain can be included.
Switzerland	NP	Yes	-	Gravity Dam: • Similar assumptions for pore pressure distribution as in Norway. Effect of drains and grout curtain can be included.
Sweden	NP	Yes	(Yes)	Buttress Dams: • See explenation below • Reference: (Energi Företagen, RIDAS, 2020 Oktober)
Austria	NP	(Yes)		Gravity dams: • Triangular distribution of uplift pressures is generally assumed with 85% of the water head at the upstream heel,
Other references/countries:				
USA/FERC	NP	Yes	Yes	Reference: • Guidelines: Hydropower projects, Chapter 3, Gravity Dams. (FERC, 2016) • Guidelines: Hydropower projects, Chapter 10-2, Buttress Dams. (FERC, 1997) • Engineer manual: Gravity Dam design (USACE, 1995)

2.5.2 Sweden – Buttress dams

Assumptions for concrete dams in Sweden are given in RIDAS, Chapter 9 “Concrete Dams” (Energi Företagen, RIDAS, 2020 Oktober), Chapter 9.1.3 "Uplift".

Pore pressure under buttress dams is reduced compared to gravity dams as the dam is drained on the downstream side. A linearly decreasing uplift can be assumed under the upstream slab/buttress head, as shown in the figure below (Energi Företagen, RIDAS, 2020 Oktober)

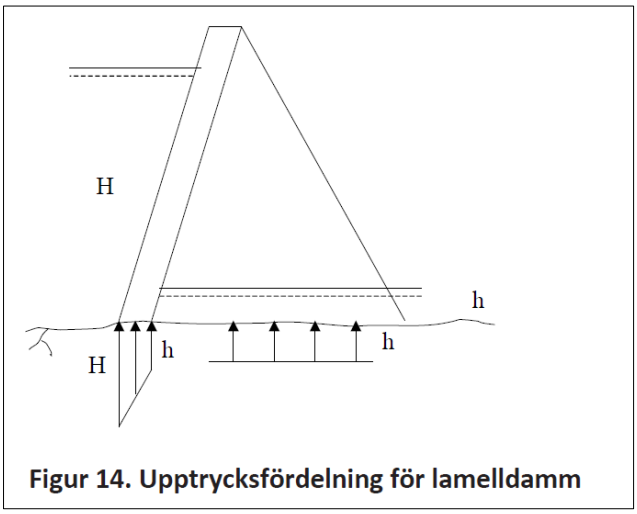

Figure 33. Pore pressure distribution according to RIDAS (Energi Företagen, RIDAS, 2020 Oktober)

If the buttress support is wider than 2 m, the pore pressure is assumed to be linearly decreasing over a distance similar to the width of the support. Similar assumptions apply for the gate piers, as shown in the figure below where “d” is the width of the pier or the buttress support.

The Swedish authorities have no exact limit when a buttress or gate pier should be considered as a gravity dam.

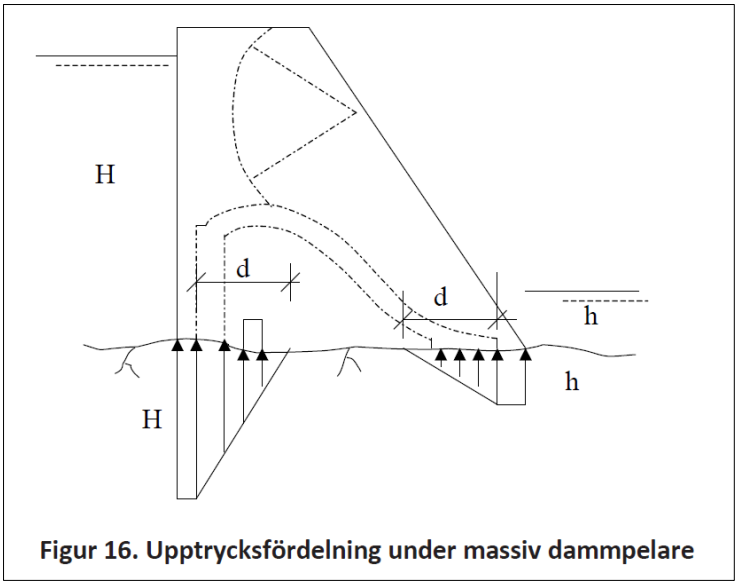

Figure 34. Pore pressure distribution for a gated pier and buttress support wider than 2 m, where d is the width of the pier or the buttress support.

We have been information from RIDAS, that the requirements are based on an article in "Dam Engineering" Vol XX, Issue 1. Here tests have been carried out on supports 2.2 m wide and 6.6 m wide. For the slenderest buttress the pressure under the support was insignificant, while under the 6.6 m wide support the pore pressure is described as significant. We have not been able to get hold of this article and therefore cannot verify the result.

2.5.3 USA (FERC)

The Federal Energy Regulatory Commission (FERC), have established Engineering Guidelines for the Evaluation of Hydropower Projects, where pore pressure requirements for dams are given in the following publications:

- Chapter 3 – Gravity Dams (FERC, 2016)
- Chapter X – Other dams - se chapter 10-2 Buttress dams (FERC, 1997)

The Federal Energy Regulatory Commission, or FERC, is an independent agency that regulates the interstate hydropower projects. FERC also regulates transmission of natural gas, oil, and electricity.

Buttress dams (Chapter 10-2)

Assumptions for pore pressure under buttress dams are given in chapter 10-2.3.2 and 10-2.3.3, where the following apply:

Uplift may be assumed to vary from headwater pressure at the upstream face to tailwater pressure at the downstream edge of the upstream face slab or arch. Uplift pressure beneath the remaining portion of the buttress or buttress footing may be assumed to be tailwater pressure.

When examining failure planes within the foundation, the uplift pressures should be treated similar to uplift pressures for concrete gravity dams. If shallow, sub horizontal discontinuities exist, uplift pressures should be calculated using cracked base type analyses.

If a buttress dam is founded on a continuous slab, uplift pressures at the concrete-to-rock interface should be treated as discussed for concrete gravity dams, as shown on the figure below.

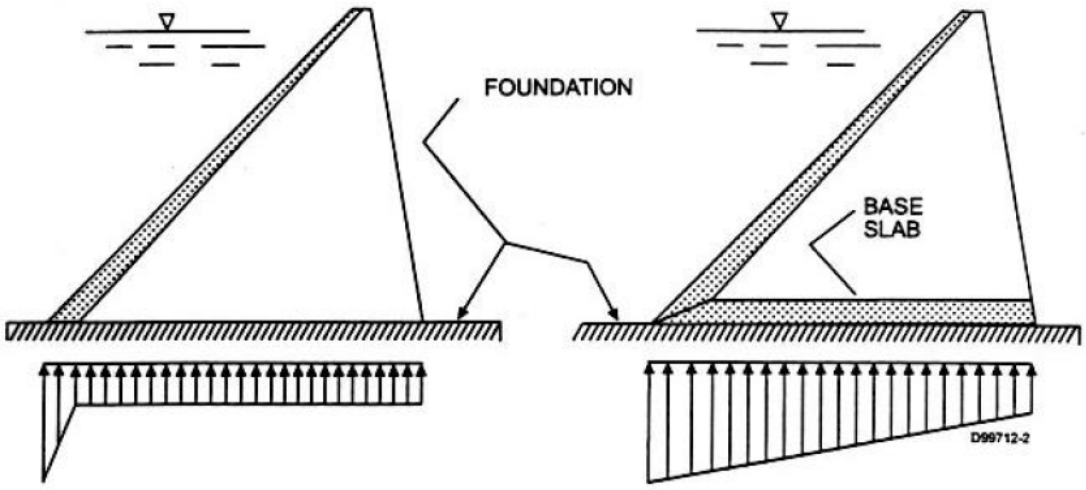

Figure 35. Uplift pressure diagram for buttress dams, figure 10-2.9 (FERC, 1997). The right figure applies if the buttress supports are founded on a continuous concrete slab.

Gravity dams with drains (Chapter 3)

Uplift at the concrete/rock interface for structures having an open verifiable drainage system should be assumed to vary as a straight line from full headwater pressure at the heel or theoretical crack tip, to reduced uplift at the drain, and then to full tailwater pressure at the toe. Assumed pore pressure head at the drain (*H3*) is dependent on the drain effectiveness, *E*, where the drain factor can be expressed as the following:

- ***T<X**: H3 = K (HW-TW) + TW*
- ***T>X**: H3 = K (HW-H4) + H4*
- Drain factor: *K = 1 – E*, where *E* is the drain effectiveness

The drain effectiveness must be verified by instrumentation, and an effective maintenance plan must be implemented. It is also assumed that the gallery is free draining.

The dam owner is responsible for evaluating the specific conditions at each project, to determine if extrapolation of drain efficiencies is valid.

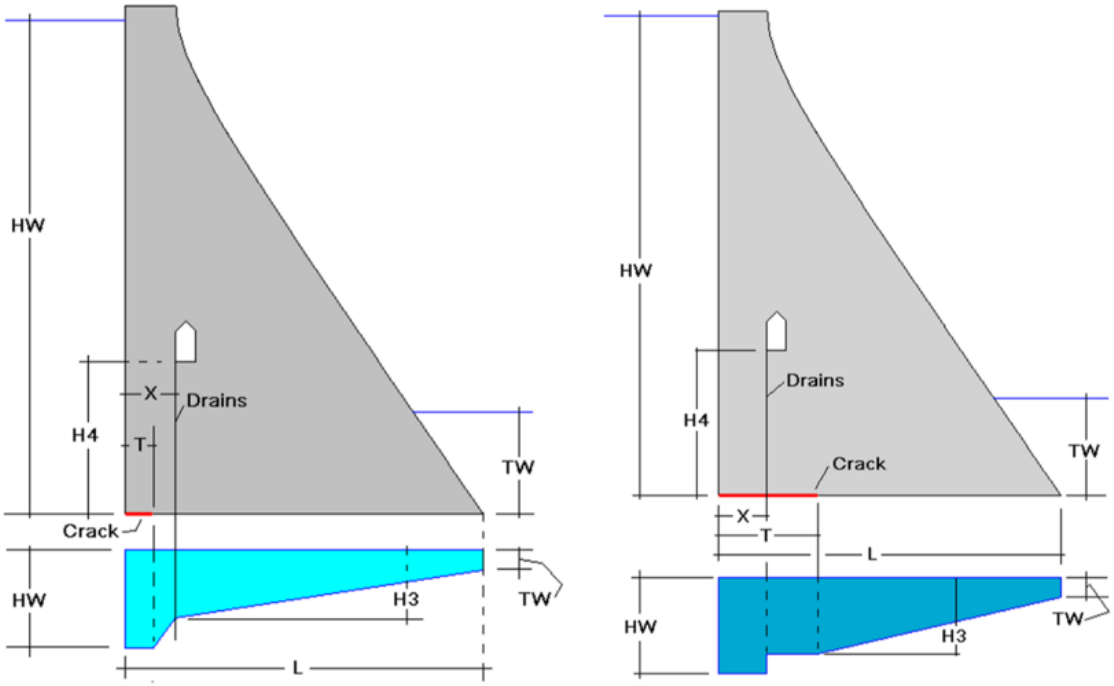

Figure 36. Assumed pore pressure at the base of concrete gravity dam with drainage and an open crack upstream the drains (left) and downstream the drains (right).

3 INSTRUMENTATION AND MONITORING

3.1 Purpose of monitoring of dams

This chapter is mainly based on (NVE/NGI, 2024), chapter 2.1. The purpose of instrumentation and monitoring of dams can broadly be divided into three categories (NGI, 1994):

- To monitor the dam's condition and behaviour for safety reasons.
- To verify that the dam's actual behaviour aligns with the assumptions made during design.
- To enhance the general understanding of dam behaviour.

The monitoring program must be carefully planned and executed according to defined objectives. The fundamental philosophy is that every instrument in a dam should have a specific purpose. If it does not have a specific purpose, the instrument should not be installed. As Professor Ralph B. Peck stated in his article on instrumentation for embankment dams (R.B., September 2001):

"*Certainly, the fundamental rule today should be that no instrument should be installed that is not needed to answer a specific technical question pertinent to the safe operation of the dam*."

Most guidelines for the instrumentation and monitoring of dams emphasize that instruments and the collection of measurement data alone do not improve dam safety. The Federal Energy Regulatory Commission (FERC, 1995), which regulates a large number of dams in the USA, points out in its guidelines for instrumentation and monitoring that instruments must be carefully selected, positioned, and installed. Data must be collected thoughtfully, carefully processed, analysed, and visualized, and this must be done within a reasonable timeframe to ensure dam safety.

A poorly planned or poorly executed monitoring program will generate large amounts of unnecessary data, causing the dam owner to waste time and money collecting and interpreting it. This can lead to confusion about the dam's actual behaviour and may result in the monitoring program being partially or entirely abandoned.

3.2 NVE requirements

In general, monitoring of Norwegian dams has not been very extensive, and is often limited to monitoring for safe operation, i.e. water level monitoring. In general terms, monitoring for this can be partly explained by the fact that Norwegian dams, generally have been built with good safety margin, so that surveillance and monitoring has not been necessary. In addition, there is mainly good quality rock even at the ground surface in Norway, since glaciations have removed most weathered rock and loose material. The ground conditions are therefore often not comparable to the geology in other parts of the world.

According to the Norwegian Dam Safety Regulations (Energidepartementet, 2009), § 7-2, the following requirement applies for instrumentation of dams:

Table 3-1. Summary of table 7-2.2 from in the Norwegian dam safety regulations (Energidepartementet, 2009), sorted according to foundation properties.

Dam type	Foundation	*Dam class*	*Water level*	*Leakage*	*Deformations*	*Pore pressure*
Embankment dam	All types	2, 3, 4	x	x	x	
Concrete- or masonry dam	All types	3, 4	x	x	x	
		2	x	x		
All dam types	**Soil, clay, moraine or weak rock**	**2, 3, 4**	**-**	**-**	**-**	**x**

As shown in the above table, Pore pressure measurements are limited to dams with foundation on loose soil or poor-quality rock.

3.3 Experience with pore pressure measurements

This report includes evaluation of five buttress dams with a total of 87 hydraulic piezometers installed. For 4 of the dams the piezometers are located at a fixed depth of about 1 m in the rock mass, placed under the buttress supports that are about 5-6 m wide. This accounts for about 70 of the piezometers.

All the dams in question are located on good quality rock foundation. The placement of the piezometers is not based on an evaluation of geology of the rock foundation. Summary of some key information is given in the table below:

Table 3-2. Key information of the dams and sensor output (total 87 sensors).

Dam	Dam height	Foundation	Grout curtain?	Total leakage	No. of piezometers
A	21 m	Fairly good to good/very good	Yes	Not visible	16
B	19 m	Fairly good to good	No	<0.2 l/s	24
C1 and C2	12 m	Good to very good	No	< 0.1 l/s	28
D	14 m	Very good	No	Not visible	19

3.3.1 Installation of piezometers

It is important that the sensors are installed correctly. Here are some recommendations for installation:

- The filter should be saturated before installation. This means the tip of the sensor should be unscrewed and the sensor filled with water.
- In dry holes, the sensor should be installed upside down.
- Boreholes should be filled with water when the hole is sealed.

- There are no specific requirements for the drilling method. Both core drilling and impact drilling can be used.
- The diameter of the borehole is not critical, but it should be slightly larger than the sensor itself to prevent jamming and to allow for backfilling with sand/gravel around the sensor.
- Signals from the sensor should be checked both before and after installation to ensure the sensor is functioning properly.

3.3.2 Sources of error

There are many people involved in achieving good and accurate measurement data. The potential for misunderstandings is high in the process, which includes selecting sensors, ordering, setup, installation, reading, and interpreting of data, etc.

Correct installation depends on a good installation instruction. This can be addressed by having the supplier or another dedicated person to follow the sensor from delivery to installation and software setup.

The lifespan of the sensors is difficult to predict. Generally, a sensor of good quality that is properly installed and functions well in its first year can have a lifespan of between 10 and 40 years.

Some possible sources of error that have been identified in this project are:

- Damage to the sensor and/or cable during transport and installation. This can be prevented by testing the sensor before and after installation.
- Installation errors.
- Incorrect selection of sensor type.
- Damage because of too high pressure.
- Incorrect setup to collect and present data.
- Errors in reading, evaluation and understanding the measurement data.
- Malfunction of the sensor and limited sensor lifetime.

4 ENGINEERING GEOLOGY AND ROCK MECHANICS

The main focus in this chapter will be on issues related to engineering geology and rock mechanics which are important for characterizing water flow and pore pressure build up at the foundation of concrete dams. In practice, flow and pressure build up are governed mainly by discontinuities (joints and fractures), and factors related to discontinuities therefore will be described in most detail in the following, and to a lesser extent issues related to intact rock.

4.1 Permeability of rocks and rock masses

The effective porosity of most rocks is rather low and the communication between individual pores rather poor. This is the case particularly for hard rocks like in Norway, which in the great majority of cases have porosity < 1 %, see the table below. Exceptionally, for Permian sandstone found in SE-Norway (Brummundal area), porosity of more than 15 % has been measured and in sandstones from the North Sea porosity of more than 30 %. For the great majority of Scandinavian cases the rock porosity is however very low (< 1 %).

Table 4-1: Effective porosity of some Norwegian hard rocks tested at NTNU (Nilsen, 2016)

Rock type	Effective porosity
Basalt (Permian)	0.11%
Monzonite (Larvikite)	0.61%
Diorite (Trondhjemite)	0.84%
Gneiss	0.75%
Quartzite	1.09%
Marble	0.48%
Limestone	0.58%
Sandstone	0.22%

Hydraulic conductivity (k), also referred to as the coefficient of permeability, is the most commonly used parameter for characterizing water flow. k (in m/s) represents the coefficient of permeability in Darcy' equation:

$$v = Q / A = k \, x \, i$$

where: v = flow velocity (m/s)
Q = flow rate (m^3/s)
A= flow area (m^2)
i = hydraulic gradient

Typical Scandinavian hard rocks have very low porosity and the communication between pores is rather poor. The contribution of porosity to hydraulic conductivity therefore will be close to zero and the hydraulic conductivity of in-situ rock mass will be governed by the frequency and properties of discontinuities.

The value of hydraulic conductivity depends on the nature of the rock mass as well as the nature of the fluid. Most commonly it refers to water as fluid, and in present chapter this is also the case.

The specific permeability K (in m^2, often referred to simply as permeability) depends on the nature of the rock mass only (and not the nature of the fluid). The relationship between k and K is defined as:

$K = k (\mu / (\rho \times g)) = k (\nu / g)$

where: μ = dynamic viscosity of the fluid = 1.3 mPa s (millipascal seconds) for water at +10˚C

ν = kinematic viscosity of the fluid (= 1.3×10^{-6} m^2/s for water at +10˚C)

ρ = density of the fluid

g = gravitational acceleration (= 9.81 m/s^2)

The joint aperture has great influence on flow rate. For a system of parallel, smooth joints Louis (1969) found the following relationship between hydraulic conductivity and joint parameters:

$k = (g \times e^3) / (12 \nu \times s)$

where: e = joint aperture (m)

s = joint spacing (m)

ν = kinematic viscosity (m^3/s)

For doubling of aperture, the hydraulic conductivity according to the Louis-equation is increased by a factor of eight. The Louis and Darcy-equations are however both based on idealized laminar flow conditions, and the Louis equation also assumes a joint geometry based on a simple parallel-plate model. Since rock joints are rough and in many cases also coated or partly filled with minerals, water flow often follows irregular, narrow channels/pipes, and the Louis and the Darcy-equations therefore have limited value. Both are however important for understanding the basic aspects of water flow in Rock joints.

Figure 37 gives an overview of typical *k*-values for rocks and soils. The hydraulic conductivity of in-situ rock mass is governed by the extent of jointing and the character of the joints which may both vary within wide ranges. As shown in the figure jointed igneous and metamorphic rocks may have hydraulic conductivity similar with that of sand, while unjointed rocks of the same types may have a conductivity less than for marine clay.

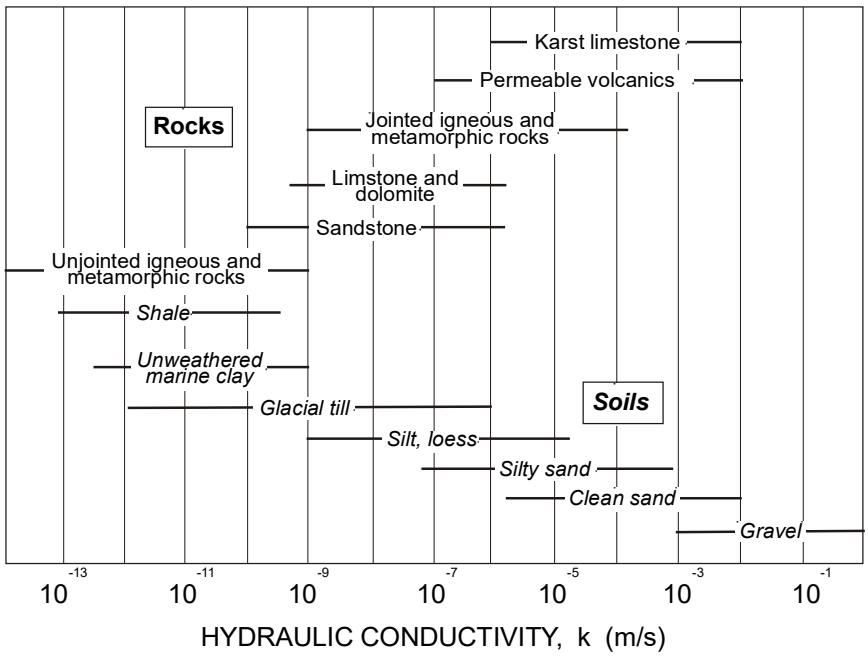

Figure 37: Characteristic permeability of rock mass compared with soils (Freeze & Cherry, 1979)

Due to complex geological prehistory and the feature of most in-situ rocks to have predominant joint orientations (joint sets), it is common to have inhomogeneity and anisotropy also regarding hydraulic conductivity. Due to stress confinement the aperture of joints is normally reduced with depth and the conductivity therefore is also reduced as illustrated by the example in Figure 38. Joint infilling/gouge material may also to a considerable degree reduce the hydraulic conductivity.

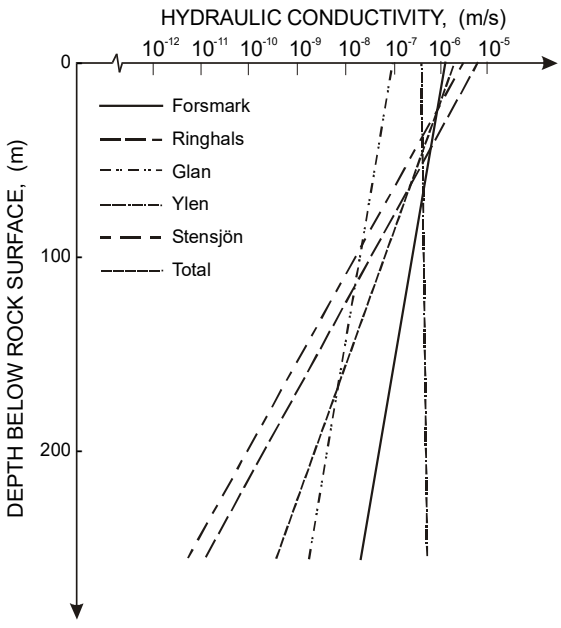

Figure 38. Hydraulic conductivity as function of depth below ground for Swedish test sites in Precambrian rocks (Carlsson & Olsson, 1977)

It should also be noted that small aperture joints deform more relative to its initial size compared to large apertures. This indicates that additional loads will reduce the permeability in rock foundations with small aperture. For larger apertures additional load will have less effect on the permeability (EPRI, 1992).

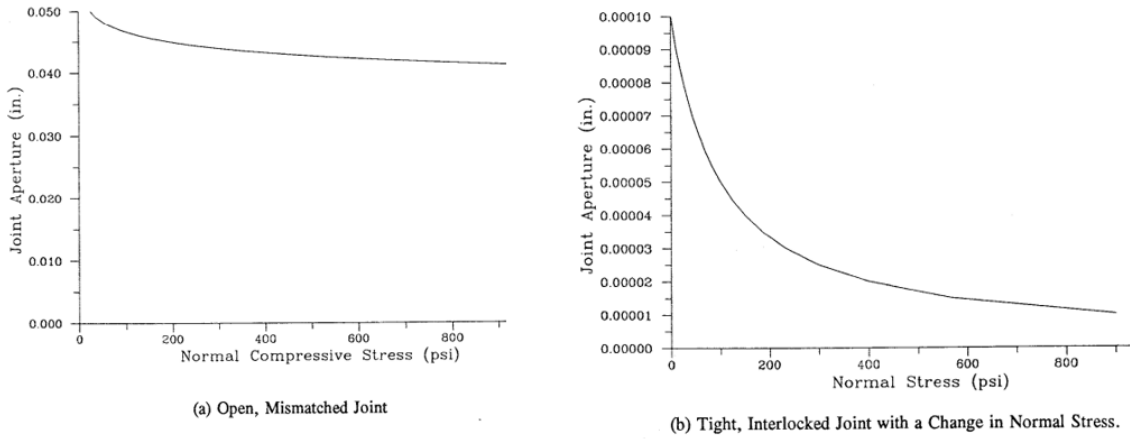

Figure 39. Change in joint opening with change in normal stress for open joints (figure a) and for tight joints (figure b) (EPRI, 1992).

4.2 Key fracture parameters

As discussed above, water flow of and pressure build up in rock mass will in practice be governed by discontinuities. Several factors may be of significance in this connection, but in most cases, these will be the most important:

- Orientation
  Flat-lying fractures may cause direct uplift (hydraulic jacking, with acceleration of water flow) and are therefore the most unfavourable for the base of a concrete dam. For the abutments, steep joints may have similar jacking effect. The orientation of fractures is normally given as strike/dip or dip direction/dip, see Figure 40.

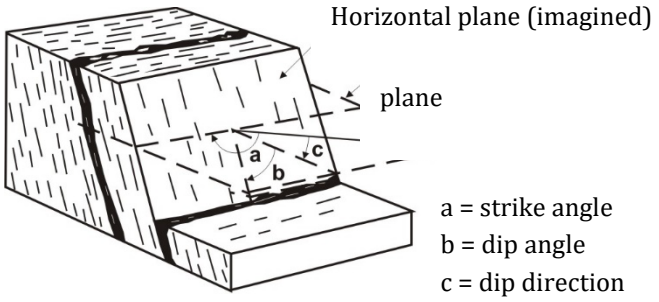

Figure 40: Terms related to joint orientation

- Joint spacing
  Most commonly, this parameter is given as average spacing between fractures of each joint set (e.g. 0.2 m for foliation joints, 0.7 m for north westerly dipping cross joints and 2 m for vertical joints). For drill cores, joint spacing is normally given as RQD-number (relative extent of drill core pieces longer than 10 cm).

- Length/continuity, also referred to as persistence
  This is the key factor regarding scale, although water flow (and failure planes) may also follow a stepwise path represented by smaller fractures. Very distinct fractures may have

persistence > 20 m and in most cases have higher permeability than less persistent fractures, see Figure 41.

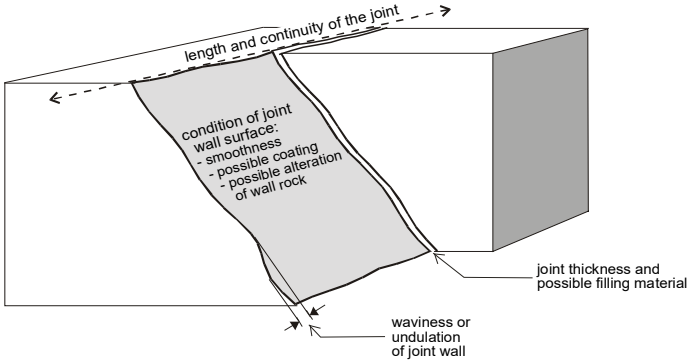

Figure 41: Length/continuity and other factors of main interest for joint mapping (Nilsen & Palmstrøm, 2000)

- Aperture/thickness,
  Aperture directly affects permeability as discussed above in relationship with Louis' equation. Very tight joints may have aperture < 0.1 mm and open joints aperture > 10 mm (Bieniawski, 1984).

- Infilling, coating
  A thin mineral coating on fracture walls normally will not affect permeability much, except from cases with dissolution of calcite which may in some cases have a significant effect. More common is however that thicker infilling of clay minerals (several millimeters and in some cases several centimeters) are washed out, leaving open pipes or channels with water flow while the remaining filled joint is impermeable. As result, water flow often is restricted to minor parts of a fracture, while the rest is dry as illustrated in Figure 42, right.

Figure 42: Left : Concentrated flow-pipe/channel in fracture intersecting deep tunnel (Kvilldal HPP, from NTNU slide-archive), Right: Water leakage from very continuous joint at face of long rock slope; leakage is not evenly distributed, but concentrated to certain sections/flow channels (photo B. Nilsen).

- Roughness
  Large scale roughness (waviness, undulation of the fracture plane) may significantly

increase permeability compared with more planar/smoother fractures. This is mainly due to the tendency of irregular discontinuities more easily to develop flow channels/pipes. Smaller scale roughness (irregularities in joint wall) normally has less effect on permeability

- Rock stress
  High rock stress has the effect of compressing fracture walls and thus reducing permeability. This is confirmed by practical experience as illustrated in Figure 38. Large gravity dams and concrete arch dams may have significantly favourable effect by increasing the normal stress on joints and thus reducing permeability. For smaller dams, like most Norwegian buttress dams this effect will however be negligible. As discussed earlier, surface-parallel fractures caused by high tangential stress and low normal stress at the bottom of a valley (so-called exfoliation joints,) may be particularly open and quite persistent.

For larger scale discontinuities such as weakness zones and faults the key significant factors will be similar as described above for fractures. The potential consequences of encountering a weakness zone may however be considerably more severe than those of crossing smaller scale fractures. As consequence of unfortunate incidents on several projects it has therefore been recognized that a dam site with risk of encountering a fault or weakness zone should never be selected. The failure of the foundation of Malpasset dam in 1959 (see Figure 43) is a tragic example of catastrophic consequences of underestimating potential consequences of faults. It also illustrates that intersecting discontinuities may cause collapse (in this case wedge failure) of the dam abutment, with water pressure caused by prolonged heavy rainfall representing the triggering factor. The dam failed during first filling, with water level rising above Normal Water Level after a heavy rainfall. See also case description in chapter 5.3.1.

Figure 43: Failure of left abutment of Malpasset dam due to unfavourably oriented fault dipping 45-50° upstream and foliation fractures dipping 40°W (plot in stereographic projection, upper hemisphere). Left photo from (Duffault, 2012), sketch to the right from (Goodman, 1993).

4.3 Engineering geological mapping

The engineering geological conditions and accessibility of dam sites may vary considerably from case to case, and there is therefore no standard procedure for mapping. Discontinuities such as fractures

and faults (which should as far as possible be avoided) are however always the most important factors for evaluating risk of water leakage and foundation instability and therefore should be of main focus in mapping. Some discontinuities, as discussed in Chapter 2.2 are more important regarding risk of water leakage and stability than others, and at the start of mapping it is therefore always wise to spend some time on evaluating which discontinuities are the most important and to have greatest focus on these in the further mapping.

In many cases the bottom of the river valley will be covered by soil as shown in the example in Figure 44 and in such cases, interpretations need to be done based on available data from previous geological mapping of the abutments and surrounding areas.

Figure 44: Example illustrating fracturing with varying orientation and persistence at dam abutment.

Mapping of rock types and their mechanical characteristics are included at an early stage of any engineering geological investigation. In Norway most rocks are strong, and locations without weathering normally not difficult to find. For dam sites the quality of the intact rock is therefore seldom a problem, except for cases when sliding along discontinuities (as in the case in Figure 44) or at the contact between concrete and bedrock represents a potential problem. In such cases data on rock strength is needed for estimating the shear strength of the potential sliding plane. Also, data on the mechanical properties of the intact rock are needed as input in many models for numerical analysis of foundation stability.

Some rock types, in Norway mainly restricted to limestone and marble, are soluble and may contain karstic tunnels and caves with a high potential for leakage and should whenever possible be avoided for location of dams.

The orientation of joints (strike and dip or dip direction and dip) is measured using a geological compass, and the data is typically presented either as a joint rosette or, more commonly, in a

stereographic projection. An example of a simple joint rosette is shown in Figure 45. The number of joints within each selected strike interval is represented by the length of the blade in the joint rosette (with 6 as maximum number in Figure 45, corresponding to the periphery circle in the rosette). The advantage of using the joint rosette is that for users who are not familiar with presentation of joint data it is easier to understand intuitively than the stereographic projection.

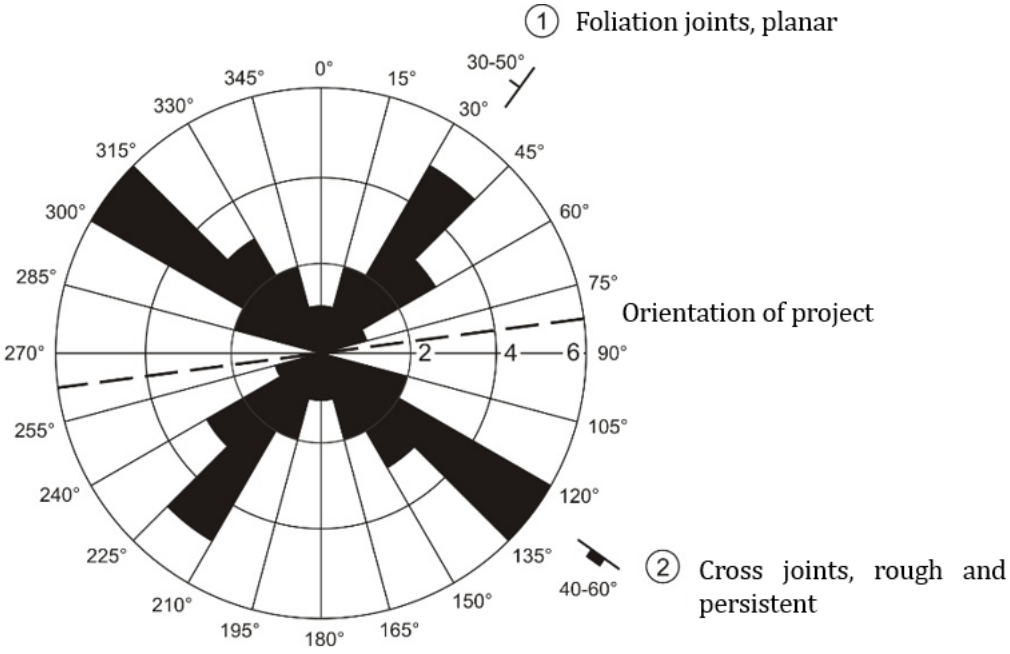

Figure 45: Joint orientation presented in a simple joint sorsette.

Joint data presented in stereographic projection is more difficult to understand intuitively but provides more detailed information than the joint rosette. The method is based on the spheric projection principle, which provides a three-dimensional impression of orientation. As illustrated in Figure 46 it is imagined that the respective joint plane is located with its dip and dip direction through the center of the sphere. The intersection between the plane and the sphere is referred to as the great circle. Next step is that one half of the sphere is removed. In Engineering geological practice today, only the lower hemisphere is used (in contrast to what is done for Malpasset in Figure 43). The pole of the plane is defined as the intersection point between sphere and the normal to the joint plane from the center of the sphere, see Figure 46.

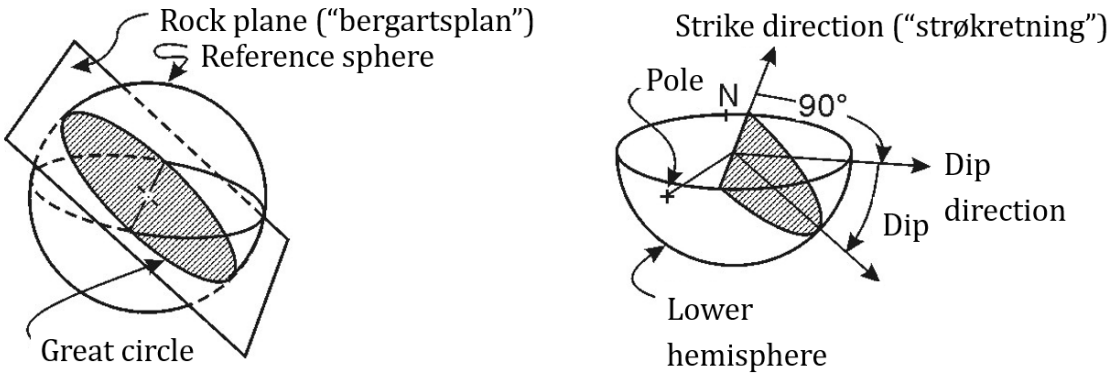

Figure 46: Definition of great circle and pole in stereographic projection

An example of presentation of joint data in stereographic projection is shown in Figure 47. Each point in the left Figure represents a pole, and thus the strike and dip of a certain joint. The direction from a pole towards the center of the stereonet represents the dip direction (= strike direction ± 90°), while the graduation along the center line gives the dip angle (dip angle = 90° for poles at the periphery and 0° for poles at the center), i.e. steeper joint the further away from the center. Right part of Figure 47 is a contoured version of the pole plot, showing the percentual distribution of poles/joints within a circle with area 1/100 of the periphery circle of the stereonet.

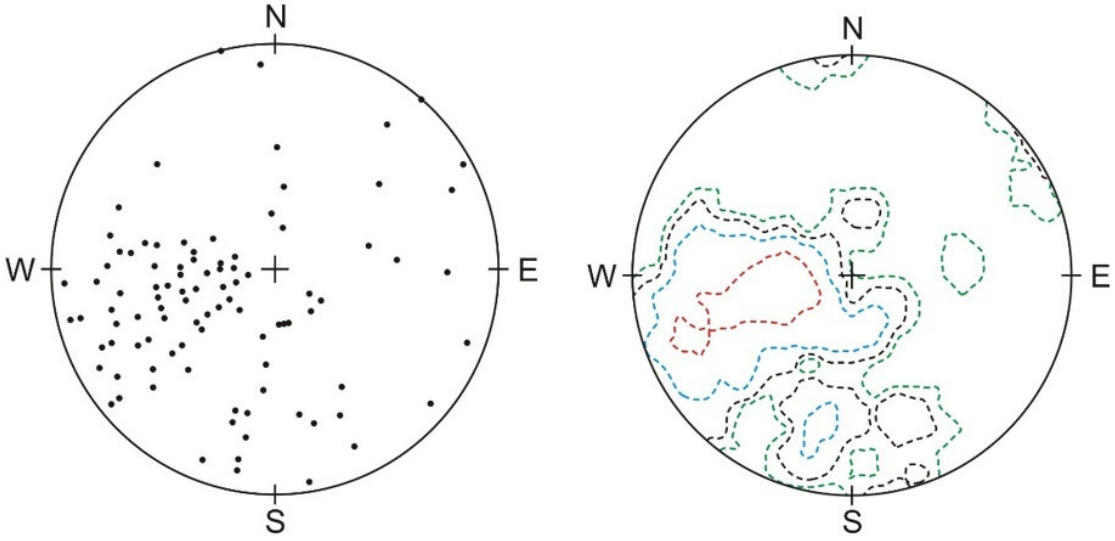

Figure 47: Joint poles (to the left) plotted in polar projection (Schmidt net, lower hemisphere), and contoured plot (to the right) with contour intervals representing 1, 2, 4 and 8 (red) pole density

It is important to be aware that the methods for presentation of joint data described above will provide realistic results only when the field measurements have been done in such a way that they provide a realistic picture of the in-situ conditions. High quality performance of the in-situ mapping is therefore crucial.

The degree or extent of fracturing is most commonly given as average spacing between fractures withing one certain joint set. Joint set means set of fractures with the same strike and dip. For example in the joint rosette in Figure 45 there are two distinct joint sets; one set of foliation joints and one set of cross joints. In addition, there are a few joints with other orientations. As alternative to "average spacing" the extent of fracturing may also be given as a range (i.e. 0.5 – 1 m) for each joint set, volumetric joint count (joints per m^3), etc.

The roughness of fractures most commonly is given as Joint Roughness Coefficient (JRC) as illustrated in Figure 48. JRC may be estimated empirically by comparing with standard profiles as shown to the left on the figure or based on using a ruler and measuring the maximum depth of irregularities as shown to the right. JRC and JCS (described in Chapter 6.5) are key parameters for estimating friction angle of rock joints based on Barton &Bandis (1990) empirical criterion, which is briefly described at the end of Chapter 6.5.

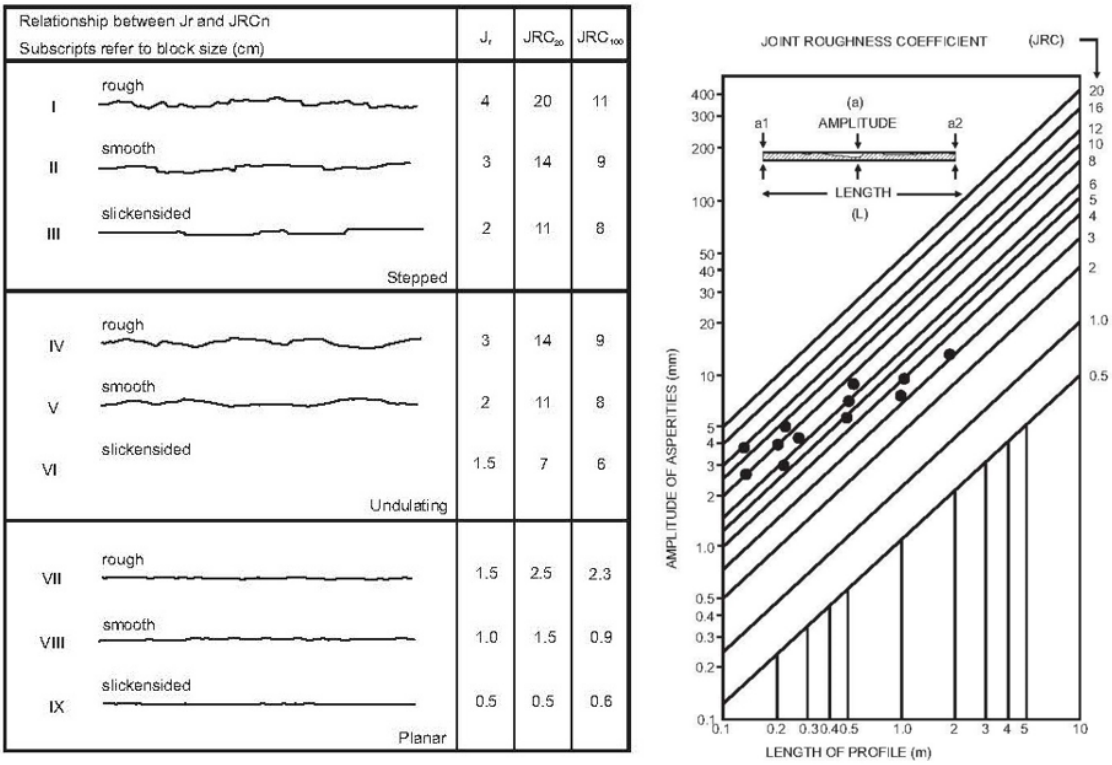

Figure 48: Estimation of JRC based on a) measuring roughness amplitude (left, modified from (Bandis, S. C.; Lumsden, A. C.; Barton, N., 1981) and b) empirical diagram for joint length 20 and 100 cm respectively (right, modified from (Barton, 1988).

Mineral coating on the joint surface by slick mineral such as mica, chlorite, talc and clay minerals may strongly reduce the friction. Thicker infilling, most commonly consisting of chlorite, clay minerals and calcite in addition to reducing friction will in many cases have a sealing effect and thus reduce the permeability.

All factors described above have effect on permeability and friction of fractures and should be included in engineering geological investigation. Their relative significance will however vary from project to project, and how much emphasis should be placed on each of them has be carefully evaluated for each individual case.

4.4 Rock mass classification

For characterization of the engineering geological conditions of a project site, use of classification systems is common procedure. The most commonly used classification system in Norway and many other countries is the well-known Q-system (NGI, 2015), which is however primarily aimed at rock mass classification for estimating rock support requirement for underground excavations (tunnels, rock caverns etc.), and not much applicable for dam foundations.

An alternative classification system which is also commonly used is RMR, the Rock Mass Rating (Bieniawski, Z.,R., 1989) which is based on many of the same input-parameters as the Q-system plus some additional, and provides rating not only for tunnels, but also for slopes and foundations, see Table 4-2,

Table 4-2: Diagram for estimation of basic parameters included in RMR, (Bieniawski, Z.,R., 1989)

PARAMETER			Range of values // **RATINGS**						
1	Strength of intact rock material	Point-load strength index	> 10 MPa	4 - 10 MPa	2 - 4 MPa	1 - 2 MPa	For this low range uniaxial compr. strength is preferred		
		Uniaxial compressive strength	> 250 MPa	100 - 250 MPa	50 - 100 MPa	25 - 50 MPa	5 - 25 MPa	1 - 5 MPa	< 1 MPa
		RATING	**15**	**12**	**7**	**4**	**2**	**1**	**0**
2	Drill core quality RQD		90 - 100%	75 – 90%	50 - 75%	25 - 50%	< 25%		
		RATING	**20**	**17**	**13**	**8**	**5**		
3	Spacing of discontinuities		> 2 m	0.6 - 2 m	200 - 600 mm	60 - 200 mm	< 60 mm		
		RATING	**20**	**15**	**10**	**8**	**5**		
4	Condition of discontinuities	Length, persistence	< 1 m	1 - 3 m	3 - 10 m	10 - 20 m	> 20 m		
		Rating	**6**	**4**	**2**	**1**	**0**		
		Separation	none	< 0.1 mm	0.1 - 1 mm	1 - 5 mm	> 5 mm		
		Rating	**6**	**5**	**4**	**1**	**0**		
		Roughness	very rough	rough	slightly rough	smooth	slickensided		
		Rating	**6**	**5**	**3**	**1**	**0**		
		Infilling (gouge)	none	Hard filling		Soft filling			
			-	< 5 mm	> 5 mm	< 5 mm	> 5 mm		
		Rating	**6**	**4**	**2**	**2**	**0**		
		Weathering	unweathered	slightly w.	moderately w.	highly w.	decomposed		
		Rating	**6**	**5**	**3**	**1**	**0**		
5	Ground water	Inflow per 10 m tunnel length	none	< 10 litres/min	10 - 25 litres/min	25 - 125 litres/min	> 125 litres /min		
		$p_w / \sigma 1$	0	0 - 0.1	0.1 - 0.2	0.2 - 0.5	> 0.5		
		General conditions	completely dry	damp	wet	dripping	flowing		
		RATING	**15**	**10**	**7**	**4**	**0**		
p_w = joint water pressure; $\sigma 1$ = major principal stress									

B. Rating adjustment for discontinuity orientations

		Very favourable	Favourable	Fair	Unfavourable	Very unfavourable
RATINGS	Tunnels	**0**	**-2**	**-5**	**-10**	**-12**
	Foundations	**0**	**-2**	**-7**	**-15**	**-25**
	Slopes	**0**	**-5**	**-25**	**-50**	**-60**

C. Rock mass classes determined from total ratings

Rating	100 – 81	80 – 61	60 - 41	40 - 21	< 20
Class No.	I	II	III	IV	V
Description	VERY GOOD	GOOD	FAIR	POOR	VERY POOR

D. Meaning of rock mass classes

Class No.	I	II	III	IV	V
Average stand-up time	10 years for 15 m span	6 months for 8 m span	1 week for 5 m span	10 hours for 2.5 m span	30 minutes for 1 m span
Cohesion of the rock mass	> 400 kPa	300 – 400 kPa	200 - 300 kPa	100 - 200 kPa	< 100 kPa
Friction angle of the rock mass	< 45º	35 – 45º	25 - 35º	15 - 25º	< 15º

The RMR-system is considered more suitable for dam foundations than the Q-system and therefore recommended to be used for classification of dam site rock mass quality. More explanation and comments on the various parameters and the use of RMR are given in Chapter 6 "Case studies of selected Norwegian dams", which includes description of classification based on the RMR-system for 5 Norwegian dam sites.

As part of an engineering geological dam site investigation, also GSI (Geological Strength Index) should be estimated since this parameter is a common input for calculating rock mass strength in numerical models. Estimation of GSI should be done on-site based on diagram as shown in Figure 48.

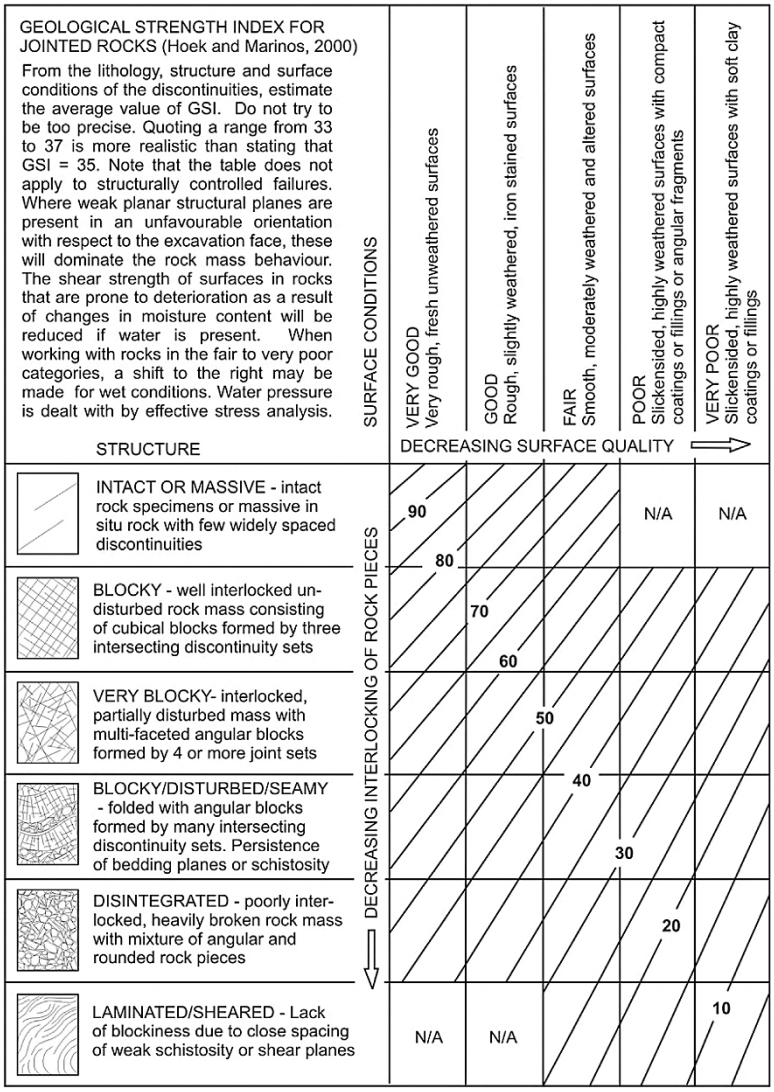

Figure 49: Diagram for estimation of GSI (Hoek & Brown, 2019)

The RMR system has been used for estimation of rock mass quality for several dam projects around the world. The main differences and advantages regarding dam foundation evaluation compared with the Q-system is that RMR includes additional relevant parameters, such as rock strength, length/persistence and aperture of discontinuities, and adjustment factor for discontinuity orientation. Lack of including rock stress may be counted in disfavour of RMR, but the main counterargument against RMR is the imperfect way that water pressure is included. A new classification system, DMR (Dam Mass rating) therefore was proposed by (Romana, 2003) and (Romana, 2011). The DMR is derived from RMR, and in addition to "basic dry" RMR includes new adjustment factor for dam stability and a correction factor for direction of dam axis and joints.

Since DMR was proposed more than 20 years ago, few examples of practical use of the method have been found in literature. The Beni Haroun dam in Algeria (120 m high RCC gravity dam, described by Kebab et al. 2020), and the Khorram-Roud dam site in Iran (Shafiel, et al., 2007) are among the few relevant cases that have been found by literature search.

Particularly aimed at hydropower and dam foundation evaluation, (Konow & Engseth, 2017) in their report to Energi Norge included a chapter 5 “Evaluation of the bedrock”, where five classes (0 to 4) were described for definition/classification of the rock mass conditions. The proposed system has obvious similarities with the RMR-system, but deviates from it on certain issues, e.g. no factor for groundwater conditions and by the way that classes are defined.

Due to the obvious advantages of basing classification on an internationally recognized and commonly used system it was found logical to use the RMR-system in this DSHP-project. The main weakness of the RMR-system, the imperfects of the ground water factor, may be compensated by additional evaluation of this important issue.

4.5 Mechanical properties of rock and rock mass

Mechanical properties, including strength of intact rock and in-situ rock mass, are not among the parameters which are first thought of when it comes to permeability and uplift forces. In cases where sliding may contribute to instability and possible abutment collapse, like at the Malpasset dam (Figure 43), rock strength may however be a key factor, and also in cases where failure intersects bridges of intact rock.

Most reliable determination of rock strength and elasticity parameters (E and ν) is done by testing drill cores in laboratory, but for a quick and fairly accurate estimation in-situ rock strength type L Schmidt hammer and a correlation diagram as shown in Figure 49 may be used.

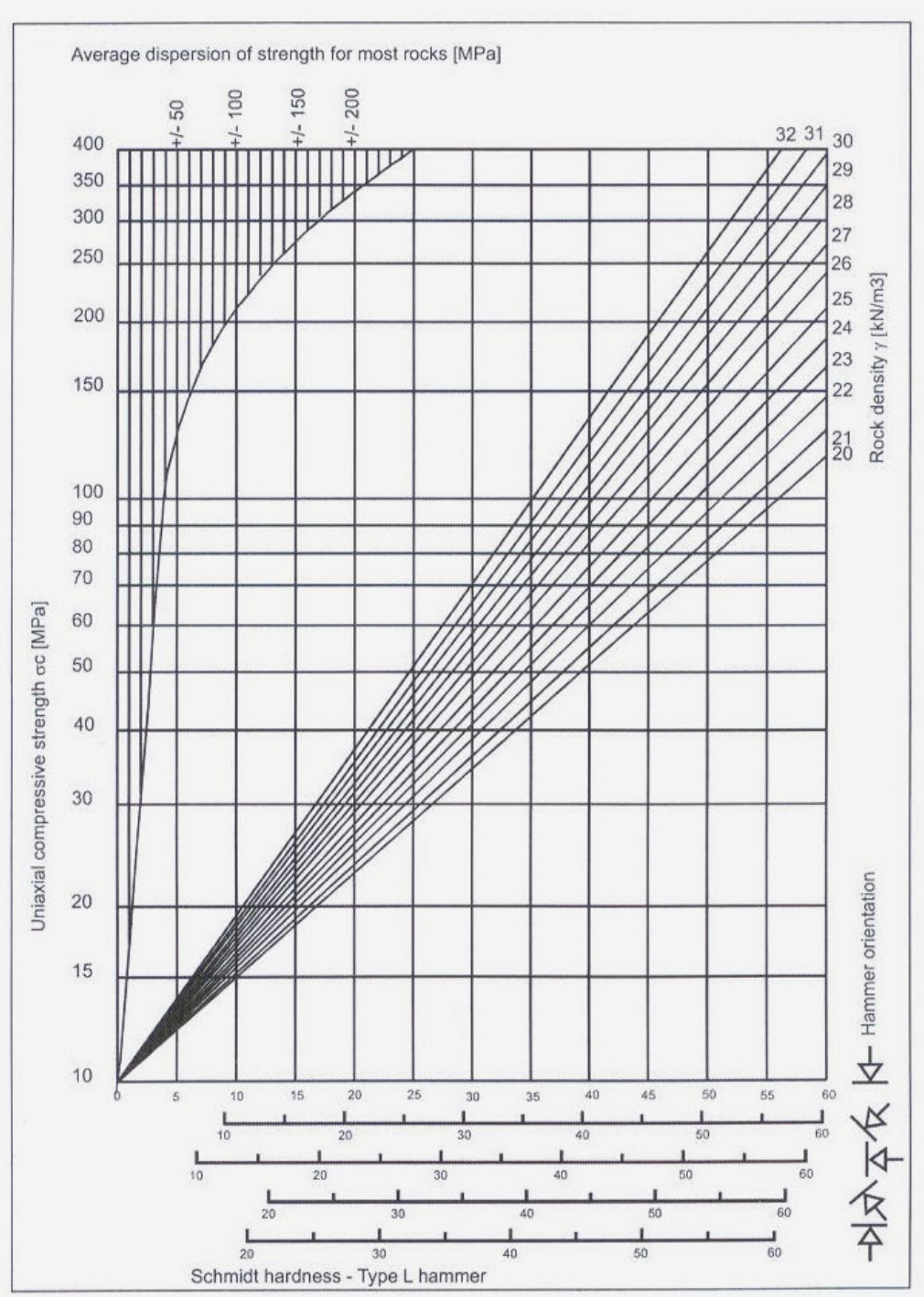

Figure 50: Diagram for conversion of Schmidt hardness to UCS (Hoek & Bray, 1981)

It is important to be aware that the strength of any rock type may vary within wide ranges, as illustrated by Figure 51. When exact determination of rock strength is needed, it is therefore required to test the rock from the respective project site, and not rely on data found in literature.

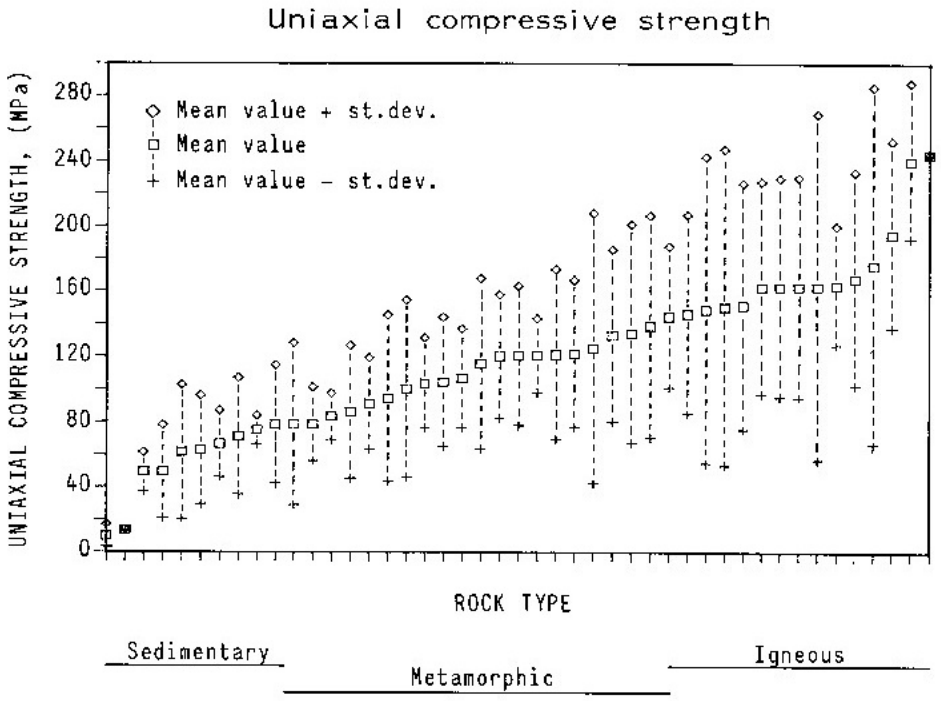

Figure 51: Variation of UCS-results for Scandinavian rock types for tested at NTNU/SINTEF. Modified from (Hanssen, 1988)

Determination of peak shear strength of fractures (τ) is most commonly based on the Barton-Bandis empirical equation (Barton & Bandis, 1990):

$\tau = \sigma_n * \tan [JRC * \log (JCS/ \sigma_n) + \phi_r]$

where: σ_n = effective normal stress

JRC = Joint roughness coefficient (see Figure 48)

JCS = Joint wall compressive strength (based on Schmidt hammer and diagram in Figure 50)

ϕ_r = residual friction angle (found in laboratory by using tilt table)

For more detailed descriptions of the procedures for determining mechanical properties of rock and rock mass, including fractures, reference is given to (Nilsen & Palmstrøm, 2000), (Grøneng & Nilsen, 2009) and relevant ISRM-recommendations such as (ISRM, 1979) and (ISRM, 2009).

4.6 In-situ monitoring

Monitoring of in-situ hydraulic conductivity of the rock mass is most commonly done by Lugeon-testing, where a section off a borehole (normally around 3 m long) is isolated by installing packers as illustrated in Figure 52, and water under high pressure is pumped into that section. The Lugeon value (L) is defined as water loss in l/min per meter borehole at an overpressure of 10 bar (1 MPa). The test may also be done for a section between the borehole end and one packer located in the borehole, during or after boring of the hole. It is therefore important also to describe the monitoring method when results from Lugeon testing are presented.

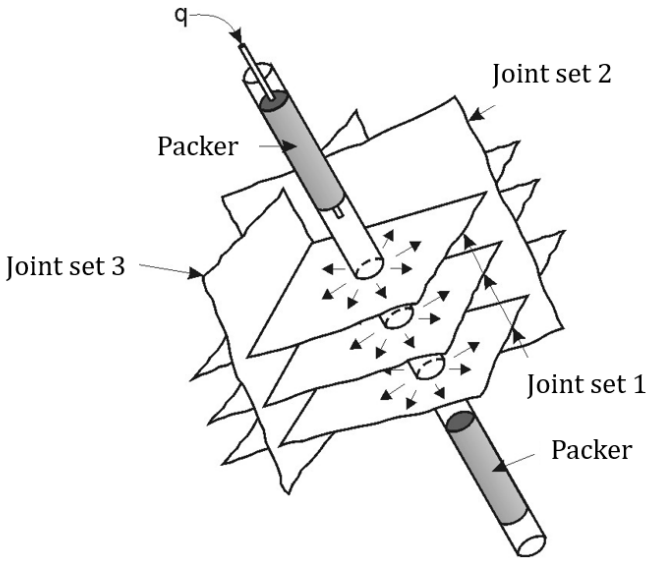

Figure 52: Principle sketch of Lugeon testing with 2 packers in the borehole

A commonly used classification of Lugeon-values and the character of fractures corresponding to respective L-intervals is shown in Table 4-5. A value of 1 Lugeon for homogeneous, isotropic conditions corresponds to hydraulic conductivity $k = 1.3 \times 10^{-7}$ *m/s*. When evaluating results, it is however important to be aware of the uncertainty represented by potential piping effects as described in chapter 4.2; very high water loss will be measured if the borehole intersects a pipe while a borehole intersecting the same fracture a small distance away from the first will have no water loss if it does not intersect the pipe.

Lugeon-value	Classification	Fracture character
<1	Very low	Very tight
1-5	Low	Tight
5-15	Moderate	Some partly open
15-50	Medium	Some open
50-100	High	Many open
>100	Very high	Dense system of open

Table 4-3: Commonly used classification and evaluation of monitored Lugeon-values (Quinones-Roso, 2010)

For monitoring groundwater pressure, piezometers installed in boreholes are used. There are several types of extensometers which will not be discussed in detail here. What is however particularly important to keep in mind regarding geology is that the same uncertainty exists as for

monitoring of hydraulic conductivity; joint wall roughness and piping may cause water pressure to be very unevenly distributed in the fracture. To choose the maximum value of monitored pressure as representative for an entire fracture plane may therefore cause a considerable overestimation of total, resultant pressure. In most cases, the average of monitored values probably will represent a more realistic estimate of resultant pressure than maximum value. A fracture plane may therefore cause a considerable overestimation of total, resultant pressure. In most cases, the average of monitored values probably will represent a more realistic estimate of resultant pressure than maximum value.

5 LITERATURE STUDY

Originally, this report intended to include a comprehensive literature review. During the initial review it was however found that NGI was already working on a R&D project related to this on behalf of NVE, and in April 2024 the final report from this project was published (NVE/NGI, 2024).

It was found that the list of literature in the NGI-report included most of the relevant references which had been identified during the review in this project and therefore the literature study in this report was downscaled.

A brief review of literature references is however given in the following. A brief description of the most relevant literature is also given in this chapter, where pore pressure and buttress dams has been given extra attention.

A complete list of relevant references from the literature search of this project, with links for downloading is included as Chapter 8 of his report.

5.1 Literature search based on Databases

5.1.1 NTNU databases

Search on the NTNU database for theses and peer-reviewed journal papers; NTNU open https://ntnuopen.ntnu.no/ntnu-xmlui/ for «concrete (alt. "buttress" and "slab") dam uplift pressure» gives several references. The great majority is, however, related to gravity dams and friction/risk of sliding. Some of the references are still of interest for this project, such as:

- Rognes, Marie (Master thesis, 2014): Poretrykk under betongdammer fundamentert på fjell. https://ntnuopen.ntnu.no/ntnu-xmlui/handle/11250/242505. Based on literature review of 4 gravitation dams, 1 in Norway, 2 in Germany and 1 in Austria. Site visit to the 2 in Germany.
- Bista, Dipen; Ulfberg, Adrian; Lia, Leif; Gonzalez-Libreros, Jaime; Johansson, Fredrik; Sas, Gabriel (2024): Numerical parametric study on the influence of location and inclination of large-scale asperities on the shear strength of concrete-rock interfaces of small buttress dams. Journal of Rock Mechanics and Geotechnical Engineering. https://ntnuopen.ntnu.no/ntnu-xmlui/handle/11250/3141504
- Løkke, Arnkjell (Doctoral thesis, 2018): Direct finite element method for nonlinear earthquake analysis of concrete dams including dam–water–foundation rock interaction. https://ntnuopen.ntnu.no/ntnu-xmlui/handle/11250/2564067
- Stangvik, Renate Musum (Master thesis, 2017): Shear strength of the rock-concrete interface at Kalhovd dam. https://ntnuopen.ntnu.no/ntnu-xmlui/handle/11250/2457150
- Stølen, Peter (Master thesis, 2012): Målsetdammen - Sikkerhet mot glidning i platedam. https://ntnuopen.ntnu.no/ntnu-xmlui/handle/11250/242324

Only the latter of the references mentioned above is focusing on buttress dam, while the first on the list above is to the highest degree discussing the importance of pore water pressure.

Search on the database Compendex/Engineering village, which is among the leading within engineering disciplines and available at NTNU, gives a high number of references of similar type as those for NTNU- open, and also some relevant for concrete slab- and buttress dams, such as:

- ICOLD European Club (2004): Working Group on Uplift Pressures under Concrete Dams. Final report, 30p.

Although 20 years old (no newer version has been found) this report is very interesting and highly relevant. Covers many of the issues of particular interest for this project. Regulations and recommendations from many countries are well described, such as Switzerland, USA (EPRI), UK and Italy (also for buttress dams). Swedish rules are mentioned, but not described in detail.

- Ruggeri G. (2004) ICOLD European Club; Sliding safety of existing gravity dams – Final report. European Working Group on the safety of existing gravity dams, 111p. https://britishdams.org/assets/documents/conferences/2004/reports/sliding.pdf

Contains descriptions of rules and regulations in various countries, mainly regarding safety against sliding, but also regarding uplift pressures.

- Avella (1993): An analysis of a worldwide status for monitoring and analysis of dam deformation. M.Eng. report, Department of Surveying Engineering, Technical Report No. 167, University of New Brunswick, Canada, 272 pp.

Interesting review of dam monitoring, including Worldwide Status (although a bit old).

- Enzell (2023): Toward Realistic Failure evaluations for Concrete Buttress Dams. Licentiate thesis, KTH Stockholm 2023. 55 pp.

Mainly on failure of concrete of the dam itself, and not of the rock foundation. Including 3D numerical analysis

- Zee et al (2011): Pore pressure in concrete dams. J. Geotech. Geoenvironmental Eng.2011, 137(12): 1254-1264.

Interesting references to international experience, but not focusing on buttress/slab concrete dams.

- Spross et al (2016): On the pore pressure measurements in safety reassessments of concrete dams founded on rock. Georisk: Assessment and Management of Risk for Engineered Systems and Geohazards, Volume 8, 2014 - Issue 2

Mainly focusing on importance of drainage system and the connection between malfunctioning of drainage system and probability of dam failure, 30p.

- Nordström, E., Malm, R., Blomdahl, J., Tornberg, R., Nilsson, C-O. (2015) Optimization of dam monitoring for long concrete buttress dam. Paper presented at ICOLD Symposium, 13-20 June, Stavanger, Norway., 17 pp.

Also in the Compendex/Engineering village search it was found that very few of the resulting references were focusing significantly on water pressure at the foundation of concrete slab/buttress dams.

5.1.2 ISRM-database

Search on www.OnePetro.org , the database of ISRM (the International Society of Rock Mechanics) gives several additional hits for the same terms as used in the NTNU-search described above.

- Johansson (2020): Managing uncertainties in sliding stability re-assessment of concrete dams founded on rock. Franklin Lecture, Eurock 2020.
- Scott et al (2001) Design and analysis of foundation modifications for a buttress dam. US Symp. On Rock Mechanics, 2001.
- Celestino et al (2015) Probabilistic assessment of uplift pressure under concrete dams. ISRM regional Symposium.
- Da Silva (2015) Clogging of drains and its influence on the stability of concrete dams. ARMA 2015
- Duffault (2011) What modern rock mechanics owe to Malpasset dam failure. 12th ISRM Congress, Beijing.
- Goodman, R (1993): Engineering geology - Rock in Engineering Construction, p.170-172 Vaiont slide and p 327-330 Malpasset Dam failure.

As for the other database searches described above, it was found that very few of the resulting references were focusing significantly on water pressure at the foundation of concrete slab/buttress dams.

5.2 Buttress dams - Cases

Buttress dams are not a dominant dam type, as described in chapter 1.3. The general design rules are therefor often not very specific in the different national codes, regulations or design practice.

Design pore pressure for some specific dams is therefore given in this chapter.

5.2.1 UK, Hydraulic structures, 4th edition (P. Novak, 2007)

The textbook "Hydraulic structures, 4th edition" (P. Novak, 2007), is a much used and a well-recognised textbook for postgraduate students.

In the textbook, The Shira buttress dam is used as a design example of buttress dams. The dam is a round headed buttress dam with a length of 725 m and height of 45 m high. The dam is located in the Scottish Highland and was commissioned in 1954.

The textbook gives the following description of solid head buttress dams:

The structural form of the buttress dam (see figure below) has two important consequences with respect to primary loads. First, uplift pressures are effectively confined to the buttress head, resulting in the modified uplift distribution shown in the figure below. Pressure relief drains are therefore only necessary in exceptional cases. As a further consequence of the form the vertical component of the water load on the sloping upstream face is very much enhanced relative to any gravity profile. Stability against overturning is therefore a less meaningful design criterion.

In structural terms the massive buttress dam is constructed from a series of independent 'units', each composed of one buttress head and a supporting buttress, or web. Each unit has a length along the axis of the dam of about 12–15m. Structural analysis is therefore conducted with respect to the buttress unit as a whole. The sliding stability of one complete unit is investigated in terms of FSS, sliding factor or, more usually, FSF , shear friction factor, in accordance with the principles of these approaches as outlined in Section 3.2.3, (P. Novak, 2007). The design minimum values for FSS and FSF are normally comparable with those required of a gravity profile.

Stress analysis of a buttress 'unit' is complex and difficult. Modern practice is to employ finite element analyses to assist in determining the optimum shape for the buttress head to avoid undesirable stress concentrations at its junction with the web. A trial profile is established on the basis of previous experience, the selection of a round head or a diamond head being largely at the discretion of the designer. The profile details are then modified and refined as suggested by initial stress analyses.

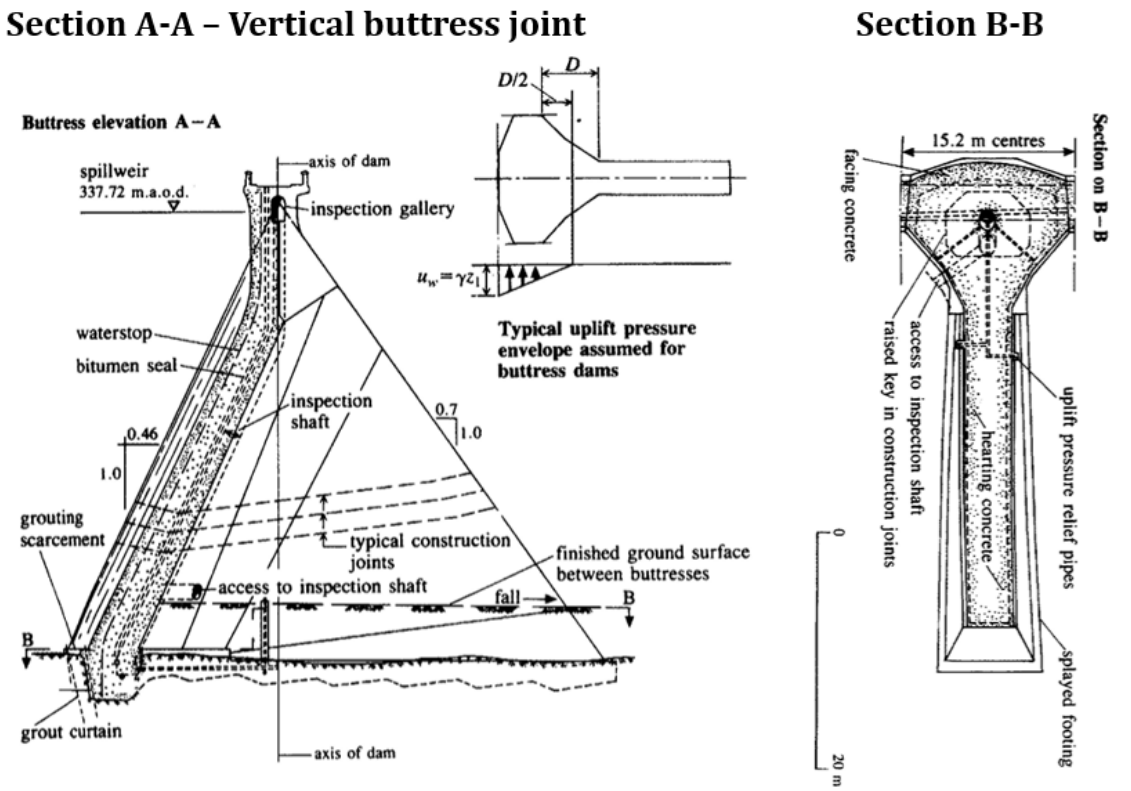

Figure 53. Shira buttress dam, UK. The proepressure dirstribution is shown on the sketch in the middle top of the figure.

5.2.2 Brazil; Itaipú Buttress dam

This case is based on (IABSE, 1983), Edition C-25. This edition was dedicated the construction of the Itapú hydroelectric power plant, with 30 pages giving details about the design and construction. IABSE structures is a well-recognised technical magazine and is published in collaboration with the magazines Constructions AIPC and IVBH Bauwerke.

The Itaipú dam, is the world's highest buttress dam with a height of 196 m and is of the type Solid Head Buttress Dam, where each buttress head is about 24 m wide along the dam axis.

The dam was built between 1975 and 1982, on the border between Paraguay and Brazil. The total dam length is almost 8 km and the reservoir stretches about 160 km northward form the dam. Itaipú HPP is one of the world's largest hydroelectric projects. It has 20 generators of 700 MW each (total 14,000 MW) and in 2016 a total of 101 TWh was produced.

The uplift pressure distribution under the dam is shown in the below figure. The following pore pressure distribution apply for ULS and ALS:

- Upstream of the dam and downstream of the powerhouse, uplift pressure equals the upstream and downstream head of water (Hu and Hd) respectively down to the rock discontinuity (El. 20).
- Between the upstream and downstream longitudinal underground drainage tunnels (El. 20), the uplift pressure Ho is constant and equals the distance between ground surface and the rock discontinuity elevations (El. 35 to 40 and El. 20).

- Between the grout curtains and the drainage tunnel upstream, there is a linear uplift pressure Variation (from Hu to Ho).
- At the downstream drainage curtain the uplift equals H0 + 0.33. (Hd - Ho) and from there the uplift pressure has a linear variation increasing to Hd at the downstream grout curtain and decreasing to Ho at the downstream drainage tunnels.
- Both Underground tunnels will normally be pumped and subsequently H0 o approximately. For safety reasons however and because of possible damage to the pumps, the above indicated uplift value Ho has been maintained.

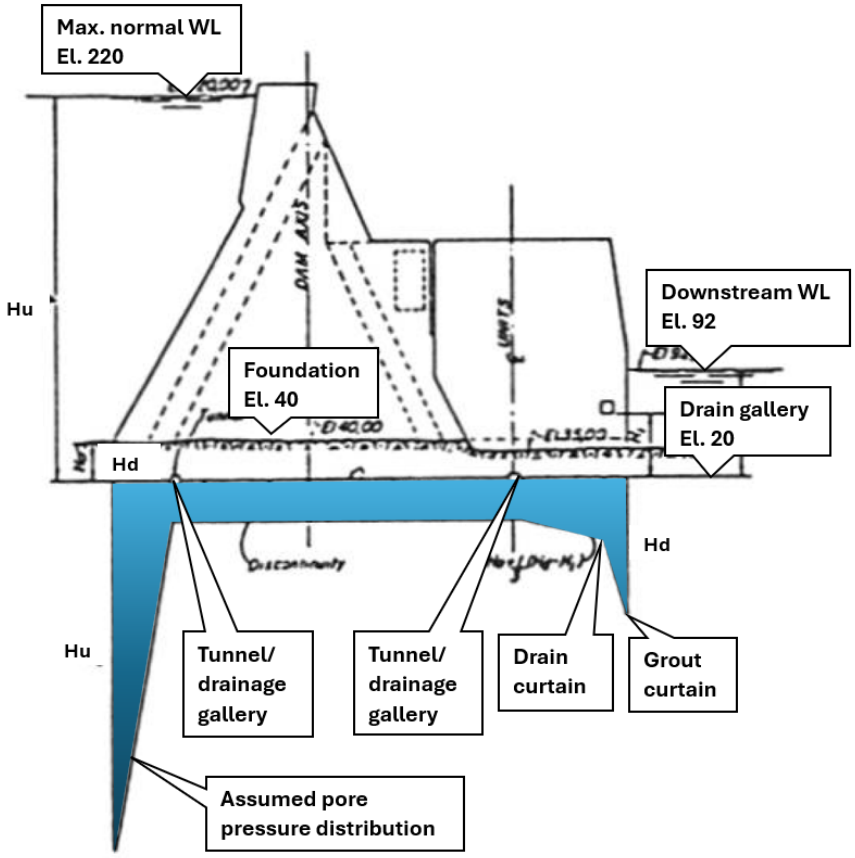

Figure 54. Dam Itaipú: assumed pore pressure distribution for design (IABSE, 1983)

5.2.3 Sweden; Storfinnforsen buttress dam

Storfinnforsen is buttress dam located in the northern part of Sweden at Faxälven River. The dam is a Solid Head Buttress dam has the following layout:

- Hight; 41 m high at its highest point.
- Length: Buttress dam is 800 m long, while the total dam length is more than 1200 m
- Buttresses (se figure below):
    - Buttress head is 8 m wide and 1.2 m thick at the top and up to 2.6 m thick at the base. The buttress head is constructed as a slab resting on one buttress support.
    - Buttress supports are 2 m wide.

The dam owner has installed 180 piezometer sensors in the dam with the intention of always monitoring the dam's behaviour and to also, create warnings and alarm system if the structural integrity and safety of the dam is below the required level.

This summary refers to a Numerical simulation conducted as a degree project at KTH (M. Abdi (KTH), 2022). The analyses were limited to monolith M42 which is the tallest monolith at Storfinnforsen buttress dam.

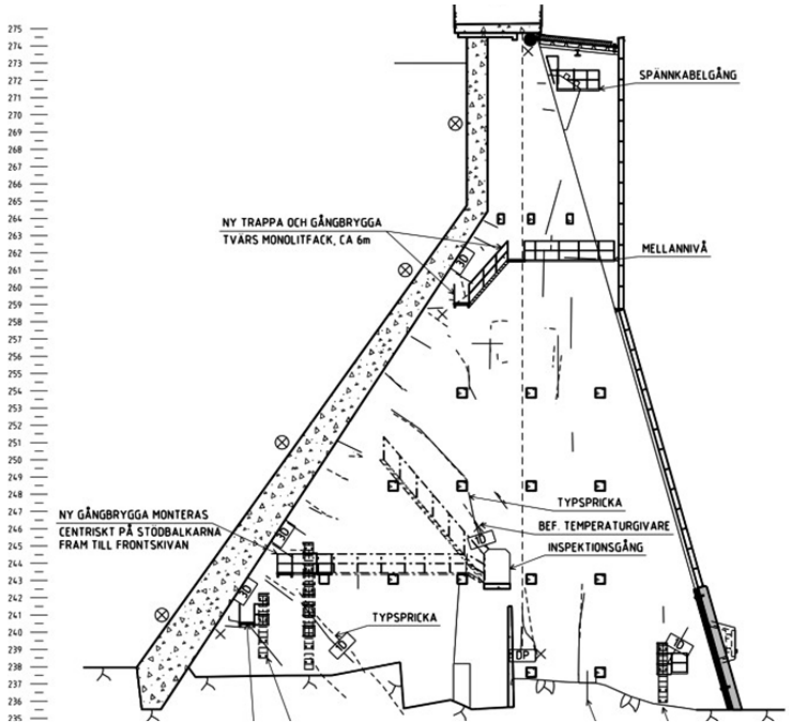

Figure 55. Section of the buttress M42. Level top dam; El. 272 masl. and foundation between el. 238 masl. (upstream) and el. 234 masl. (downstream).

To identify the most realistic pore pressure, several model parameters were assessed and tuned with respect to the measured values. The table below describes the different cases for pore pressure distribution shown in the following figure. Case 4d alt.3G was selected as input for the numerical simulation that is presented.

Case (line colour)	Assumptions for pore pressure distribution
4d alt.3G (purple)	**Combines both realistic field conditions and a satisfactory hydraulic head close to the measured values.**
4a (yellow)	Resembles the lower limit condition for the current state of the monolith with fully air-filled drains
4b (orange)	Resembles the upper limit condition for the current state of the monolith with fully water-filled drains
1 (full line, black)	Gravity dam: Drainage and the grout curtain are not included, according to RIDAS guidelines, chapter 9.1.3 (Energi Företagen, RIDAS, 2020 Oktober)
2 (dotted, black)	Gravity dam: Effect of just drainage is included, according to RIDAS guidelines, chapter 9.1.3 (Energi Företagen, RIDAS, 2020 Oktober)
3 (dotted, black)	Gravity dam: Effect of both drainage and grout curtain is included, according to RIDAS guidelines, chapter 9.1.3 (Energi Företagen, RIDAS, 2020 Oktober)

Table 5-1: Assumptions for pore pressure distributions

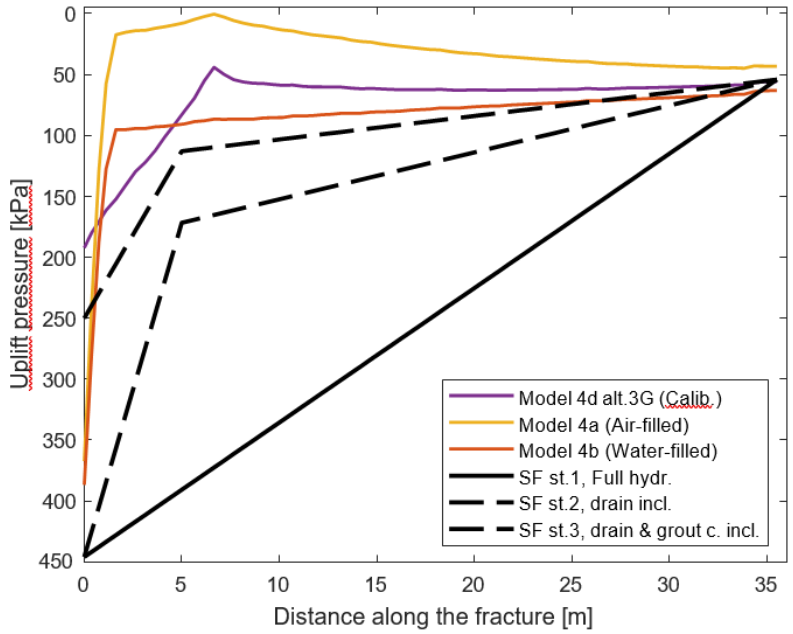

Figure 56. Pore pressure distribution for different cases. 0 = upstream Heel of the dam and 35 = downstream toe of the dam. Model 4d alt. 3G is used for the results presented below. (M. Abdi (KTH), 2022)

One of the findings from the analysis was that safety factors increase with increasing depth of the fracture in question, i.e. the shallower fractures are those of most concern. The results for one fracture are show in the figures below.

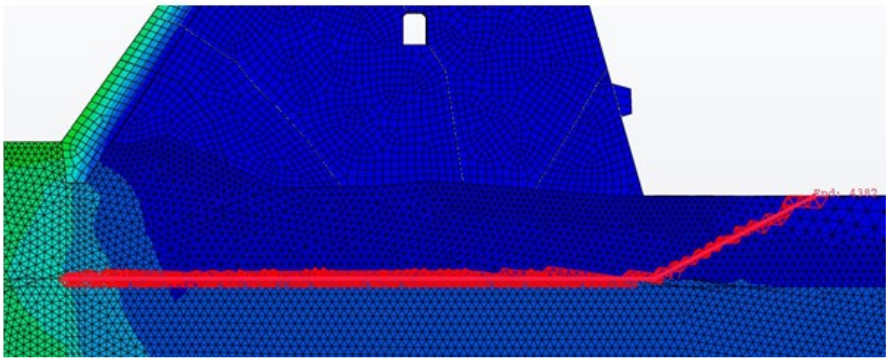

Figure 57. Illustration of the fracture, case B. (M. Abdi (KTH), 2022)

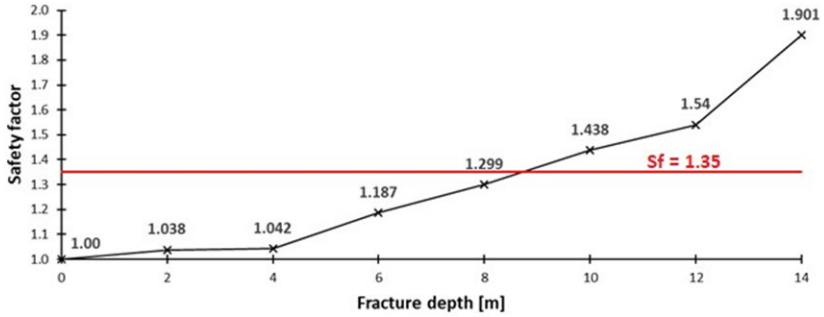

Figure 58. Safety factors vs. fracture depth, Case B and 4d alt.3G. (M. Abdi (KTH), 2022). Selected pore pressure gives a safety factor of 1.00 at the dam base.

5.3 Other cases/other references

5.3.1 Malpasset dam

The Malpasset dam was an arch dam, north of Fréjus on the French Riviera. It collapsed on 2 December 1959, killing 423 people in the resulting flood. The dam was 222 m along the crest and 66 m high.

The Malpasset dam is an interesting case as the failure mode of the foundation is probably one of the most thoroughly analysed cases in damengineering. The incident resulted in changes of dam designing, where the concept of uplift was extended from gravity dams to arch dams. It also gave developments in the measure of rock properties (in the lab as in the field), and in the analysis of rock mass stability and its dependency to groundwater pressure.

Most of the experts described the succession of events as the following (Duffaut, 2012):

i. The dam thrust creates a more impervious barrier into the rock mass deep below the dam.
ii. The low rock modulus lets open a fissure along gneiss foliation, wider and deeper where rock is more deformable.
iii. The water thrust inside the fissure increases as the square of the depth as the resultant is parallel to the fault it can move the "dihedron" upwards;
iv. Lacking support from its base, the shell asks more from the thrust block, which cannot afford and gives up;
v. Arching having vanished, monoliths will fail in bending.

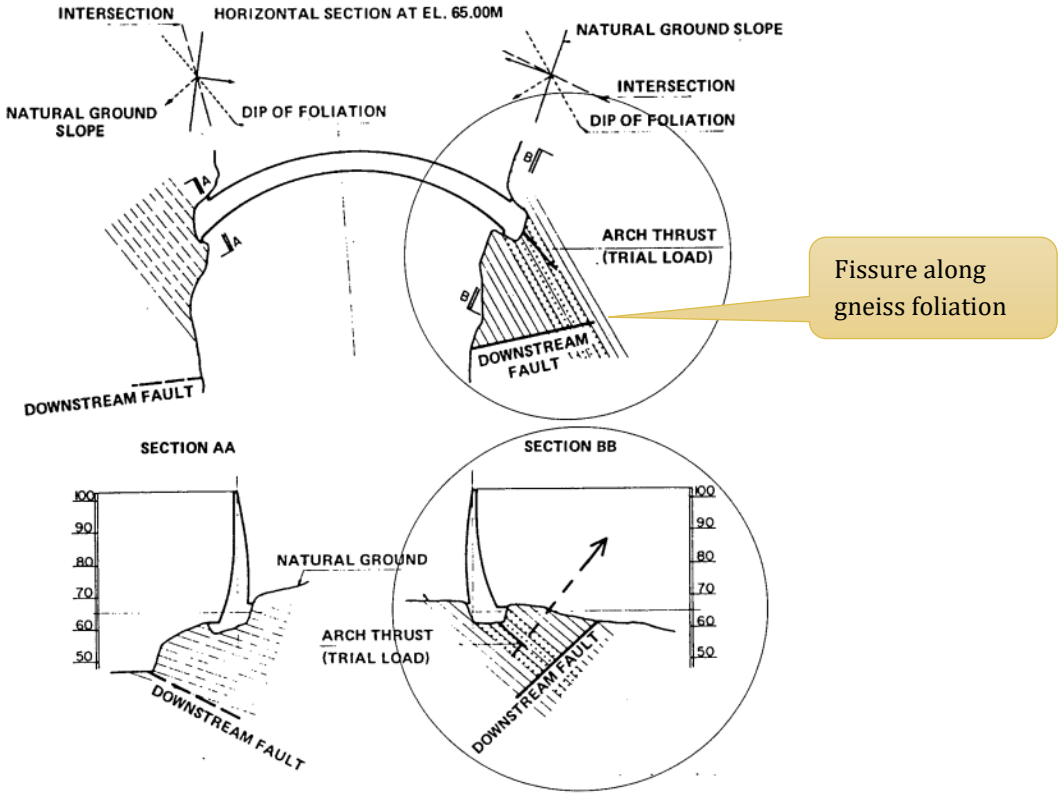

Figure 59. Relations between geologic structure in abutment of Malpasset Dam and arch. Circles indicate left abutment conditions. Dashed arrow (added) in Section BB is direction of uplift force. (USACE/ERDC, 2002)

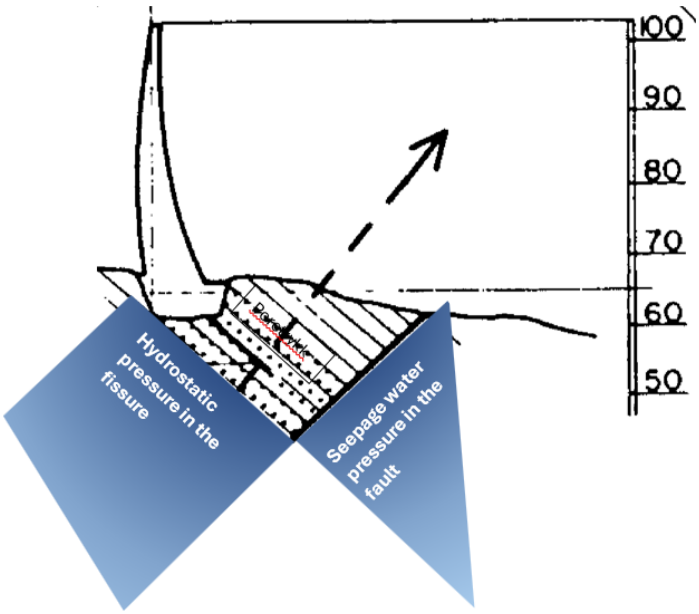

Figure 60. Illustration of the pore pressure in the left abutment under the arch.

5.3.2 ICOLD European Working Group on Uplift Pressure

This study (ICOLD, 2004) also gives a literature study of the current knowledge based on the reports listed below and carried out by the following organisations:

- EDF (France): C Brunet, M Poupart, D Rossignol. "Analyse de la piézométrie observée en fondation des barrages poids en beton", Crans Montana Symposium, 1995
- Swiss National Committee of Large Dams: Schweizerisches National Komitee für Grosse Talsperren. Arbeitsgruppe Auftrieb. "Auftrieb bei Betonsperren",1992
- EPRI (USA): A G. Strassburger. "Uplift Pressures in Existing Concrete Dams". Research Project 1745-27, 1988
- EPRI (USA): Stone and Webster. "Uplift Pressures, Shear Strengths and Tensile Strengths for Stability Analysis of Concrete Gravity Dams". EPRI TR-100345, Vol. 1, Project 2917-05, 1992

It is summarised that the common motivation behind all these studies is the acknowledgement that design assumptions about the effect of drains, grout curtains, cut-offs, and other methods of controlling and limiting uplift pressures, have never been fully validated. This becomes of particular interest in the safety reassessment of existing dams, where many questions and differences of opinion arise as to uplift assumptions. Many dams would require modification to meet updated safety standards. A better understanding of the interaction of structural features and uplift pressure distribution can contribute to avoid unnecessary modifications.

The report gives a comprehensive summary of the basic background and theory related to dams and pore pressure, techniques for numerical analysis and also drain maintenance and cleaning.

5.3.3 Study carried out by EPRI (USA)

The Project "Uplift Pressures, Shear Strengths and Tensile Strengths for Stability Analysis of Concrete Gravity Dams" (EPRI, 1992), was developed in 1989-1992, after the conclusion of a previous EPRI Project, to examine some aspects of the subject in more detail.

In addition to uplift pressures, the Project also aimed to establish ranges of shear and tensile strengths and cohesion values for concrete-to-rock interfaces. As far as uplift pressures are concerned the objectives of the three-year study were the following:

- Evaluate geological conditions, foundation treatment, and foundation drainage with respect to their influence on uplift.
- Evaluate drain cleaning methods.
- Develop a rational approach for extrapolating measured uplift to design flood levels.

A comprehensive study of uplift pressures at existing gravity dams was undertaken to meet these objectives. Data from over 150 gravity dams was reviewed and 17 well-instrumented host dams were selected. The selected dams were built between 1912 and 1974 and ranged from 30 to 170 m in height. A variety of sedimentary, metamorphic, and igneous rock foundations were represented.

The report (EPRI, 1992) is one of the main references in this report and is referred to in other relevant sections. However, some of the other findings may be of interest and has not been included in other chapters in this report. A short description of these findings is given here:

- **Response variation in water pressure:** Without exception, the data collected and examined showed no significant time lag between changes in headwater level and changes in uplift pressures. Reviewing some of the occurrences of time lag reported in literature they can probably be attributed to a misinterpretation for example by the delayed response of open standpipe piezometers. Open standpipe piezometers require that the water flows into the pipe raising the elevation of the water surface before an increase in pressure is registered. The time required for this flow depends on the permeability of the foundation and the magnitude of the pressure change, and it can result in the illusion of a time lag. For this reason, open standpipes are not suitable for monitoring the effects of rapid changes in reservoir elevation at dams with low permeability foundations.
- **Seasonal Uplift Variations**: The expansion and contraction of the concrete, resulting from seasonal air temperature variations, change the load distribution on the foundation and can consequently change the joint aperture and the uplift pressure distribution. This aspect was investigated in detail by (EPRI, 1992) by considering examples from published literature and data from the host dams and by theoretical finite elements analyses. The theoretical analyses showed that in winter the vertical stress near the heel is less compressive than in summer and the load that was originally at the heel is transferred downstream. As a result, the foundation behaves like a tapered joint and the uplift pressures increase (se illustration in Figure 22).

6 CASE STUDIES OF SELECTED NORWEGIAN DAMS

Pore pressure measurements from four Norwegian dams have been reviewed and assessed in this report. The assessment includes the following elements:.

- Mapping of the bedrock, with the aim of finding a suitable methodology for evaluation of the rock mass in dam foundation, as well as to reveal unfavourable fracture sets with regard to pore pressure and the placement of meters.
- Reproduction of measurement values, location, etc.
- Evaluation of results from the measurements.

In this chapter details from geology mapping and visualization of measured data are presented for each dam. The dams are named dam A, B, C1 and C2 and D for anonymity. Dam A is a traditional Norwegian slab buttress dam. Dams B, C1, C2 and D have buttresses that have been strengthened and is therefore defined as "Heavy Buttress Dam" according to (Energidepartementet, 2009).

However, dam A has a bottom gate placed on a concretes slab on the rock foundation in the highest section. Although the dam is a traditional Norwegian slab buttress dam, the gated section with the bottom slab will be comparable to a solid head buttress dam, where the buttress head and support is a continuous structure cast on to the bedrock.

Dam B, C and D differ from Dam A, as they have a box drain between the upstream slab and the downstream buttress support and are therefore freely drained downstream the water seal/slab. Pore pressure in the contact zone between the structure and the bedrock is therefore generally not possible.

Table 6-1. Key information of the dams and sensor output (total 87 sensors).

Dam	Dam height	Foundation	Grout curtain?	Drainage	Total leakage	No. of piezometers	Correlation PP and WL[9]?
A	21 m	Fairly good to good/very good	Yes	No	Not visible	16	Yes – for 1 piezometer
B	19 m	Fairly good to good	No	Drainage Galley (box drain)	<0.2 l/s	24	No
C1, C2	12 m	Good to very good	No	Boxdrain	< 0.1 l/s	28	No
D	14 m	Very good	No	Boxdrain and drainage curtain	Not visible	19	No

Figure 61 illustrates the placement of boreholes and sensor (sensor and surrounding sand is shown

[9] PP = Pore Pressure - WL = water level

in red) in relation to the rock surface (shown with green line).

All the sensors are close to the surface and are positioned to measure pore pressure at the rock/concrete interface (Dam A) or directly below the rock surface under the buttresses (Dams B, C and D). All boreholes are quite short and would need to match the rock joints exceptionally well in order to intersect these. The placement of the boreholes is generally schematic and standardized, and does not take into account the more random orientation/location of rock fractures. The measured pressure is not calibrated against a locally measured barometric pressure, for any of the dams. Only one of the dams are including the pressure in the transition between the rock and the concrete.

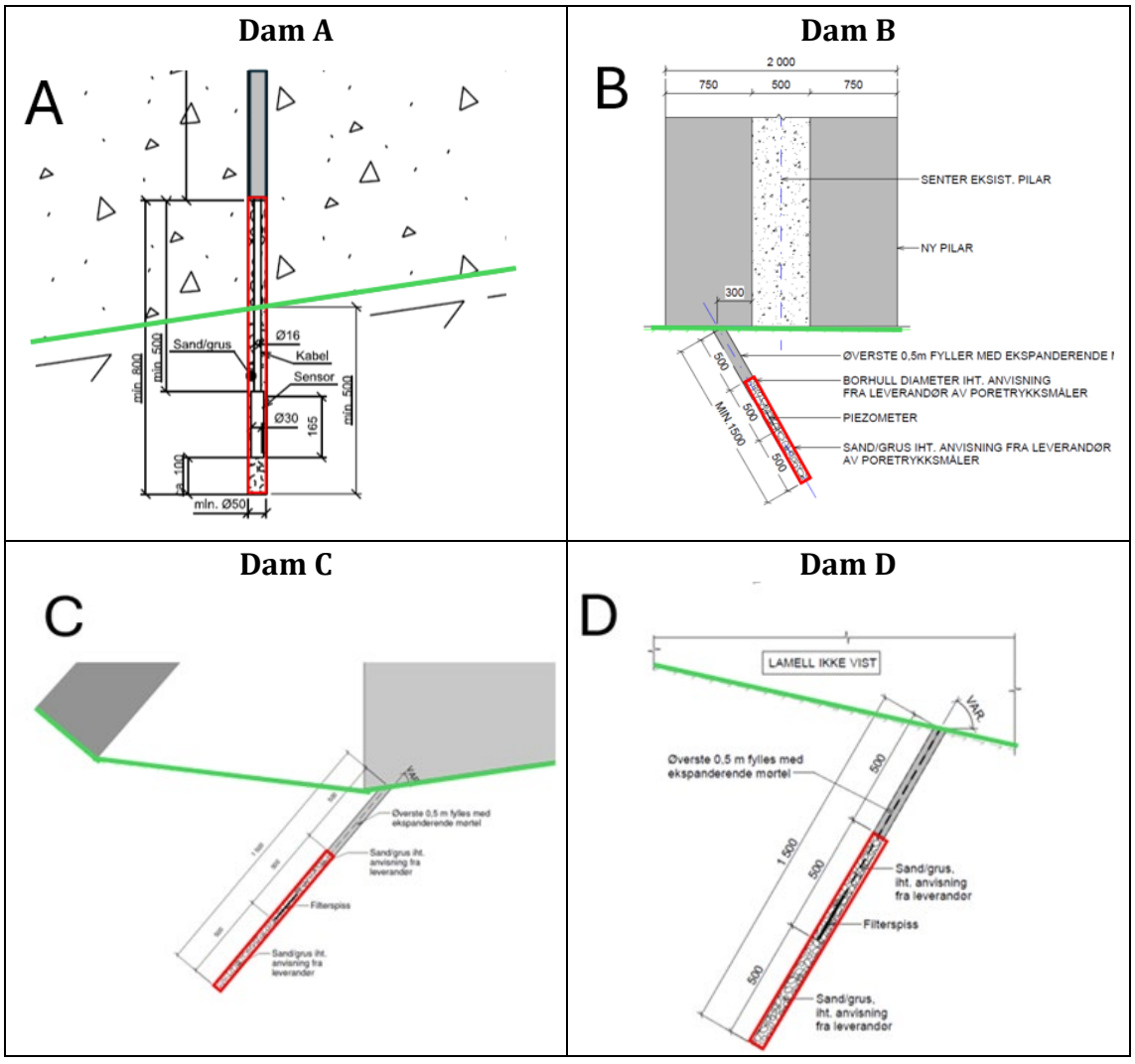

Figure 61: Typical placement of borehole, sensor and grouting, for the 4 sites, Figure 61 shows the more general placement of the sensor in the dams.

In Dam A, Piezometers have been installed underneath the bottom slab (related to a water gate) in the center of the dam and in the rock on both sides. Some of the measured values correlate well with the water level in the reservoir. In Dam A the sand in the borehole is extended through the intersection between the concrete and the rock in order to include this joint/intersection in the measured pressure. This is not done for any of the other three dams where pressure is measured

from 1.5 m to 0.5 m depth.

In Dam B the pilar have been strengthened to a new width of 2 m. The sensor is placed underneath the centre of the pilar as shown in Figure 61. The measured values relate best to the outside atmospheric pressure. This dam is quite close to meteorological weather stations and reliable barometric pressure could be fund. There is no correlation with the water level in the reservoir, and the values are small. It is believed that these sensors measure the depth of the water column in the drainage borehole that is placed right next to the sensors.

In dam C1 and C2 every other section (between the existing buttresses) is filled with concrete. Two Piezometers are placed in the centre of the section filled with new concrete. An opening is kept for drainage towards the upstream side as shown in Figure 61. The measured values are small and as for dam B corelates well with the atmospheric pressure but not the water level in the reservoir. These dams are further from any meteorological weather stations and reliable barometric pressure could not be fund. About half of the sensors are reporting negative values indicating that something is wrong with the measurement, calibration or the storage.

In dam D every other section (between the existing buttresses) is filled with concrete, and an opening is kept for drainage towards the upstream side. Two Piezometers are placed in the centre of the section filled with new concrete, similar to Dam C. The Piezometers are placed similar for Dam C as shown on Figure 62. There are no measurements of pore pressure that are connected to the upstream water level. No measurements of pore pressure is also expected as the dam has a drainage curtain upstream the piezometers.

Figure 62 shows the location of the sensors in the different dams.

Evaluation of the pore pressure measurements in this report, show that the drainage gallery between the upstream slab and the buttress support, eliminates the risk of pore pressure under the buttress supports. This also applies for with very wide buttress supports. No pore pressure was measured in any of the 47 piezometers that were installed in the dams with an upstream drainage gallery (dam C1, C2 and D). These dams have “very wide” buttress supports, that are 6 m wide, and with an upstream drainage gallery.

Dam B has different design with slenderer buttress supports that are 2 m wide. No pore pressure was detected by the 24 piezometers installed in this dam. This result corresponds with previous studies described in chapter 2 of this report, where it is concluded that pore pressure cannot develop under slender buttress support.

For buttress dams without an upstream drainage gallery, however, there are indications that pore pressure can develop under very wide buttress supports (>5-6 m wide). We see tendencies to this in one of 16 piezometers installed in dam A. it is likely that this sensor intersects a quite vertical rock joint and thereby will not cause uplift. Development of pore pressure uplift under “very vide” buttress supports, will in any circumstances be site-dependent and will therefore vary with foundation conditions and with dam height (i.e. upstream water pressure).

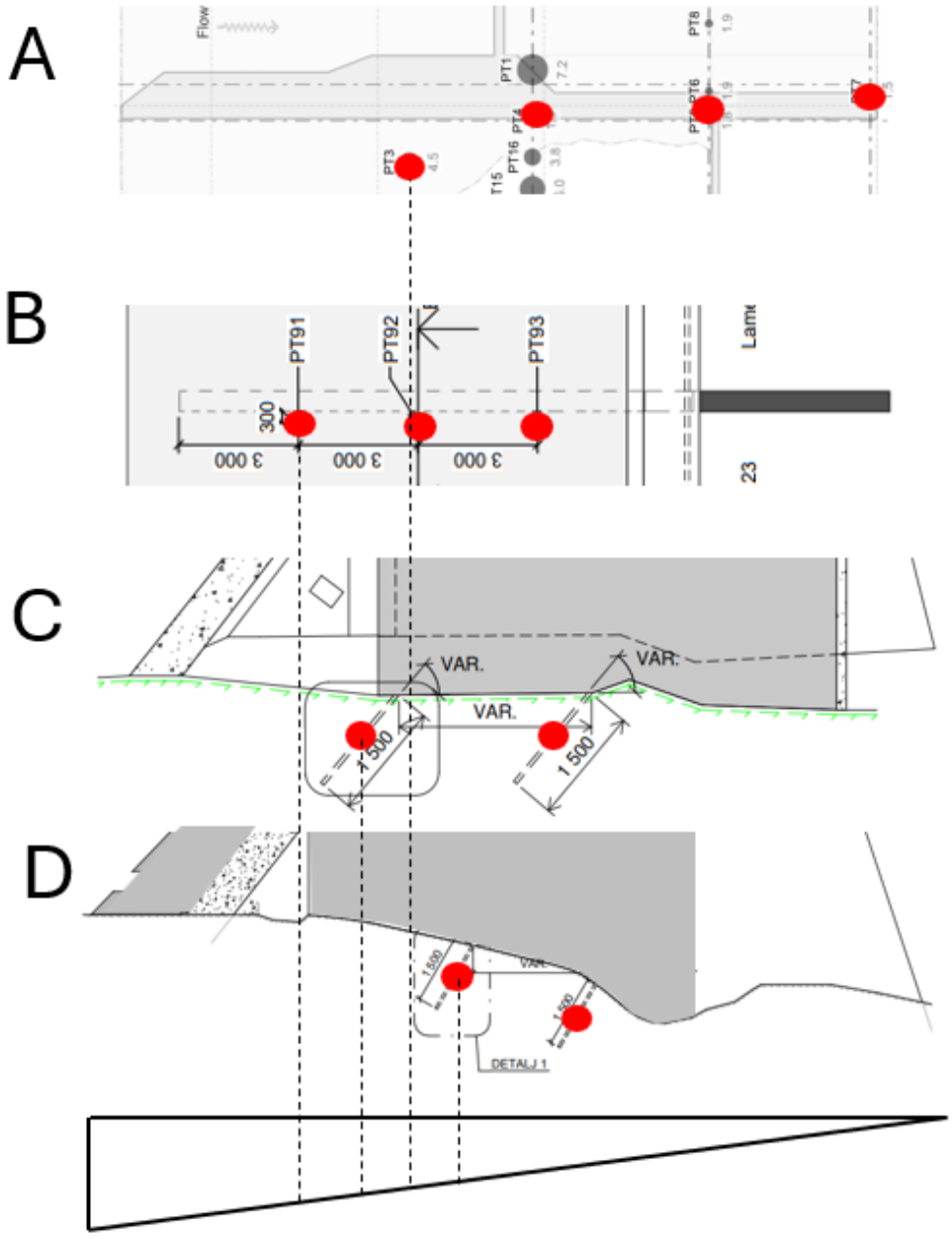

Figure 62: Typical geometric placement of sensors. Viewed from above (A and B) and in vertical section through the dam (for C and D). Upstream face to the left and position of piezometers shown by red dots. Position of furthest upstream sensor indicated by vertical dotted line against a triangular distribution.

Table 6-2 below summarizes the data that have been provided by dam owners. The dams are listed based on the significance of findings rather than the number of sensors or datapoints. Factors contributing to interesting findings include the complexity of the interface between the dam foundation and its surroundings, or sensors that penetrate water-conducting cracks. These factors influence how pore pressure evolves beneath the dam, yielding more interesting results.

Table 6-2: Overview of the sent data

Dam	No. of sensors	Time period	Timestep	Complementary instrumentation	Distance to measurment of atm.	Note
A	16	Okt. 21 – Okt 24 → 3 years	1 hour	WL	40 km	~55 % evenly spaced empty cell
B	24	Nov. 23 – Nov. 24 → 1 year	2 hours 40 min	WL	20 km	continuous, but some sensors with only 0s
C	22 + 6 (C1 + C2)	Mar. 2022 – May 2024 → 2 years + 2 months	1 hour	WL, temp	55 km	Mostly continuous, but big gaps
D	19	June 2019 – June 2024 → 5 years	.		2 km	Manual measurements; 17 points total

The datasets lack information on units and details regarding corrections made between sampling, storage and SCADA. Correction for variations in atmospheric pressure has not been performed in the received data. There are several potential sources of error in pore pressure measurements that must be considered during sensor placement, installation, and data interpretation. Refer to Section 3.3 for a more detailed description of installation procedures and sources of measurement error.

6.1 Dam A

6.1.1 General overview of the dam

The dam was built in the 1980s with a maximum height of 21 m and a length of about 60 m. The dam has 10 buttress sections and gravity sections against the abutments. The highest section with a gate has a bottom slab against the rock surface. The dam is a traditional Norwegian slab buttress dam, and there have been no major modifications to the dam structure since construction.

Although the dam is a traditional Norwegian slab buttress dam, the gated section with the bottom slab will be comparable to a Solid Head Buttress Dam, where the buttress head and support is a continuous structure cast on to the bedrock, and this is where the 16 piezometers have been installed.

After a flood incident, the downstream foundation was strengthened with rock bolts. In addition, loose rock blocks were secured with a massive concrete slab. The downstream side of the supports and the frost wall was also strengthened with a concrete wall and rock bolts.

Initially, the consultant recommended to install drains in the foundation inside the inspection gallery on the downstream side of the grout curtain. However, NVE wanted piezometers to be installed, to measure the pore pressure under a concrete slab under the bottom gate. This concrete slab is cast on the foundation in the highest section. The drain was therefore not installed, as there would be no purpose to measure the pore pressure of a drained foundation.

A total of 16 piezometers have been installed under the concrete slab under the bottom gate. The sensors are placed along 5 axes, of which 2 axes are along the dam axis and 3 axes perpendicular to the dam axis (i.e. along an upstream - downstream line).

Six of the piezometers are placed in rock at different depths (2 sensors at 1.5 m, 3.0 and 4.5 m below the surface, respectively. The rest of the sensors are placed to measure pore pressure at the rock/concrete transition or directly under the concrete slab.

There is a grout curtain under the upstream slab. In the highest section under the bottom gate, there are 3 rows of grouted holes under the foundation slab.

There has not been observed any visible leakage from the dam or the foundation.

Figure 63. Downstream side of the slab buttress dam. Free overflow spillway along the dam crest.

Figure 64. Downstream the bottom gate. Rock bolts and concrete slab to secure the downstream foundation are visible on the downstream foundation.

Figure 65. Cables to piezometer P14, P15 and P16.

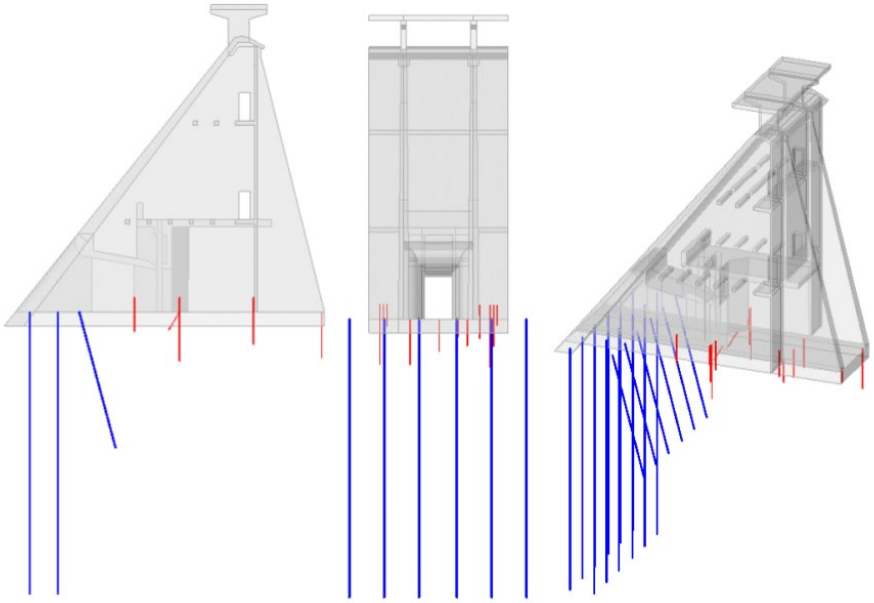

Figure 66. Grout curtain at dam A, shown as blue lines, and locatiosn of piezometers,shown as red lines. Left: Section with the upstream side to the left. Middle: Front view of the midsection. Right: 3D illustration of the grout curtain and the dam section.

6.1.2 Description of the bedrock

The dam is located in coarse-grained granitic migmatite belonging to a large Gneiss-migmatite-granite-complex of Precambrian age. On geological bedrock map from NGU (1:250.000, paper version, Sigmond 1975), strike NW-SE to NNW-SSE and dip to the East are indicated for foliation/ schistosity at locations near the damsite.

Site visit with engineering geological mapping was carried out 15.8.2024. As basis for the mapping, geological and topographical maps were used (NGU, 2024), (Kartverket, 2024). In addition, results and evaluations related to previous work on stability of rock slopes immediately downstream the dam was useful as background material for this study (Nilsen, 2019). Detailed information on extensive pre-grouting in 1980-1981 of the rock mass at the base of dam, instrumentation and monitoring results is given in (Dr.techn.Olav Olsen, 2024).

As shown in Figure 67, the bedrock was found to be generally well exposed in the downstream slopes of the dam foundation. Most of the mapping was therefore done from the surface, but in addition observation and some engineering geological mapping was also done from inside the dam.

Figure 67: Exposed rock in the downstream slopes of the dam foundation. Left: Migmatitic gneiss at the northern valley side. Mainly massive, but with very distinct exfoliation joints having required heavy rock support. Right: granitic gneiss at the southern valley side, very massive at the middle and upper part, more fractured at lower part.

Figure 68. Intermediately fractured, granitic gneiss between support F and G at the bottom of the dam.

The bedrock at the dam foundation was found to be mainly massive and without any distinct

foliation/planar structure. Near the bottom of the river valley, the character was however less massive, and at the northern side of the river valley side distinct, persistent exfoliation (surface-parallel) fractures caused instability/sliding in the downstream slope during heavy rainfall in September 2019. After this incident, the unstable section of this slope was stabilized with rock anchors and concrete structures.

Figure 69 and Figure 70 further illustrate the rock conditions. Details on rock strength and fracturing are given below.

Figure 69: Left: Heavily fractured granitic gneiss at bottom of southern valley side, near support F. Right: massive granitic gneiss near top of southern valley side, between support H-I.

Figure 70. Left: Fractured migmatitic gneiss at bottom of northern valley side, near support E. Right: pegmatitic migmatite undercut by persistent exfoliation joints at middle/upper part of northern valley side.

6.1.2.1 Rock strength

As discussed in Chapter 4, rock strength is not the most important factor regarding rock mass permeability and water leakage. It is however one of the input parameters for calculating RMR, and therefore was included in the site mapping based on index testing with Schmidt hammer (as described in Chapter 4.5 of this report).

The testing was performed according to ISRM-standard, i.e. 20 single tests are carried out with hammer type L and the characteristic Schmidt-hammer value R_L is calculated as the average of the 50% highest single values (ISRM, 2015). The diagram in figure 50 with estimated rock density of 27 kN/m^3 for granitic gneiss/migmatite has been used in the diagram to find the UCS-value. The results are shown in Table 6-3. The estimated UCS-values are very high, with an average of 211 MPa.

Table 6-3. Results from Schmidt-hammer testing of granitic gneiss/migmatite.

Location/ rock type	**Test values for R_L**	**Average of 50% highest R_L**	**Test direction**	**UCS based on Deere & Miller**
S-side, near support F Gran. gneiss	31-41-52-50-44-44-50-40-50-36-30-40-48-38-48-50-40-40-40-36	48,2	~45° downwards	140
S-side, between support H-I Gran. gneiss	58-64-64-64-64-52-48-58-68-62-61-64-60-60-66-56-60-60-50-48	63,8	As above	300
N-side, near support E Migmatite	66-68-52-54-62-38-44-42-32-66-38-68-50-46-30-34-44-42-44-54	58,6	Vertically downwards	250
N-side, between support B-C Pegm.migmat.	54-50-50-58-40-48-48-44-42-50-38-48-40-52-44-50-46-46-48-46	50,8	~45° downwards	155

6.1.2.2 Fracture characteristics

Results from mapping of joint orientations based on stereographic projection (see chapter 4.3 for interpretation explanation) are shown in Figure 71. As can be seen, steep cross joints striking ENE-WSW and dipping steeply (about 75-85°) towards S were found to represent the predominant joint sets. In addition, there is a second distinct set of crossjoints striking NE-SW and dipping moderately steep to NW (40-45°) and a set of sub-horizontal joints dipping gently (20-30°) towards N (i.e. in direction towards the reservoir). Also, as can be seen from the stereo plot, there are some joints in other directions, including some sub-horizontal.

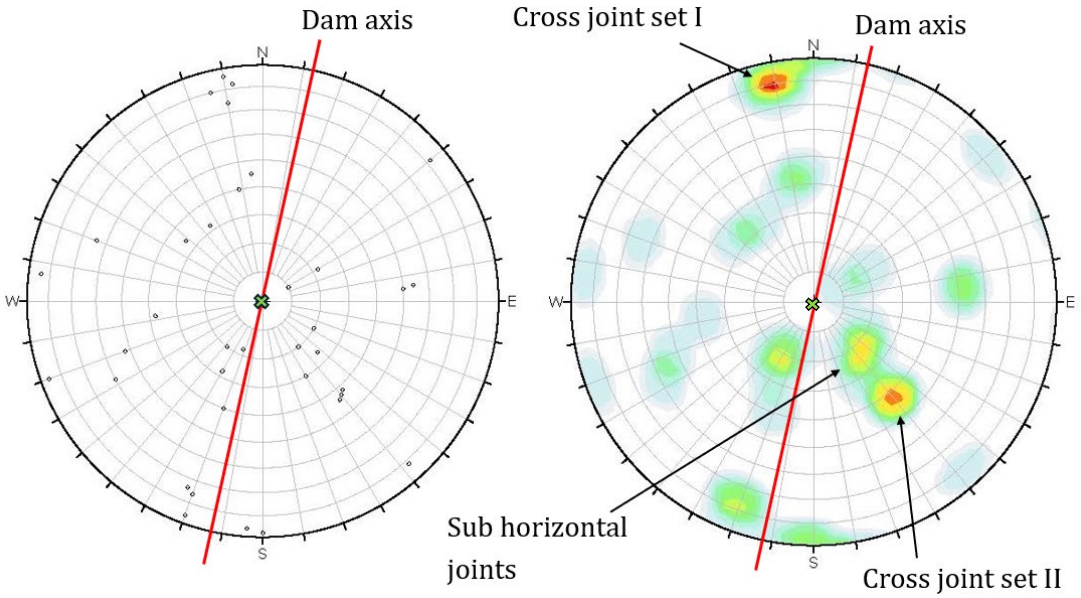

Figure 71. Distinct joints, presented as pole plots (left) and contoured plot (right) with colours representing main pole concentrations of 9-10 % (red), 8-9 % (brown) and 7-8% % (yellow), respectively. Green cross indicates vector (direction and inclination) of piezometer drillholes (in this case mainly vertical according to Olav Olsen, 2024). Number of measured joints: 36.

The degree of jointing was found to vary from very massive and massive sections for most of the dam foundation, with spacing between distinct joints of 1-2 m and more. At the bottom of the river valley (between support E-F and a few meters further to each side) the rock was found to be considerably more fractured, with typical joint spacing down to 5-10 cm.

The distinct exfoliation fractures at the northern abutment (probably caused by high tangential stress, see left part of Figure 67 are striking approx. N40°E and dipping moderately (around 35°) to SE (recognized as the green concentration just below "Cross joint set I" in Figure 71). Fractures belonging to this set are persistent and quite open, if located also further beyond the valley surface this joint set may cause build-up of considerable water pressure.

Most sub-horizonal joints dip in westerly (i.e. downstream) direction and potentially may be supplied by water from the reservoir and cause uplift pressure. For this dam, extensive grouting has however been done, which greatly reduces the risk of such potential uplift. Very little leakage was observed by surface observation at the dam foundation and by observations inside the dam.

As mentioned above, the degree of fracturing at the bottom of the river valley was observed to be much higher than further up. In addition, the bedrock at the bottom, as observed by inspection inside

the dam (see Figure 68) showed signs of weathering. This gives good reason to believe that the bottom of the river valley represents a fault/weakness zone. Detailed mapping of rock mass quality there was however not possible due to soil cover. In any case, serious consequences of this fault most likely have been prevented by the extensive pre-grouting which has been done.

6.1.2.3 Classification

Rock mass classification based on the RMR system, as described in chapter 4.4, was done during the site visit for selected, representative locations. The results are presented in Table 6-4 below. As can be seen, the ratings vary considerably in the dam foundation area. Near the bottom (as shown for support F and E in Table 6-4) the quality has been estimated as Class II-III due to generally high degree of jointing and weathering, while at the middle part of the Northern side (between support H-I) it has been classified as Class III (close to Class IV) due to the distinct exfoliation jointing. At the upper part of the Southern side (between support H-I) the estimated rating was Class I "Very good".

Table 6-4. Estimation of RMR ratings for selected locations.

Location/ parameters	**S-side near support F**	**S-side between support H-I**	**N-side near support E**	**N-side between support B-C**
1 Rock strength (UCS)	12	15	15	12
2 RQD	10	17	17	20
3 Joint spacing	10	15	10	15
4 Joint condition - persistence -separation -roughness -infilling -weatherin	22	25	25	10
5 Ground water	10	12	12	12
Rating adjustment	-15	-2	-15	-25
Rating	49	82	64	44
Class No.	III	I	II	III
Description	Fair	Very good	Good	Fair

The Q- and GSI-systems, as discussed in Chapter 4, are not considered suitable for evaluation of damsites and therefore have not been used systematically in this project. Like for the other dam sites of this study reconnaissance estimation of Q-value and GSI has however been done. Based on this characteristic Q'-values of 10-12 have been estimated for the least massive sections and around 40 for the most massive sections, which for J_w and SRF equal to 1 corresponds to "Fair" to "Good" and "Good" to "Very good", respectively. The characteristic GSI-value was found to be within the region 50 to 90, i.e. "Good" to "Very good".

6.1.3 Measurements of pore pressure

Placement of the piezometers is shown in Figure 72 and Figure 73, where they are located along five axes as summarised in the following table:

Table 6-5. Location of the piezometers along the different axis.

Axis orientation	Axis	Depth under foundation	Piezometer	Location
Along dam axis	**L1**	0-0,5 m	P1, P2, P4	Downstream bottom gate
		1,5 m	P14, P17	
		3,0 m	P15, P18	
		4,5 m	P16, P19	
	L2	0-0,5 m	P5. P6, P8, P9	In line with the frost wall
Upstream-downstream direction	**B1**	0-0,5 m	P3, P4, P5	Along Buttress support. About 1 m from axis B2
	B2	0-0,5 m	P1, P6, P7	Along Buttress support. About 1 m from axis B1 and 4 m from axis B3.
	B3	0-0,5 m	P2, P9, P10	Along Buttress support. About 4 m from axis B2.

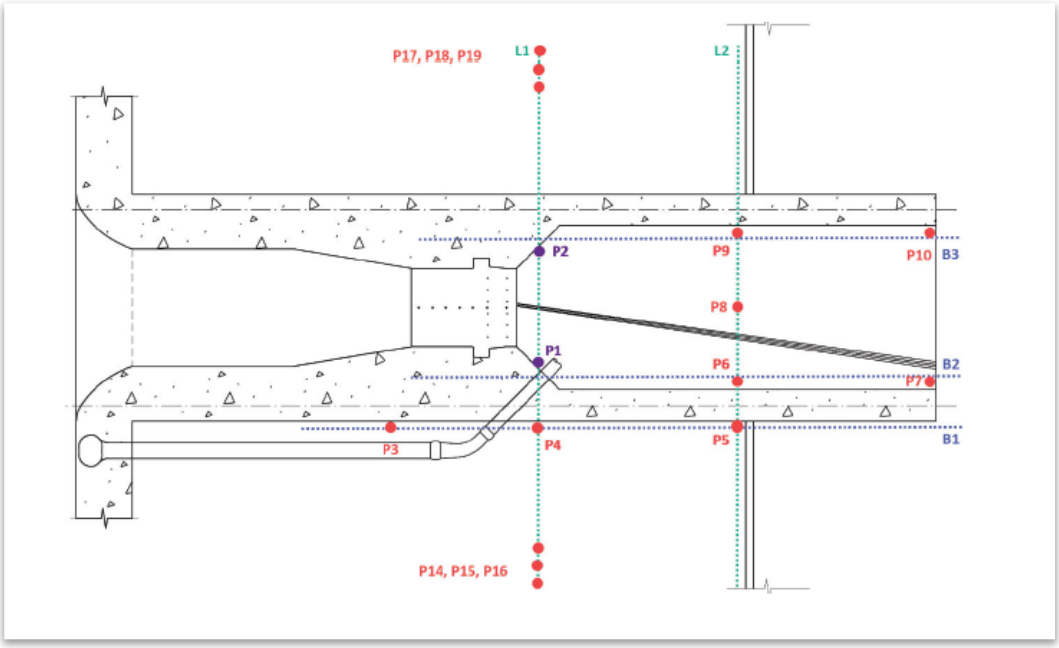

Figure 72. Plan view of the bottom gate section with the 16 sensors along 5 axes, B1, B2, B3 and L1 and L2. Upstream side to the left and bottom gate in the middle.

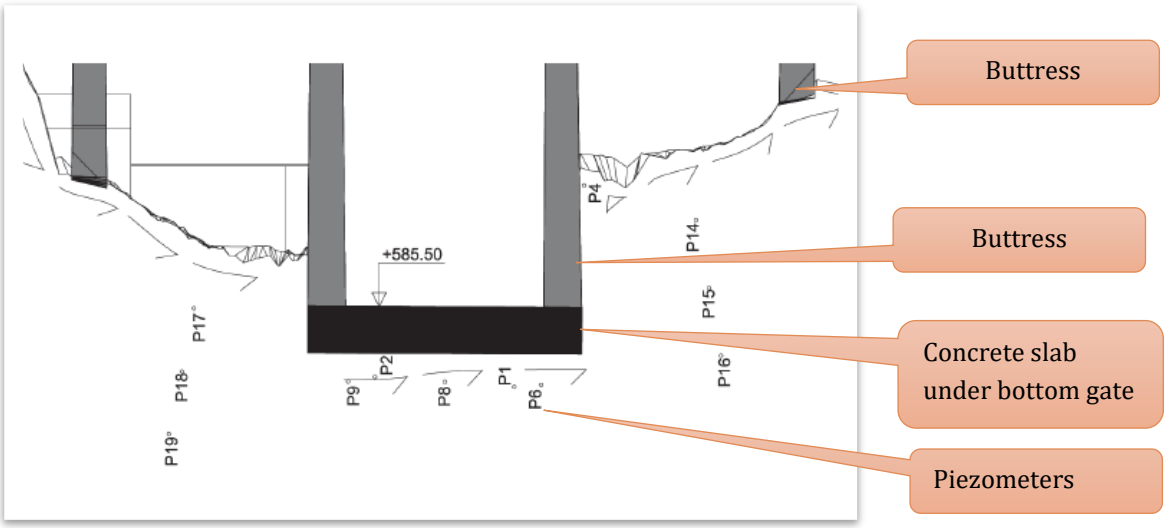

Figure 73. Downstream elevation of the concrete slab under the bottom gate, with adjacent hollow sections and buttress supports. The location of the sensors in the foundation is also shown

The analysed measurements from Dam A span from August 2021 to October 2024, and there are 16 sensors. While the available data is stored hourly, over half of the entries are missing. This presents several challenges: postprocessing becomes more cumbersome and complex, and cross-correlation analyses require aligned time series, as discussed in 6.1.3.1.

Visual representation of the time series is key to understanding the measurements. The simplest, but possibly also the most misunderstood plot is line plots. By scaling the x- and y-axis one can make any data look smooth or highly variable. Having a known reference variable, like water level, helps understanding the data significantly. The plot in Figure 74 shows the following:

1. Common variables: water level in the reservoir and atmospheric pressure from the nearest available station.
2. L1 [1]: Sensor values for axis L1, but only those beneath the bottom slab.
3. L1 [2]: Addition sensor in axis L1, all installed directly into bedrock.
4. L2 [1]: Sensor values for axis L2 right hand side
5. L2 [2]: Sensor values for axis L2 left hand side
6. L2: Sensor values for axis L3

With data for more than 3 years short-time effects disappear, but long-time trends remain visible. The water level in this reservoir varies often, and a lot. Assuming a pore pressure distribution under the concrete base like the design requirements one should see the same rapid movements in the plotted values. All but PT1 and PT15 seems to either have fewer fluctuation and/or different movement. Observations:

- PT1 is clearly corelated with the water level, probably through water-conducting cracks. (clearer in shorter timespans)
- PT2, PT3 and PT14 show very similar movement, but with a rate and intensity that does not match water level in the reservoir nor atmospheric pressure.
- PT18 have a seasonal variation, almost sinusoidal, with peak values mid-September.
- PT15 appears to be correlated with water level, but also some other variables. A similar sinusoidal pattern as PT18 is visible, but with fluctuations. Both PT15 and PT18 located on

each separate end of axis L1 and are both 3 m below the surface.

- All sensors in axis L2 and L3, PT5-PT10, have the same “jump” in late summer 2022 and 2023. They all measure small values, probably none of which is greater than the bore hole depth, i.e. no pore pressure.
- PT4 and P16 show the same movement as atmospheric pressure, atm, but opposite direction. Maybe miscalibration?

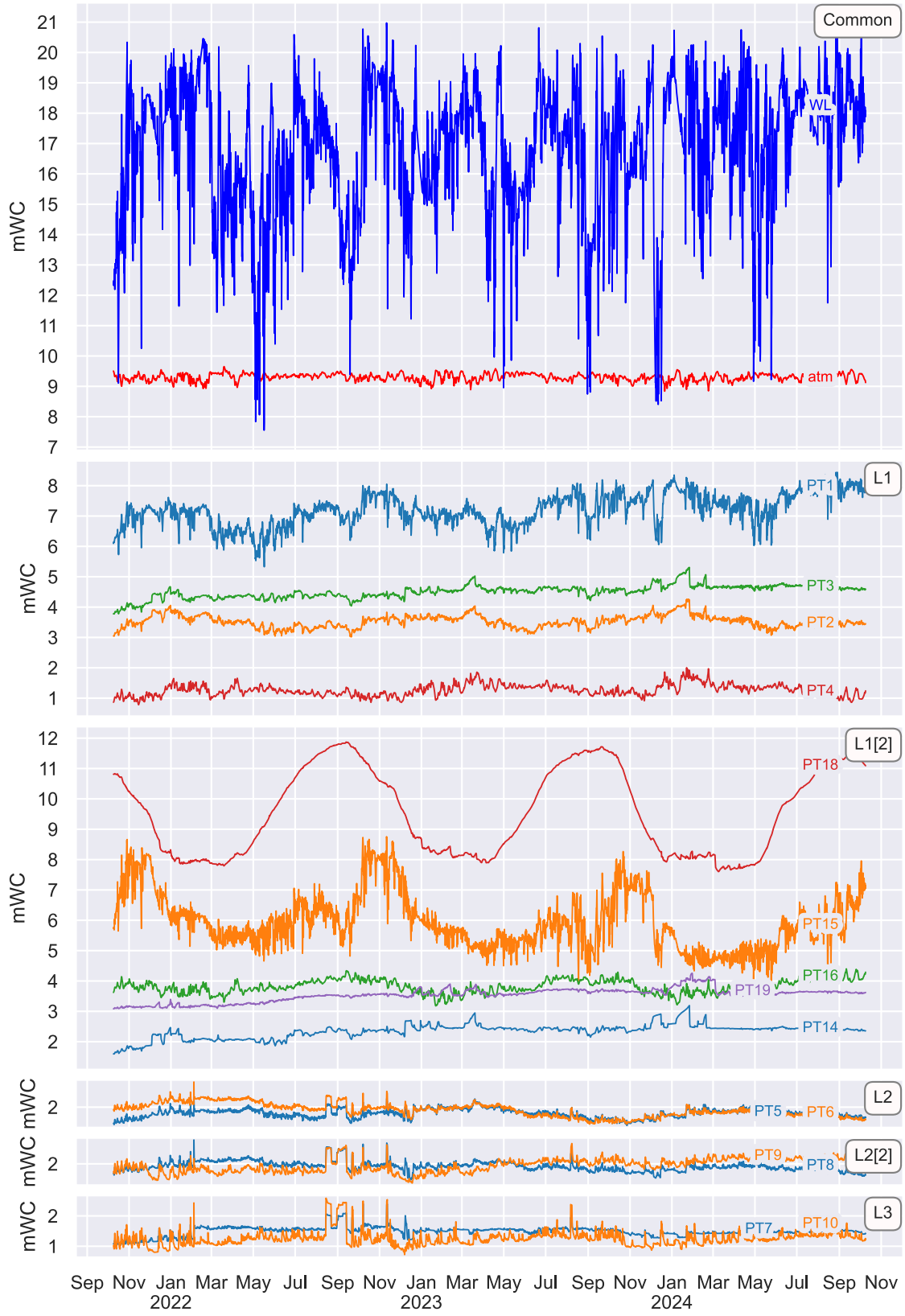

Figure 74: Line plot dam A

The plot below shows the relative position of the sensors, combined with a blue circle whose radius depicts the mean pressure and a grey circle whose radius depicts the borehole depth minus grouted part, which is set to 0.5 meters. The grey circles are plotted on top of the blue ones to identify which sensors are measuring pore pressure. In this context a sensor measuring a water column whose height is smaller than the bore hole is said to not measure pore pressure, but rather the water level in the bore. All blue circles for sensors in axis L2 and L3 are not visible, i.e. the mean value is no pore pressure.

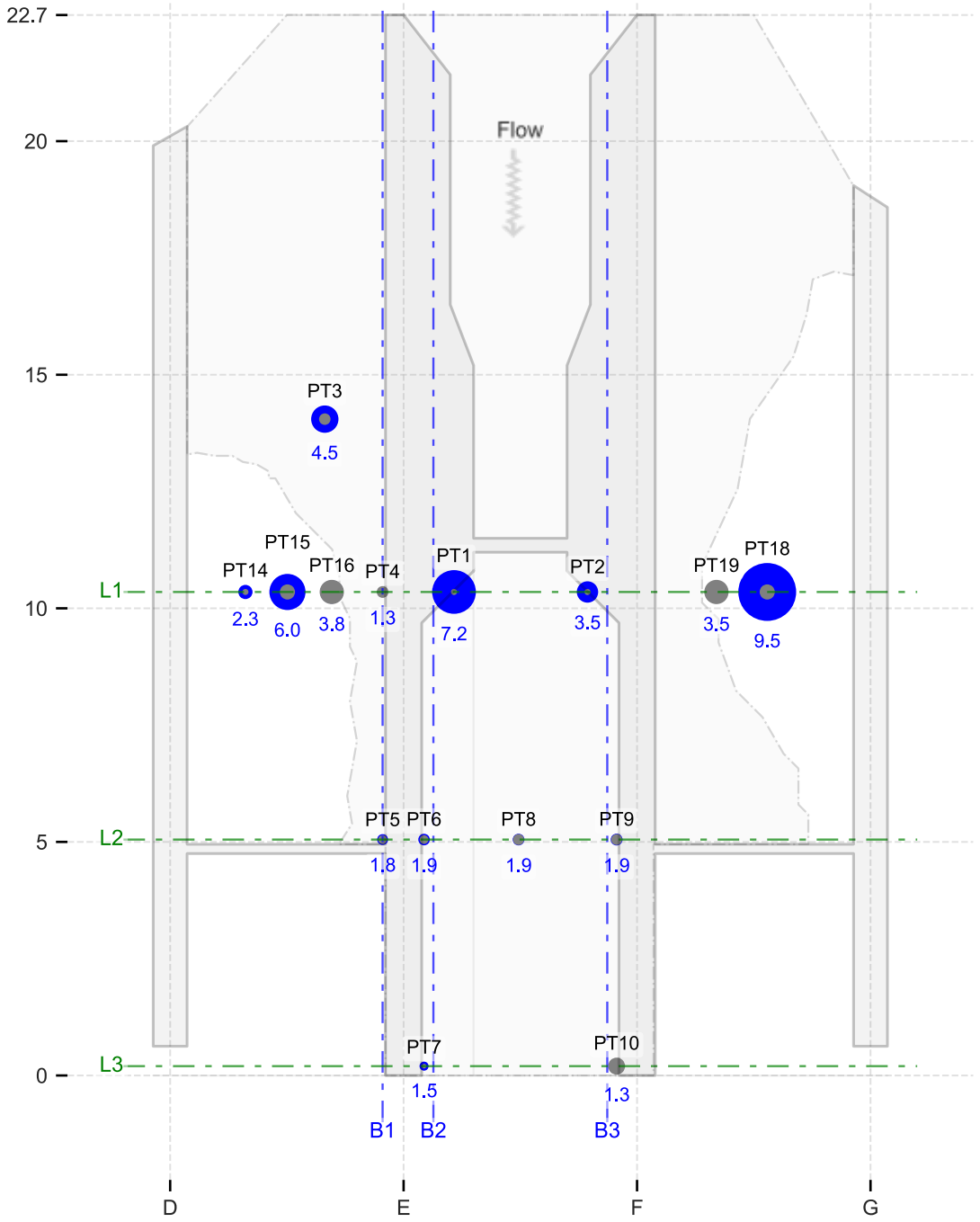

Figure 75: Sensor layout Dam A

The plot below shows the same numbers as Figure 75 but visualized as cross sections along axis B1, B2 and B3. The dotted line with dots (..•..) show sensor mean values, and the dashed line with crosses (--x--) shows sensor mean values subtracted bore hole depth minus grouted part, which is set to be 0.5 meters. Note that that negative values are zeroed, and that grout depth may vary. Note also that the concrete base is not as wide as depicted above for axis B1, see Figure 75. The plot clearly shows how the sensors in axis L1 differ, and that sensors in axis L2 and L3 seemingly is not measuring pore pressure. It does however not show the difference in installed elevation and bore hole depth. To show these differences an elevation cut though axis L1 is created, as shown in Figure 77 . The plot assumes that pore pressure from upstream side to the first sensor, is linear through the grout curtain, and is probably not correct, ie. the pore pressure on the upstream side is overestimated in the plot.

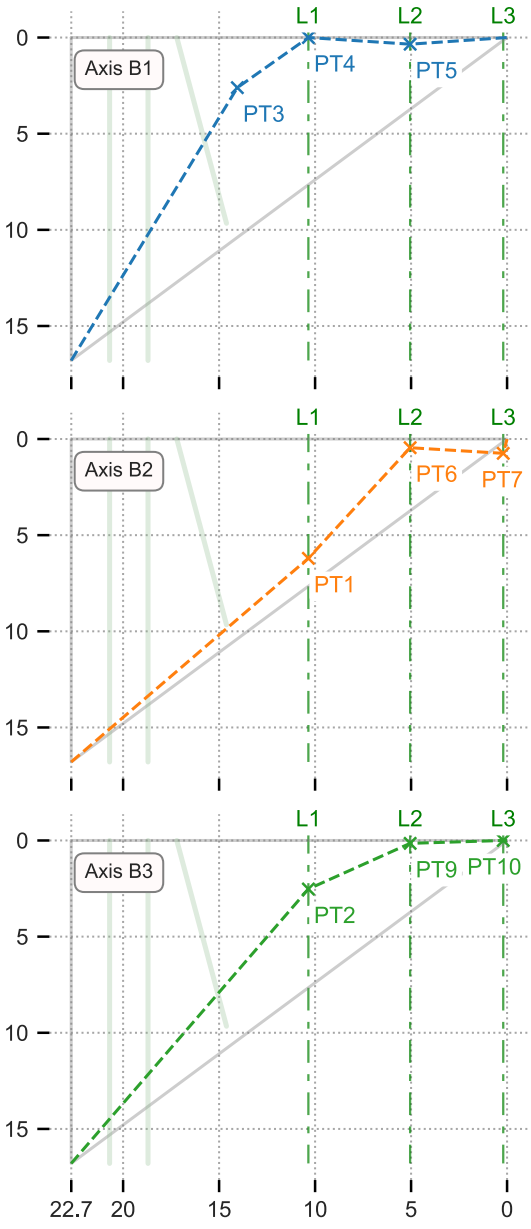

Figure 76: Pore pressure triangles. The plot assumes that pore pressure from upstream side to the first sensor, is linear through the grout curtain.

Figure 76 reveals the three-dimensional problem of identifying pore pressure under this concrete base. The base is elevated by 1.7 meters and 3.6 meters in the neighbouring sections, creating a three-dimensional challenge. Additionally, the thickness of the base varies by more than 2 meters, which is visible on the downstream side of the dam. Plot below shows a constant thickness of 1 meter for simplicity, which corresponds well with the bore hole depths.

Pressure values are visualized as equivalent water column heights, ranging from approximately 1 meter to nearly 12 meters, but without any discernible pattern. PT18, the highest water column, is sinusoidal in the line plot, Figure 74, and this is also reflected in the summer/winter distributions. This measurement is assumed to be something else than pore pressure, whether it is instrumentation error, closed cavity air pressure or a combination of such.

The measurements were demanded by NVE in order to verify the design pore pressure used. The measurements next to the concrete base was installed to confirm the values found beneath base, but due to the highly variable and uncertain values these do a better job of highlighting the challenge.

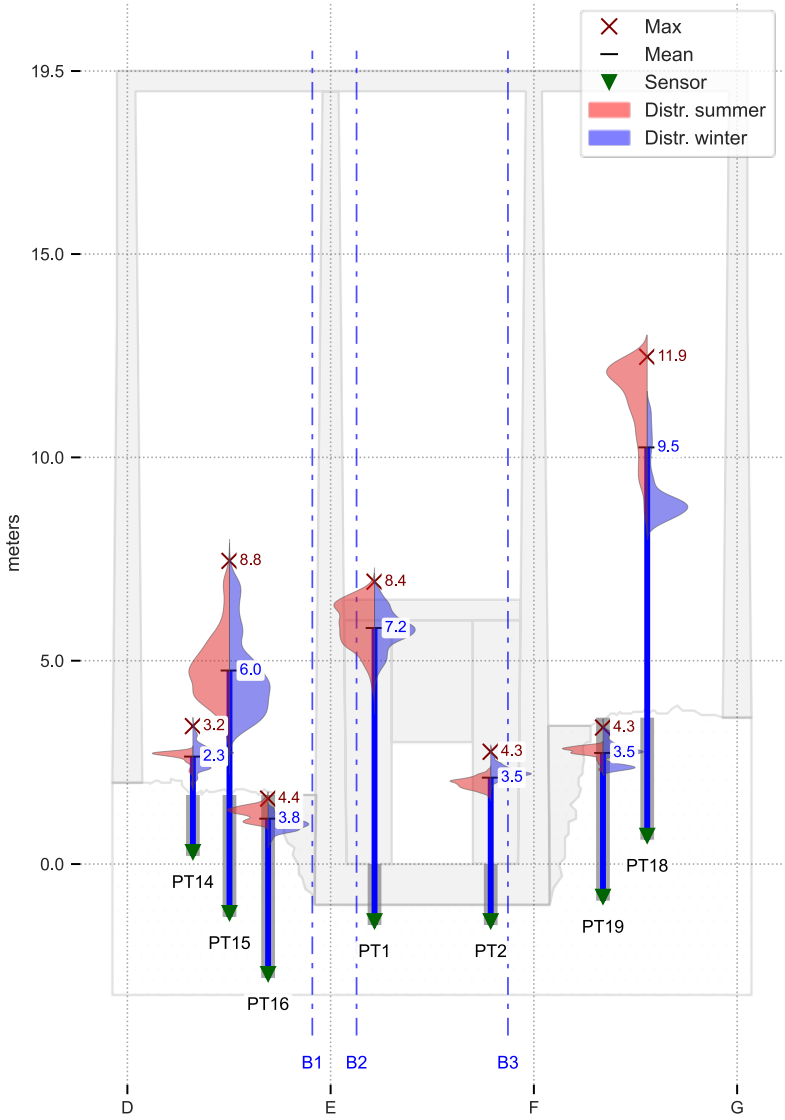

Figure 77: Elevation cut axis L1

6.1.3.1 Cross correlating timeseries

Cross correlations are useful to measure how well two time series resemble each other. To get good results, timesteps should be equal and data preferably without time-gaps to reduce the error for non-stationary effects. The measurements from Dam A are continuous but a little more than half of the values are missing. To overcome this issue, with both gaps and non-aligned timeseries, down-sampling is performed to a sampling rate of every six hours. While interpolation of missing values could have been an alternative, down-sampling was chosen to reduce the risk of introducing artificial patterns into the data. This approach works well when missing values are distributed throughout the time series. However, if missing values were concentrated into large gaps, alternative methods, such as piecewise analysis, would be more appropriate to ensure meaningful results.

Down sampling was done in a tree step process:

1. Ensure that there is one timeslot every hour, i.e. constant frequency
2. Interpolate empty timeslots by linear interpolation between known values
3. Select every 6th value

The figure below, visualizes this process. All recorded datapoints are marked with a red solid dot (•), interpolated values (every hour) between these are marked with an small red circle (o) and the chosen values are marked with a large blue circle (O). The line is solid for continuous segments, i.e. a measurement every hour, and the interpolated line is dotted to indicate gaps in the measurement where interpolation has been performed.

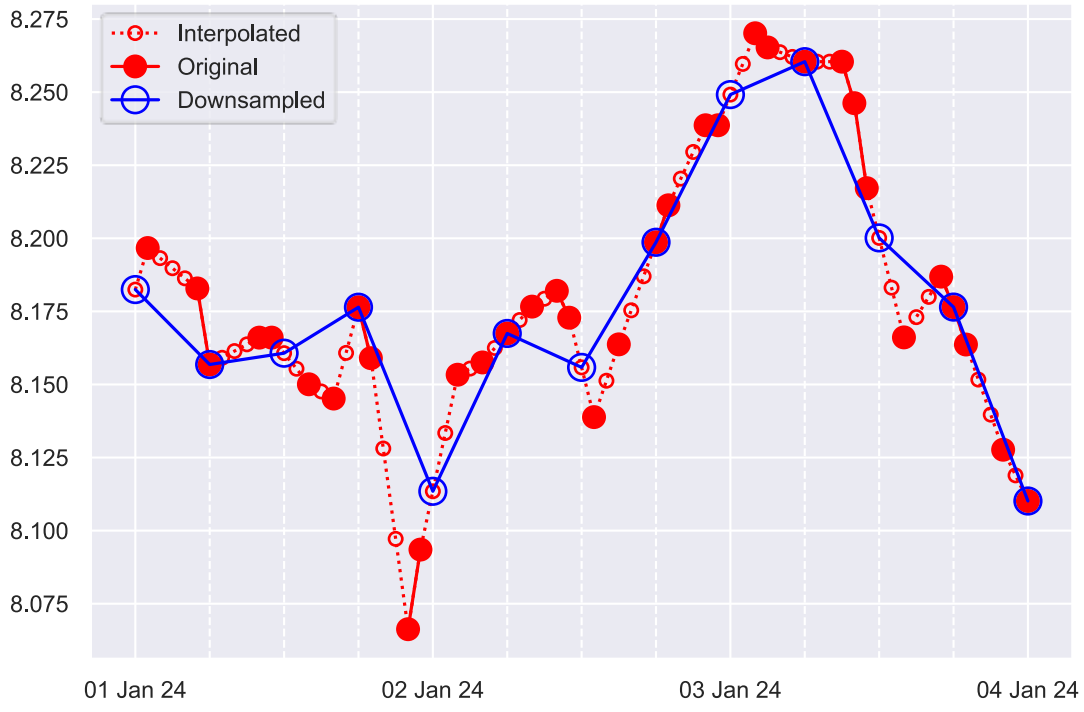

Figure 78: Down sampling of timeseries for Dam A

Note how the new signal, represented in blue with large open circles (O), modifies the original signal. Peaks are smoothed, and local variations are diminished. Whether these modifications alter the data depends on the specific context and the period under consideration. While the plot above appears heavily smoothed, recreating the same line plot over a 3-year span reveals no visible changes. This underscores the importance of reference and scale, as previously discussed.

The Pearson correlation coefficient is a normalized measure of the covariance between two series of data, with values ranging from -1 to 1. A value of 1 indicates perfect correlation, meaning the variables increase simultaneously, though their intensities may differ. -1 indicates a perfect, but opposite behaviour. 0 indicates no covariance between the two.

The plot below shows absolute value of the Pearson Coefficients between all measurements at Dam A. The correlations are mostly in the midrange, but there are more values below 0.1 (shown with a marker "x") than above 0.75 (shown with a marker "◎").

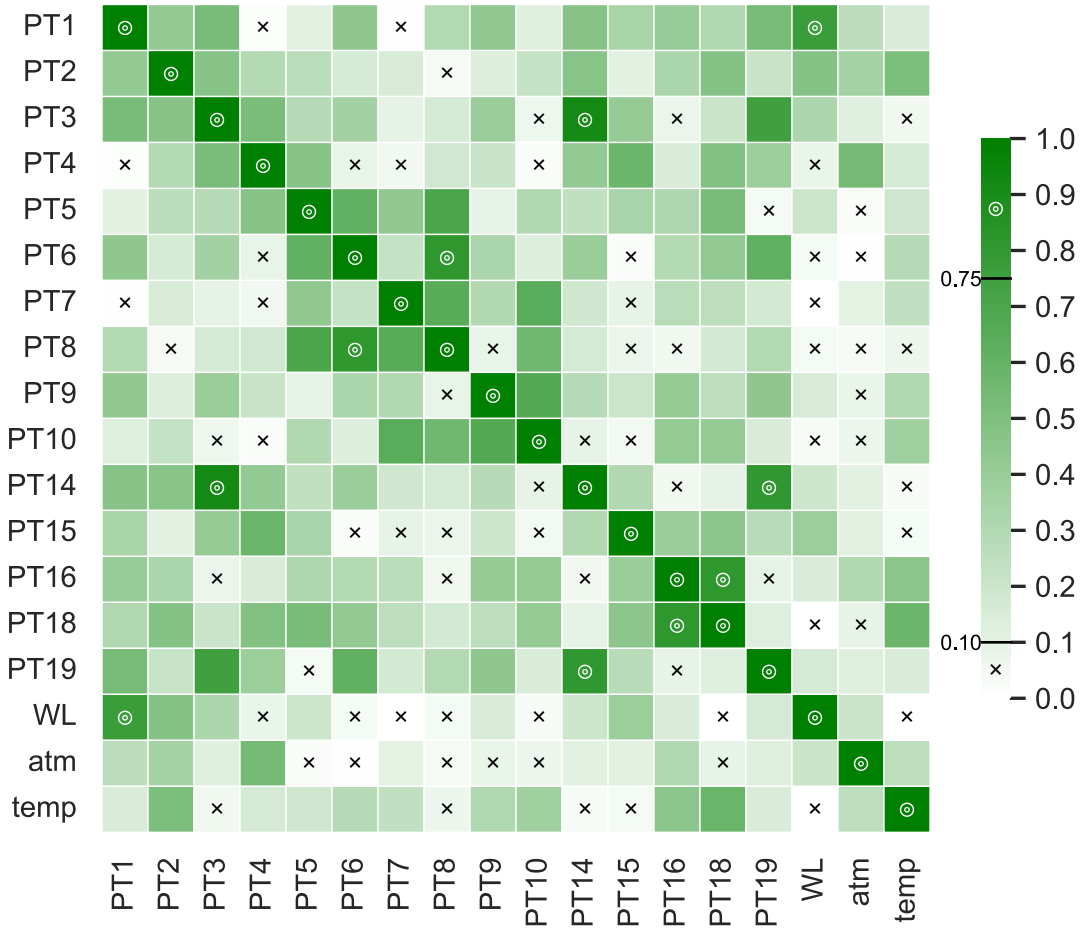

Figure 79. Pearson correlation coefficient - Dam A

In dam design, a linear relationship is typically assumed between water level and pore pressure. Under this assumption, the two variables would be perfectly correlated if the design load accurately reflects real-world conditions. PT1 and water level ("WL" in Figure 79) is above 0.75, highly correlated, as earlier assumed.

However, low correlation values should not be interpreted as falsifying the design hypothesis. Instead, they highlight the flaws of Pearson correlation and emphasize the inherently conservative nature of the hypothesis. This is best illustrated with an example: looking at PT2 and PT3 in the figure below, they are clearly exhibiting the same movement, but the overall trend differs, which is seen as variable spacing between them.

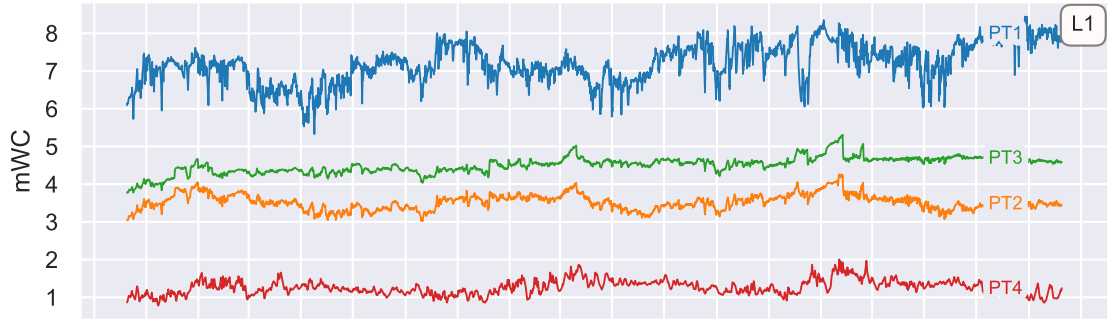

Figure 80: Extract of lineplot

Another source of low correlations is time shifts, which can occur when one variable responds to changes in another with a delay. This is likely not the case for PT2 and PT3, nor for WL and PT1, as observed by visually aligning their data in a zoomed plot. However, it must also be stated that the sampling rate plays a crucial role in detecting such delays.

According to the Nyquist criterion, the sampling frequency must be at least twice the frequency of the fastest-changing signal or the smallest expected lag. For instance, if the lag between variables is on the order of minutes, the sampling rate should be sufficient to capture changes at intervals of half that duration or less. A sampling interval of 30 seconds to 1 minute would generally suffice for detecting lags on the scale of minutes while ensuring that no significant information is lost due to under-sampling.

Given the current measurement data, which has an hourly sampling interval and contains more than half empty cells, time lag analyses are significantly limited. For example, detecting lags of less than two hours would be highly unreliable due to insufficient data resolution and missing values. As the expected lag is likely to be on the order of minutes rather than hours, the current dataset is not suitable for such analyses without additional preprocessing, such as interpolating missing data or collecting higher-resolution measurements.

While time lag analyses may be constrained by the current dataset's limitations, scatter plots and statistical visualizations can still provide valuable insights into potential relationships and correlations between variables. Figure 81 presents such a visualization, breaking down the data into four key components:

1. **Scatterplots – blue dots**
   Scatterplots are displayed in all cells except the diagonal. Each dot represents one measurement, visualizing the relationship between two variables. Scatterplots on opposite sides of the diagonal (e.g., PT1 vs. WL and WL vs. PT1) are mirror images of each other, with the x- and y-values swapped. When the axes are equal, this mirroring appears along the line x=y. A scattered circular or horizontal pattern indicates no correlation, while a clear linear trend suggests strong correlation.
2. **Distributions – blue histogram**
   The diagonal cells show the distribution of each variable as a histogram, providing an overview of its frequency and spread. These histograms offer a quick way to identify the shape of each variable's distribution, such as whether it is symmetric, skewed, or multimodal.
3. **Kernel Density Estimate (KDE) – black contour lines**
   The lower half of the matrix includes a Kernel Density Estimate applied to the scatter data. The KDE generates contour lines that indicate regions with the highest density of measurements. These transparent contours highlight clusters or patterns within the scatter, complementing the raw data points. High correlation is visually identified by elongated, non-overlapping contour lines, whereas overlapping or circular contours suggest low correlation.
4. **Linear regression – black line**
   In the upper half of the matrix, a linear regression line is fitted to the scatter data. This line provides a clear indication of the relationship between variables. When the scatter consists of numerous points, the regression line helps clarify the trend, offering an additional visual aid to assess the strength and direction of the correlation.

Figure 81 does not reveal any entirely new patterns but serves to confirm that WL and PT are correlated. Additionally, it highlights that the water level and PT1 are skewed toward higher values, while the other variables exhibit skewness toward their lower values. This skewness is possibly seasonal, suggesting that a seasonal decomposition of the data could provide valuable insights.

The line plot in Figure 74 further supports the presence of seasonal variations. To explore this, the same operations as in Figure 81 were performed, but this time split by quarter of the year. The results of this analysis are presented in Figure 81.

Examining the scatterplots in Figure 82, a faint pattern emerges where Q1 values tend to be higher than those in Q4. However, this pattern is subtle, and most scatterplots exhibit a widespread distribution, indicative of low correlations overall. Despite this, specific features, such as stripes or clusters in the scatter, hint at the possibility of linear relationships during certain periods. For instance, PT3 vs. PT2 in the lower half of the figure shows stripes suggesting periods of linearity.

The regression lines provide additional insight into these relationships. Among the variables, PT1 exhibits the strongest correlation with the water level, as indicated by its regression trend that is closely spaced and nearly the same gradient. This also indicates that the connection between PT1 and the water is permanent and not changing with season.

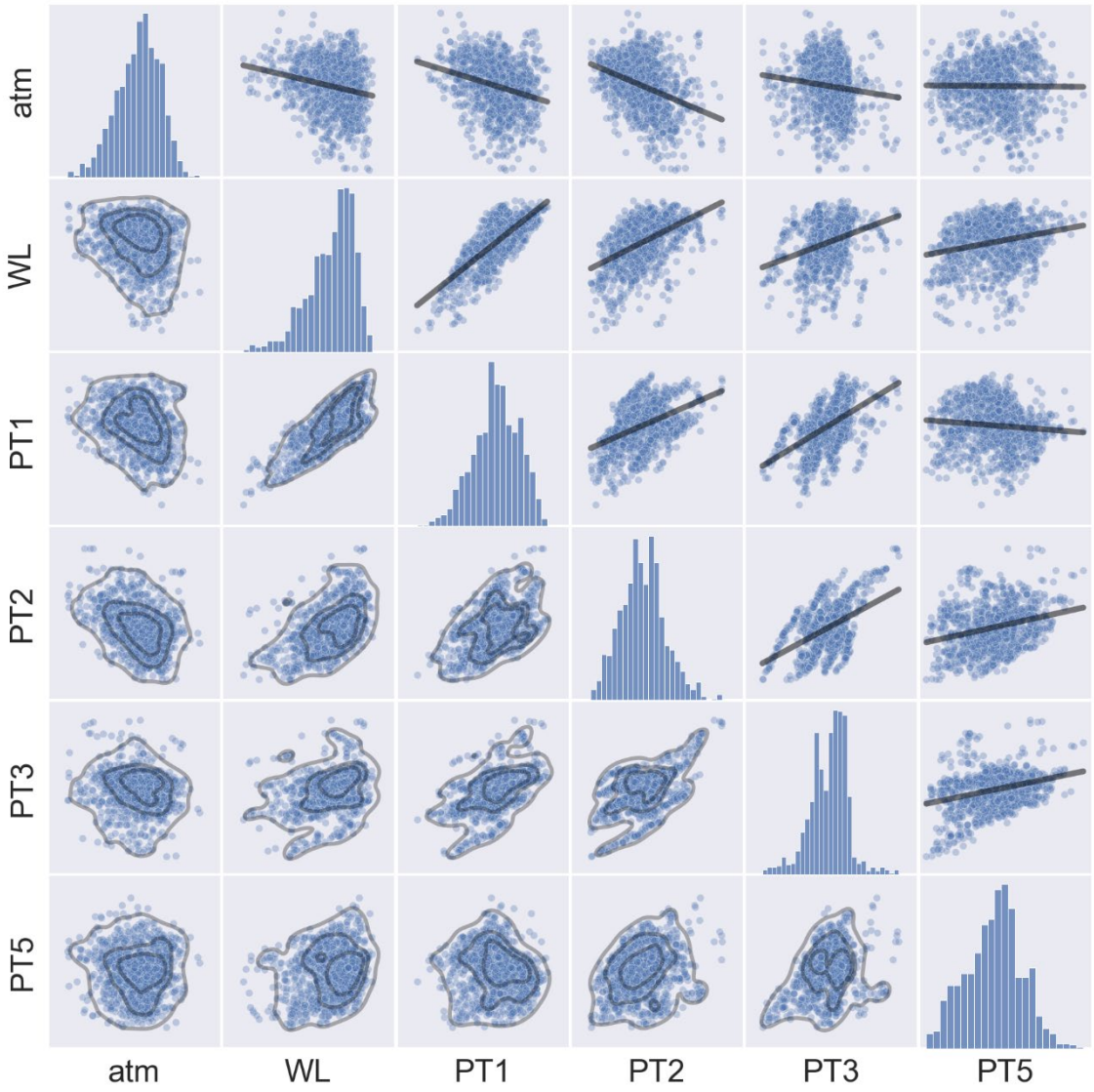

Figure 81: Scatterplot, distribution plot and linear regression

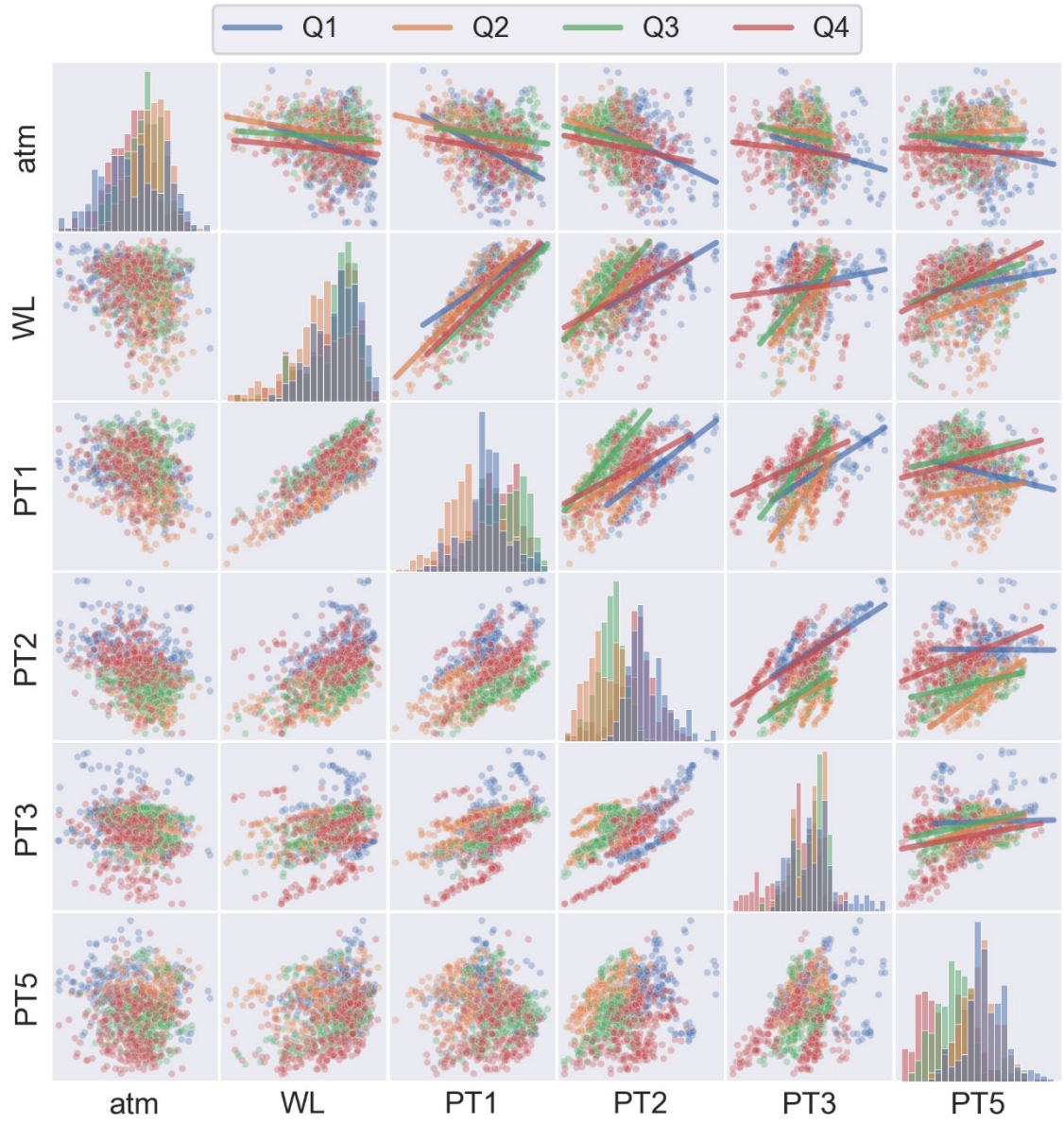

Figure 82: Scatterplot, distribution plot and linear regression per quarter

6.1.4 Assessment of results

The generally massive migmatite and granitic gneiss at this damsite are believed to have very low porosity (< 1%) and hence the permeability of intact rock will also be very low (< 10-9 m/s). In practice, water flow and pressure build-up therefore can only take place in fractures. If a borehole for piezometer installation is not intersecting any water leading fractures, no water pressure will be measured. Also, water flow in fractures is often concentrated to certain flow channels, and even if no water pressure is measured in a piezometer drillhole, it therefore does not necessarily mean that there is no water present, since the drillholes are relatively few and the monitoring sections have limited lengths. Pressure is measured in a piezometer drillhole, it therefore does not necessarily mean that there is no water present, since the drillholes are relatively few and the monitoring sections have limited lengths.

All piezometers are in drillholes near the baseplate, i.e. between sections D and G. The piezometer drillholes according to (Dr.techn.Olav Olsen, 2024) have lengths between 1.50 and 4.50 m (0.50-4.50 m drilled in rock), and almost all are vertical. The depth, placements and numbering of piezometers are described, but there are values and information in the data that makes us uncertain if it is true. Vertical drillholes may intersect sets of sub-horizontal joints shown in Figure 71 but barely the predominant set of cross joints (set I).

As described above three main joint sets; one consisting of sub-horizontal joints and two consisting of steep cross joints, have been identified. In order to obtain measurement data for all joints, the piezometer drillholes have to be drilled such that all sets are being crossed by piezometer drillholes. For evaluation of potential risk of uplift of the base plate of this dam, the theoretically most favourable orientation of piezometer drillholes is inclination 50-60^{o} towards NE. In practice, approximately vertical holes may also work well, Fracture mapping and presentation of mapping data in joint rosette as shown in Figure 71 give a good basis for choosing locations and directions of piezometer drillholes for monitoring of any pore pressure between rock surface and concrete. This illustrates the importance of geological mapping to obtain a reliable basis for deciding optimum localization and number of piezometers.

The measured values in dam A show that there is pressure contribution linked to the water level for PT1 in axis L1. PT 2 in the same axis is somewhat related to the water level, but its amplitude is hardly changed by a significant change in the water pressure. The most reasonable explanation is that the sensor PT1 is intersecting a rock joint. The relatively small change in PT 2 (and PT3 further upstream) is difficult to guess. It is also interesting to note that PT4 close to PT1 (and downstream PT3) does not measure any pore pressure. This indicate that the measurements in PT1 is very local and probably connected to a rock joint. The measurements in PT3, do indicate a pore pressure, but do not show a close connection with the upstream water level. This can indicate that the sensors are connected to a rock joint along the dam axis and not connected with the reservoir.

Ideally, if all joint sets were mapped and instrumented and transition zones between the joints were instrumented, a small area load combined with line loads from each joint would most precisely model the load on the structure from pore pressure. For instance, transverse cracks and joints in the rock or concrete combined with poor casting can result in a significant pressure in rock joints. There would however be significant uncertainties regarding the mapping of the cracks and the measurements of the pressure. From the measured data from Dam A one cannot state whether or not a triangular distribution is conservative. All measurements are on the downstream half, near edges, possibly not perforating cracks, and show great discrepancy.

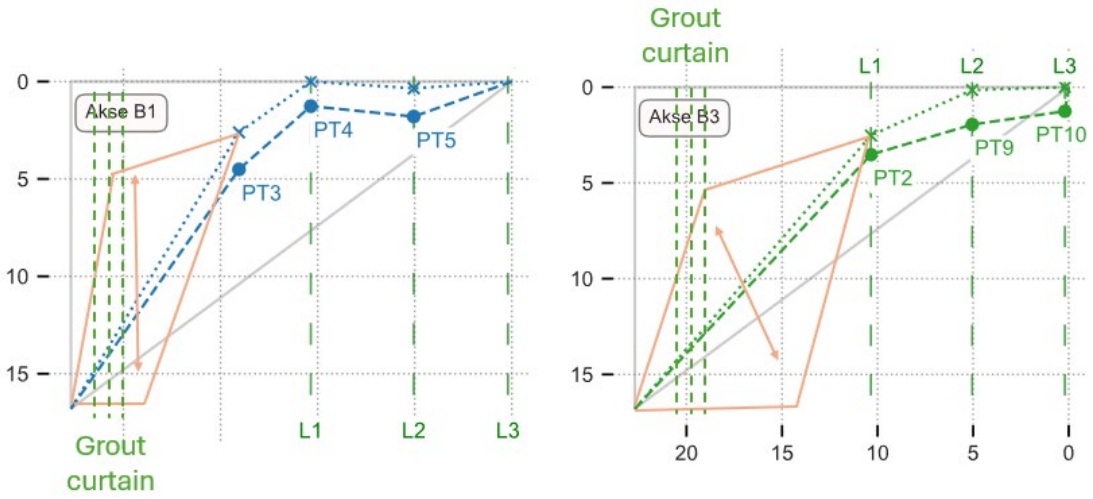

Figure 83: Uncertainty in pore pressure between axis L1 and the upstream side. Downstream of the grout curtain, lower pore pressure is the most likely

Of the 9 sensors located close to the bedrock surface, only one (PT1) show a connection with the reservoir. Further 2 sensors (PT3 and PT2) measure a pore pressure, but there is not a clear correlation with the reservoir fluctuations. In addition, 2 sensors located 3 m below the surface (PT 15 and PT18) indicate seasonal variations and measure a pore pressure. Measurements from PT15 indicate a possible connection with the reservoir, while PT18 show no connection with the reservoir.

Al in all, only 1 of 16 piezometers show a pore pressure that can be connected to the reservoir. It can therefore be concluded that the pore pressure under the dam is not evenly distributed and is generally lower than what is assumed in theory for stability assessments for this dam. The measured pore pressure is local and probably connected to water pressure in rock joints.

6.2 Dam B

6.2.1 General overview of the dam

The dam was built in 1969 with a maximum height of 19 m and a length of about 200 m, originally with 29 buttress sections and gravity sections against the abutments.

The dam was rehabilitated in 2023 and included the following:

- Gravity dam against the abutment: New concrete slab on the upstream side and dam crest
- Slab buttress dam: The area between the original buttress supports throughout the dam was filled with concrete. Against the rock foundation the supports have been expanded to a width of 2 m, so that there is a gallery 3 m onto the rock foundation. The foundation is freely drained as for a traditional Buttress dam.
- Upstream slab: New slab was cast on the upstream side of the original dam.
- Drainage gallery: There is a drainage gallery (box drain) onto the rock foundation throughout the dam. In most of the dam there is a thin concrete slab onto the rock. This slab is drained with 1 m deep drain holes at 1m centre distance. There is no drainage curtain in the foundation.
- Piezometers: There is a total of 24 piezometers installed in 8 of the buttresses supports. All the sensors are placed in inclined 1.5 m boreholes under each buttress support. As the boreholes are inclined the sensors are about 1 m under the rock surface. Installation of the sensors are similar to that of dam C and D.

There is no evidence of foundation grouting.

The leakage from the dam is estimated to 0.1-0.2 l/s.

Figure 84. Downstream side of the buttress dam. The original frost wall and buttress supports are visible form the downstream side. However, upstream the frost wall the whole dam has been filled with concrete, except the lower part over the foundation, where there is an inspection gallery.

Figure 85. Inspection gallery onto the foundation. View to the upstream side and Buttress supports to the left in the picture.

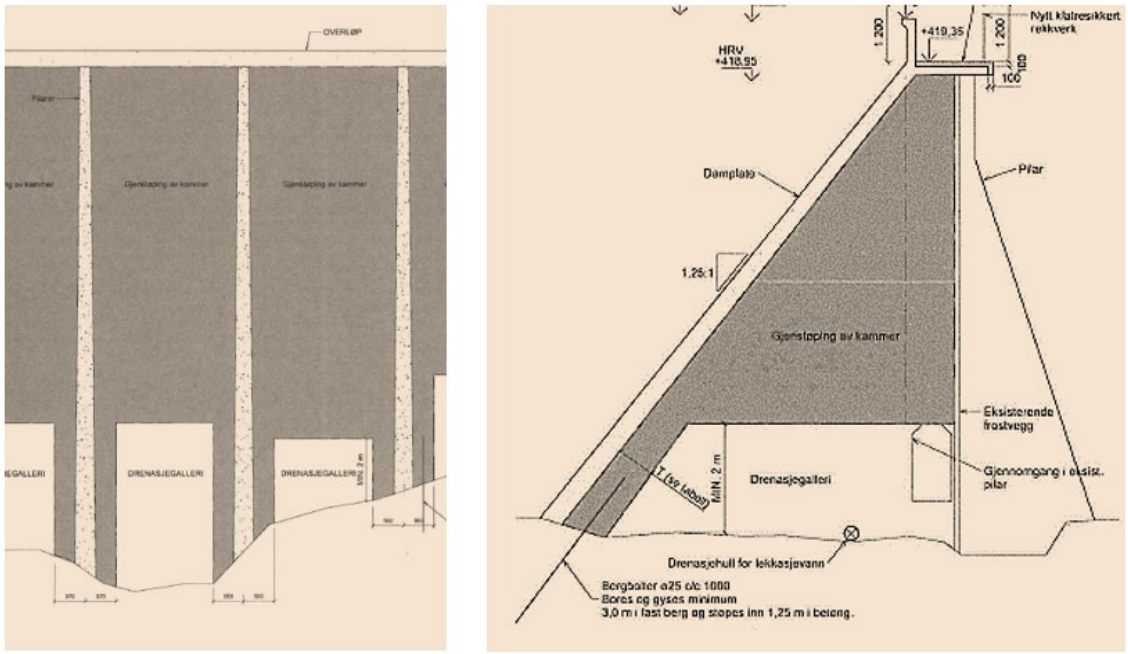

Figure 86. Drawing of the dam. Grey color is the new concrete. Inspection gallery onto the foundation. Left side showing a section of the elevation through the dam from the downstream side. Right side showing a section of the buttress

Figure 87. Drains with leakage. One pipe from each side of the dam

6.2.2 Description of the bedrock

The dam is located in syenite belonging to the Permian, igneous rocks of the Oslo-field, which contains a range of intrusive and volcanic rocks of ages around 250-300 my (NGU, 2024).

The site visit with engineering geological mapping was carried out on 24.6.2024. As basis for the mapping, geological and topographical maps were used (NGU, 2024), (Kartverket, 2024). Note from engineering geological site inspection were also available, plus excerpts from re-evaluation in 2018 and several notes on piezometer locations, monitoring results. (Norconsult, 2020), (Norconsult, 2018).

Norconsult's engineering geological note gives a systematical description of rock mass and water leakage conditions in the hollow sections inside the dam. Their investigations were however aimed primarily on evaluating friction between dam and rock foundation and contains no evaluation of water pressure or potential risk of uplift.

The mapping of the dam foundation in this case was mainly focused on hollow sections inside the dam since surface outcrops were few due to soil cover and vegetation at the surface. Some rock grouting was reported to have been done recently on the western side of the dam. It was informed by the owner that grouting had been done prior to/during construction of the dam as well. The exact extent of this grouting is however not known.

The bedrock at the dam site was found to be homogenous and isotropic, i.e. without any sign of foliation/planar structure, and mainly quite massive. Sub-horizontal joints and sets of steep cross joints were distinct almost all the way along the dam foundation, but typically the character of the rock mass varied from very massive most places to sections, particularly at the western side of the dam, with higher degree of fracturing ("moderate"). Several locations with minor leakage were observed, almost all these seeming to originate from the contact between concrete and bedrock.

Photos illustrating the rock conditions are shown in Figure 88 and Figure 89, and further details on rock strength and fracturing are given below.


Figure 88: Left: massive syenite with fractures forming tabular blocks at eastern side of dam, P27-28 approx.; Right: more fractured rock at eastern part, P18-19 approx.


Figure 89. Left: syenite with 3 distinct joint sets, including sub-horizontal, at central part of dam, P16-17 approx. Right: massive syenite at western part of dam, P5-6 approx.

6.2.2.1 Rock strength

Schmidt-hammer testing was done at three locations and characteristic UCS-values estimated as described in the corresponding section for dam A (chapter 6.1). An estimated rock density of 27 kN/m^3 for syenite has been used in the diagram to find the UCS-value. The results are shown in Table 6-6.

Table 6-6. Results from Schmidt-hammer testing of Syenite.

Location/ rock type	**Test values for R_L**	**Average of 50% highest RL-values**	**Test direction**	**UCS based on Deere & Miller**
Betw. P27-28 Syenite	46-48-40-46-53-66-48-52-58-54 60-62-58-62-50-62-64-54-48-54	60.2	~horizontal	260
Betw. P16-17 Syenite	52-56-50-58-58 46-51-58-53-55 61-46-56-51-54-56-46-58-46-51	57,1	~horizontal	220
Betw. P10-11 Syenite	58-57-63-60 58-58-57-53-53-54 50-56-53-61-51-63-59-54-60-64	60,4	~45° downwards	280

As can be seen from the table, the estimated UCS-values for the syenite are very high, with an average of 253 MPa.

6.2.2.2 Fracture characteristics

Results from mapping of joint orientations based on stereographic projection (se chapter 4.3 for explanation) are shown in Figure 90. As can be seen, sub-horizontal joints dipping gently mainly towards NE (i.e. in direction towards the reservoir) and steep cross joints striking NNE-SSW and dipping steeply towards W (60-80°) represent the predominant joint sets. In addition, there is a second set of cross joints striking NW-SE and dipping steeply to NE (75-90°) or W (70-80°) and, as can be seen from the stereo plot, also some joints in other directions. The joint sets described in Norconsult's report fits fairly well with this (Norconsult, 2020).

Results from mapping of joint orientations based on stereographic projection (se chapter 4.3 for explanation) are shown in Figure 90. As can be seen, sub-horizontal joints dipping gently mainly towards NE (i.e. in direction towards the reservoir) and steep cross joints striking NNE-SSW and dipping steeply towards W (60-80°) represent the predominant joint sets. In addition, there is a second set of cross joints striking NW-SE and dipping steeply to NE (75-90°) or W (70-80°) and, as can be seen from the stereo plot, also some joints in other directions. The joint sets described in Norconsult's report fits fairly well with this (Norconsult, 2020).

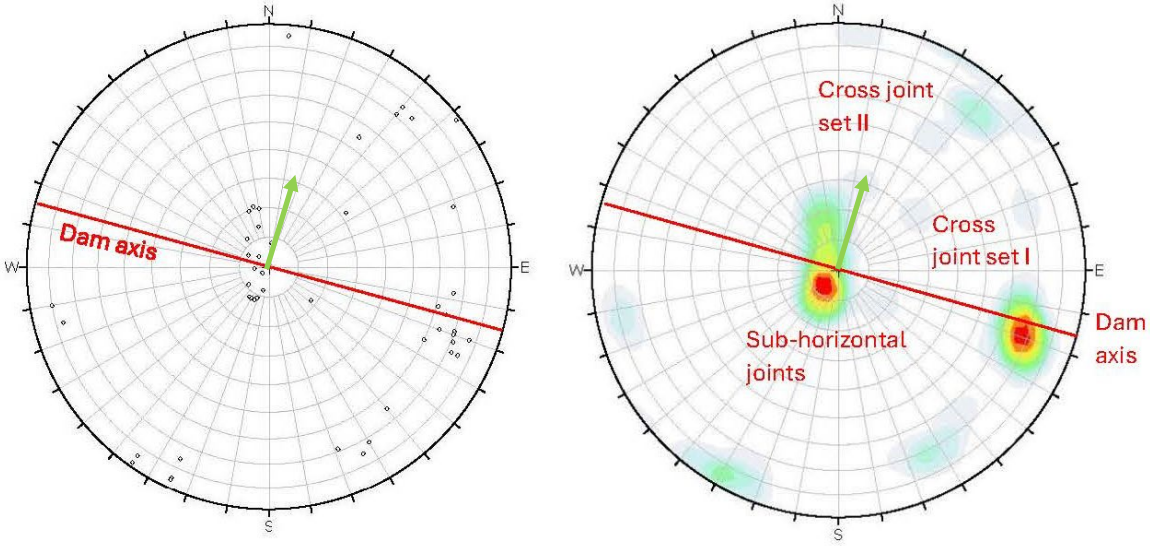

Figure 90. Distinct joints, presented as pole plots (left) and contoured plot (right) with colors representing pole concentrations of 14.4 -16 % (red), 11.2-12.8 (yellow) and 6.4-9.6 % (green), respectively. Green arrow indicates vector of piezometer drillhole (direction/inclination, approx. N15°Ø/60°N according to, drawings B-312 and B-313. Number of measured joints: 49.

The degree of jointing was found to vary from fairly low for most of the dam foundation (as shown in Figure 88 and Figure 89) to fairly high for sections at the middle of the dam (support 14- 16) and on the western side, particularly west of support 4 (as shown in Figure 89). At massive sections the spacing between distinct joints was found to be 1-2 m and more, while for the most fractured sections it was some places down to 10-20 cm.

No signs of faults or distinct weakness zones were observed, neither during mapping inside the dam nor based on surface observations of the river downstream of the overflow weir.

The sub-horizonal joints are quite distinct and continuous, with persistence of several meters, perhaps up to 5-10 m and more (exact measurement not possible due to limited area of outcrops) and in theory may cause buildup of considerable uplift pressure. Even though these fractures are favourably inclined with dip towards the reservoir, they may be fed by water from the steep cross

joints. The conditions inside the dam at the time of the geological mapping were quite humid, but the total leakage from the dam was reported to be rather low (as could also be observed at the monitoring point during this site visit).

6.2.2.3 Classification

Rock mass classification based on the RMR system, as described in chapter 4.4, has been done for selected, representative locations. In selection of "Rating adjustment" factor main emphasis has been placed on consideration of water leakage and potential uplift pressure. The results are presented in Table 6-7 below. As can be seen, the ratings for two of the locations classify as "Good" (P25-26 at the lower end, and P10-11 at the upper end of that class, respectively), and the rating for P16-17 classifies as "Fair".

Table 6-7. Estimation of RMR for selected locations.

Location	**Betw. P25-26 massive syenite**	**Betw. P16-17 more jointed syenite**	**Betw. P10-11 massive syenite**
1 Rock strength (UCS)	15	12	15
2 RQD	17	8	17
3 Joint spacing	15	10	15
4 Joint condition			
- persistence	2	2	2
-separation	5	5	6
-roughness	3	3	6
-infilling	6	6	6
-weathering	5	5	6
5 Ground water	10	15	10
Rating adjustment	-15	-15	-7
Rating	63	51	76
Class No.	II	III	II
Description	Good	Fair	Good

The Q- and GSI-systems, as explained in previous chapters, are not considered suitable for evaluation of damsites and therefore have not been used systematically in this project. Some reconnaissance estimations have however been done. Based on this, characteristic Q'-values down to approx. 6 have been estimated for most densely fractured sections and up to 50 for the most massive sections, corresponding to "Fair" and "Good - Very good", respectively for J_w and SRF equal to 1. The characteristic GSI-value has been found to be within the range 60-75, i.e. medium to high.

6.2.3 Measurements of pore pressure

Measurements from dam B has been sampled since installation in late 2023. The analysed data contains a little more than one year of measurements with a timestep of 2 hour and 40 minutes between each value. Dam B is in an area with multiple stations relatively nearby and one station approximately 20 km away is used in in the plots.

Figure 91 shows all measurements in a line plot without other adjustments than unit conversion to meter water column, mWC. The plot is divided into 10 subplots whose scale is consistent. This way comparison is easy, especially with reference variables like atm and water level (WL in figures).

Figure 91 shows the same timeseries after subtracting the variation of atmospheric pressure, i.e.:

$$s_{i.adj} = s_i - (s_{atm} - mean(s_{atm}))$$

This operation aims to detect influence of atmospheric pressure on the measurements by looking at the resulting plot as well as comparison with the original. When peaks and valleys corresponding to the atmospheric pressure in Figure 91 are completely smoothened in Figure 92, one can conclude that the measurement has direct contact with air.

Mean values, for all but PT71, are so low that the measured pressure appears to be water column in the bore holes. PT71 have some more fluctuations and almost double the mean value of the remaining sensors. The peaks of PT71 are correlated with the atmospheric pressure although there are other factors influencing this sensor. One hypothesis is leakages/rain/surface water inside the dam in addition to a deeper bore hole.
PT42 and PT43 are clearly not smoothed as the other sensors in Figure 91. Looking in Figure 92 the peaks and values have lower height than the atmospheric pressure and the other sensors. This suggest that the contact with air is restricted, possibly creating a delay and over-/under-pressure relative to the atmosphere.
The water level gets more variable when atmospheric pressure adjustment is performed. This suggest that the sensor is ventilated, i.e. already adjusted.

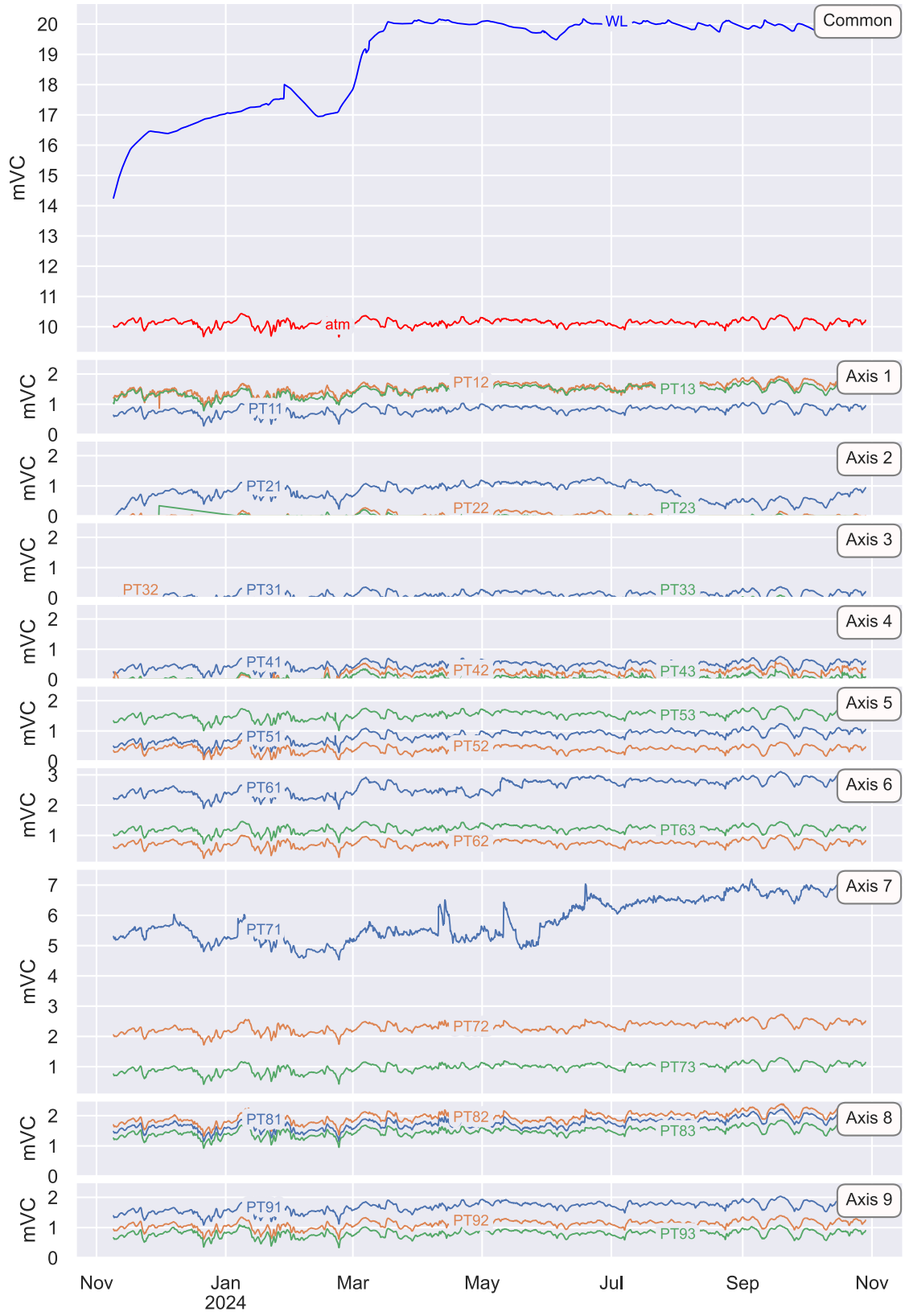

Figure 91: Line plot all axes Dam B.

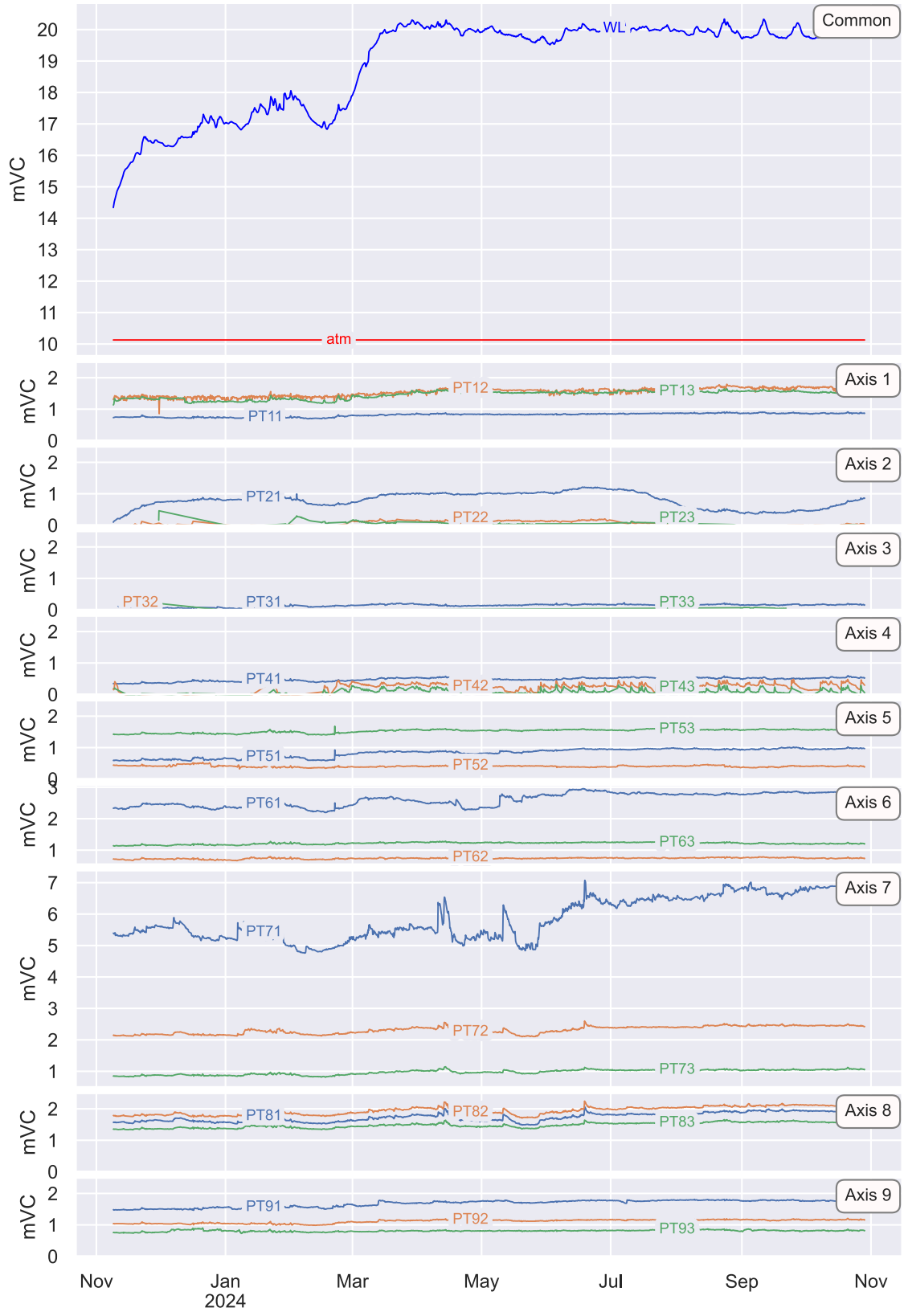

Figure 92 Line plots all axes Dam B – adjusted.

6.2.4 Assessment of results

As for Scandinavian hard rocks in general, also the syenite at Dam B is believed to have very low porosity (< 1%) and hence the permeability of intact rock will also be very low (< 10^{-9} m/s). In practice all water flow and pressure build-up will therefore take place in fractures, and if a borehole for piezometer installation is not intersecting any water leading fractures, no water pressure will be measured.

According to (Norconsult, 2019) drawing. B-312 and B-313, piezometer holes have been drilled at 60° inclination upstream of each Buttress support and vertically at the gate hatch. This corresponds to borehole direction/inclination of N15°E/60°NW and N0°E/60°NW, respectively, which is favourable with respect to the predominant sub-horizontal joint set (which is also the most decisive regarding risk of uplift pressure). The directions are less favourable for intersecting cross joints.

The lengths of the piezometer monitoring sections in rock are also here only 1 m, which is very short for a situation where the typical fracture spacing is in the range 2 m and more.

To increase the probability of intersecting water leading fractures, the direction for drilling should be selected based on data from joint mapping as presented in stereo plot. At this damsite the main fracturing, as shown in Figure 90, is sub-horizontal, and the directions of the piezometer drillholes are quite favourable, although vertical (or around 80° inclination towards NE) would be the optimum for monitoring holes (as well as drain holes), It should be reconsidered whether a hole length of 1.5 piezometer drillholes is sufficient.

The measured data show that variation is most related to the outside atmospheric pressure. Several piezometers are placed right next to borehole for drainage. We believe that the measurements are measuring the depth of the sensor and if present water inside the dam. The measurements show no indication of being linked to the water level in the reservoir. If the sensors were placed further away from the drainage and in according to a geological mapping measuring both at and between joints, small values would have indicated a well-functioning drainage in the dam.

Because all sensors have contact with air one can conclude that the measurements made are not of pore pressure, but rather borehole water columns. However, this does not directly mean that the drainage of the dam is proven effective. The image below shows a red arrow and a red circle depicting the bore hole of the sensor and the drainage hole. The distance between the sensor and the drainage hole is small and one can therefore expect contact with the water column in the bore hole if rock or concrete has crack. The hole may be tilted, giving some distance, but distance between free edges or drainage holes should be maximized to ensure that peak pore pressure is captured in measurements.

Figure 93 Picture of sensor and bore hole location/Cutout from drawings

6.3 Dam C1 and C2

6.3.1 General overview of the dam

Both dams were built in the 1950s, with the following dimensions:

- Dam 1: Hight of 12 m and length approx. 110 m
- Dam 2: Hight of 6 m and length approx. 25 m

The dams were rehabilitated in 2020 and included the following:

- Gravity dam against the abutment: New concrete slab on the upstream side and dam crest
- Slab buttress dam: The area between every other buttress support was filled with concrete, so that the buttress supports are about 5-6 m wide, while the center spacing between the supports are 10 m.
- Drainage gallery: Downstream the slab and upstream the buttress supports, are drained (box drain), and there is access to the opening through holes that are core-drilled through the old supports (hole of diameter 650 mm)
- Piezometers: There were 2 piezometers installed 1 m in the rock under each buttress support. In total 28 sensors.

There is not found any evidence that the foundation has be grouted and there is almost no visible leakage.

Figure 94. Dam C1, downstream side of the buttress dam, with gravity sections towards each abutment.

Figure 95. Dam C2, from downstream side. Gravity sections towards each abutment.

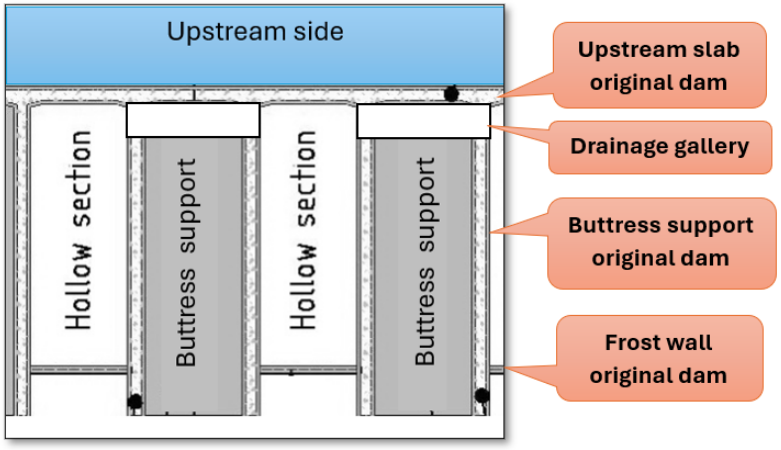

Figure 96. Plan view - typical outline of the dam

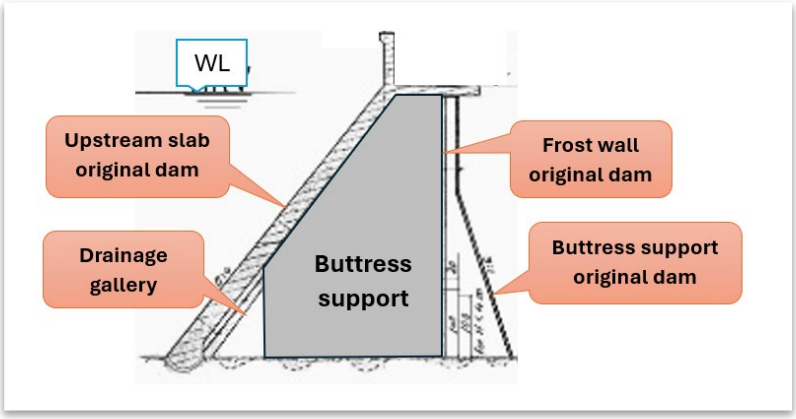

Figure 97. Section through the buttress (cast between the supports in the old dam)

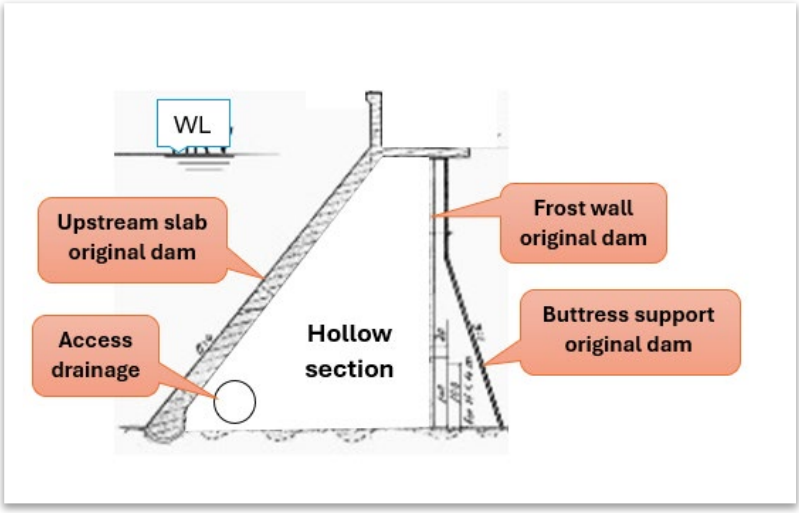

Figure 98. Section through the hollow section between the supports.

Figure 99. Dam C1 - leakage from the dam with full reservoir, about 0.1 l/s.

6.3.2 Description of the bedrock

The project is in bedrock belonging to the South-Norwegian Precambrian region, witch according to NGU here consists of shale, gabbro and amphibolite as shown in Figure 100.

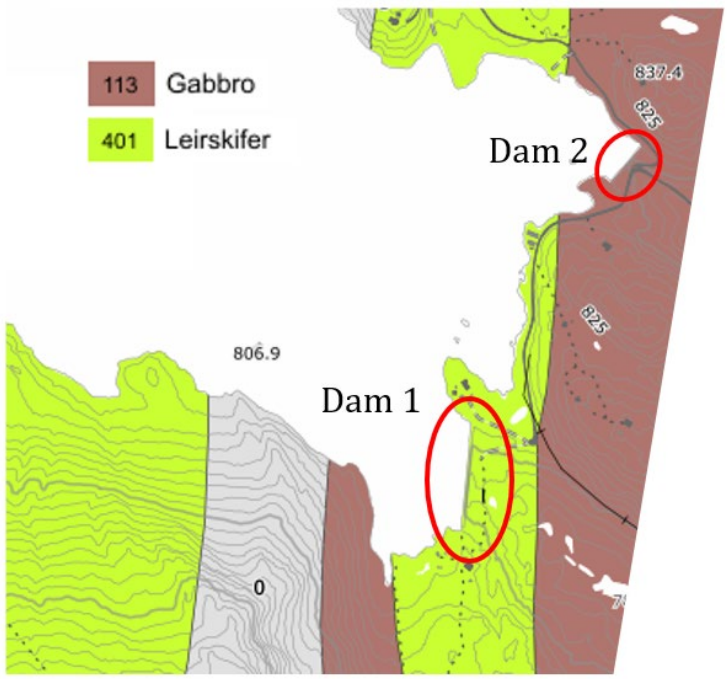

Figure 100. Geological map of the area, with the locations of the two dams indicated with red circles. Color codes: brown for gabbro and amphibolite, green for shale, yellow for quartzite and grey for area covered by soil (NGU, 2024)

Site visit with engineering geological mapping was carried out on 05.06.2024. As basis for the mapping, geological and topographical maps were used (NGU, 2024), (Kartverket, 2024). Reports with brief description of geology and drawings of dam where also used (Norconsult, 2021).

Engineering geological mapping was carried out for accessible locations inside the dam as well as for available outcrops at the downstream side of the dams. At dam 1 It was found that the bedrock was not a shale as indicated on NGU's geological map above, but a massive amphibolite/gabbro without distinct schistosity as would be seen in a shale. A certain, but not very significant, tendency of planar structure/ banding was observed at some, few places. At the central part of dam 1, migmatite could be an appropriate term.

At dam 2 the bedrock was similar to what was is described above for dam 1, but even a bit more massive.

The degree of jointing was generally low at both dam sites, with persistent rough cross joints representing the most distinct joint set. and not joints along the planar structure/foliation. Photos illustrating the rock conditions at the two dam sites are shown in Figure 101, Figure 102 and Figure 103. Further details on rock strength and fracturing are given below.

Figure 101: Dam 1: Amphibolite with visible foliation at hollow section between support 3-4.

Figure 102. Dam 1: Very massive amphibolite at chamber between support 5 and 6 (left) and mixture of massive and more fractured amphibolite/migmatite at the entrance to hollow section support 5-6 (right).

Figure 103. Dam 2: Very massive amphibolite between P7-Ø1 (left) and migmatite at N-end (right).

6.3.2.1 Rock strength

As discussed in Chapter 4, rock strength is not the most important factor regarding rock mass permeability and water leakage. It is however one of the input parameters for calculating RMR and therefore was included in the site mapping based on index testing with Schmidt hammer (as described in Chapter 4.5 of this report).

The testing has been performed according to ISRM-standard, i.e. 20 single tests with type-L hammer and the characteristic Schmidt-hammer value R_L calculated as the average of the 50 % highest single values (ISRM, 2015). The diagram in Table 4-2, with estimated rock density 30 kN/m^3 is used to find the UCS-value. The results are shown in Table 6-8.

Table 6-8. Results from Schmidt-hammer testing of dam 2 rock.

Location/ rock type	**Individual R_L-readings**	**Average of 50% highest R_L-values**	**Test direction**	**UCS based on Deere & Miller**
Betw. P7-Ø1 Amphibolite	50-44-35-40-42-40-46-42-44-38 40-44-38-38-44-54-44-48-38-44	45.6	~45° downwards	155
At N-end Migmatite	32-34-38-38-34-30-42-34-32-38 32-46-40-32-38-40-34-38-30-34	39.0	As above	110

Due to malfunctioning of the Schmidt hammer during this site visit, testing according to the standard procedure was possible only for the two locations shown in Table 6-8, both at the N-end of dam 2. For other locations where classification based on RMR was performed, UCS was estimated based on experience and evaluation of results from Schmidt hammer testing from dam 2.

6.3.2.2 Fracture characteristics

The rock mass at both dam sites was found to be generally quite massive with low degree of jointing. Foliation/planar structure, which is often representing the main joint set, could be observed only a few places, i.e.at dam 1 between support 3 - 4; 4 - 5; and 15 - 16 and at dam 2 between support 3-4. The few distinct joints in this direction were tight and not very continuous. Sub-horizontal joints were not commonly observed, but appeared locally, particularly between support 9-12 in dam 1.

Cross joints, i.e. joints crossing the rock structure, were predominant at both dam sites and had a length/persistence of several meters. Most cross joints were quite rough. The joints in general were found to be very tight and impermeable. Practically no seepage from joints were observed, except for a minor exception for the area between support 5 and 6 at dam 2 where a small seepage seemed to come from a cross joint with aperture a few tenth of a mm. The main conclusion is however that the rock mass at both dam sites had very little leakage, even though according to the dam owner, no rock mass grouting has been done.

Results from mapping of joint orientations presented in stereographic projection (see chapter 4.3 for explanation) are shown in Figure 104 and Figure 105. for dam 1 and dam 2, respectively. As can be seen, steep cross joints (dip angle 70-90°) represent the predominant joint set at both dam sites, with strike/dip ENE/70-90°NNW at dam 1 and NE-SW/70-90°NNW at dam 2.

Foliation/planar structure was observed to be less distinct, although visible in some places. At dam 1 strike NNE-SSW to NNW-SSE and dip 70-90°E (occasionally 70-90°W) is most common for this type of structure/jointing, as would be expected based on the orientations of rock formations shown in Figure 100. It is also partly coinciding with Joint set S2 in Norconsult's report. At dam 2 foliation/planar structures are scarcer and have orientation ENE-WNW/60-90°N (occasionally 60-90°S), which is quite different from that at dam 1. This might be due to folding, or also by the fact that due to limited number of outcrops few joints were possible to measure at dam 2.

Sub-horizontal joints were scarce but occasionally observed at dam 1.

At both dam sites the degree of jointing is mainly quite low, with spacing between distinct joints of 1-2 m and more. Some places have less spacing, down to 40-50 cm. Particularly this is the case at the foundation for highest part of dam 1. The jointing at the two damsites has been found to be quite unsystematic/ random, as expected for the actual rock types and the complex tectonics of this region.

The main conclusion based on this engineering geological mapping is however that the bedrock at the foundation of these two dams however must be characterized as very massive, as will also be reflected by the results for rock mass classification in next chapter.

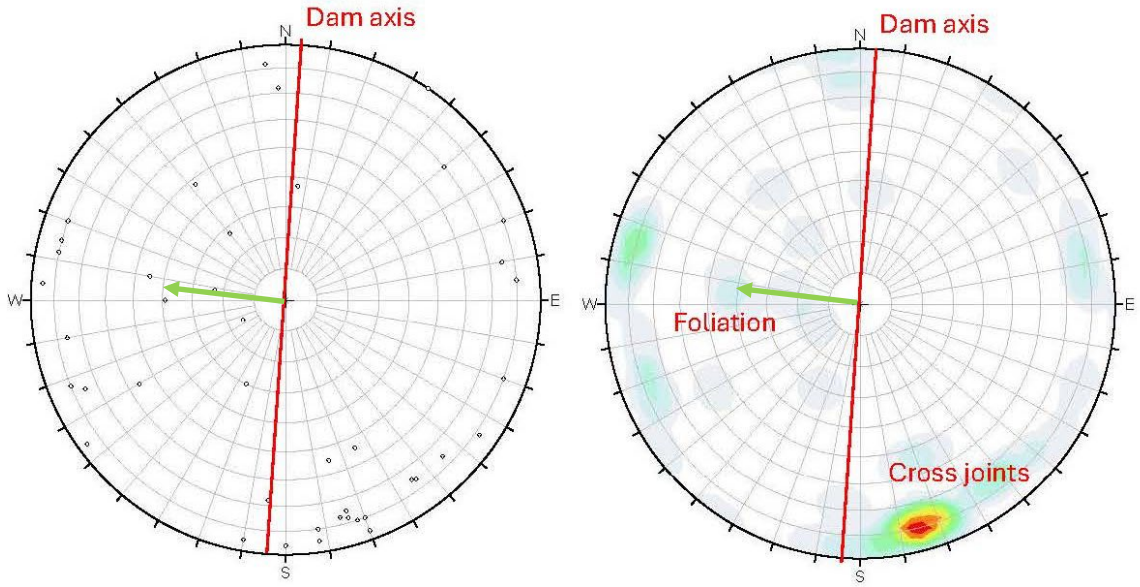

Figure 104. Distinct joints mapped at dam 1 presented as pole plots (left) and contoured plot (right) with the colours representing 13-15 % (red), 10-12 % (yellow) and 6-9 % (dark green) pole density, respectively. Green arrow indicates vector (direction and inclination) of piezometer drillholes. Number of joints mapped: 42.

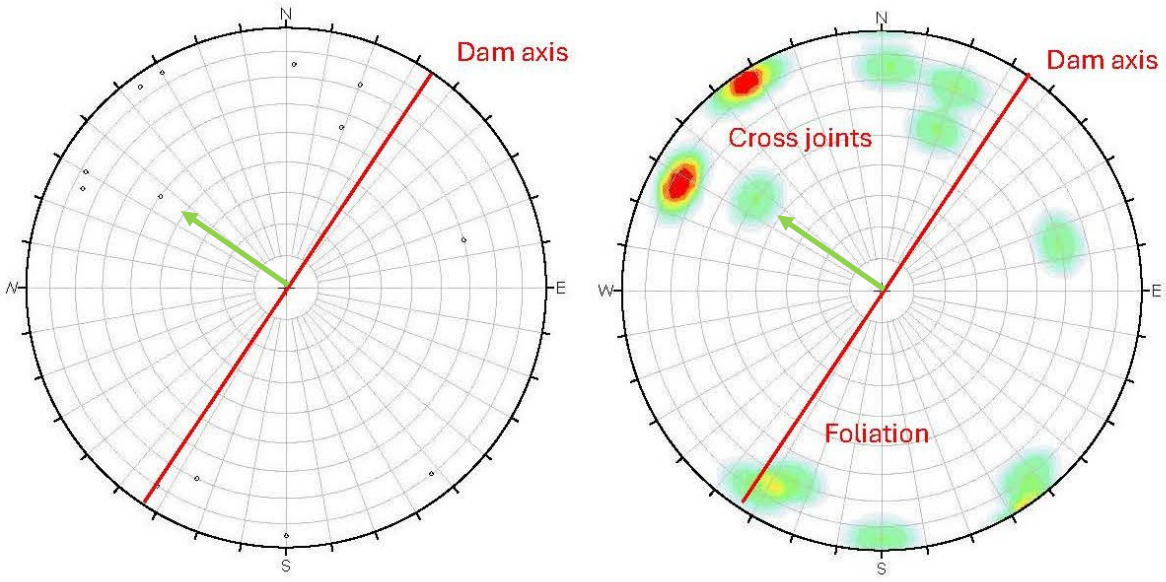

Figure 105. Joints mapped at dam 2 presented as pole plots (left) and contoured plot (right) with the colours representing 13-15 % (red), 10-12 % (yellow) and 6-9 % (dark green) pole density, respectively. Green arrow indicates vector (direction and inclination) of piezometer drillholes. Number of joints mapped: 13.

At both dam foundations cross joints as well as foliation joints are so steep that problems due to uplift pressure caused by these are not regarded realistic. Such joints may however in theory feed water down to sub-horizontal joints which have been observed at dam 1 (shown in Figure 105. as poles plotting close to the centre of the stereonet).

6.3.2.3 Classification

Rock mass classification, primarily based on the RMR system, has been done for selected, representative locations as described in chapter 4.4. The results are presented in Table 6-9 below.

Table 6-9. Estimation of RMR for selected representative locations at dam 1 and 2.

Location	Dam 1 ratings			Dam 2 ratings	
	Betw. P3-4	**Betw. P5-6**	**Near P11**	**Betw. P7-Ø1**	**At S-end**
1 Rock strength (UCS)	12	12	12	12	12
2 RQD	20	20	17	20	20
3 Joint spacing	15	18	15	20	15
4 Joint condition					
- persistence	2	2	2	4	2
-separation	6	6	6	6	6
-roughness	5	5	6	5	6
-infilling	6	6	6	6	6
-weathering	6	6	6	6	6
5 Ground water	10	10	10	15	15
Rating adjustment	-2	-2	-2	0	0
Rating	80	83	78	94	88
Class No.	II	I	II	I	I
Description	Good	Very good	Good	Very good	Very good

As can be seen from Table 6-9 the ratings are good and very good for both dams, with slightly better results for dam 2 than for dam 1. The two locations at dam 1 which classify as Class II "Good" are however also very close to class" Very good" (the lower limit is at 80/81).

As discussed in chapter 4 the Q-system, which is very commonly used in many countries (including Norway) is not considered suitable for evaluation of damsites and therefore has not been used systematically in this project. Some reconnaissance estimation of Q-value and GSI, which is commonly used also today for rock engineering purposes has however been performed.

Based on this characteristic Q'-values (Q-value with J_w and SRF equal to 0 in the formula $Q = RQD/J_n \times J_r/J_a \times J_w/SRF$) of 20-50- have been found for dam 1 and around 70 for dam 2, which for J_w and SRF equal to 1 corresponds to "Good to very good" and "very good", respectively. The characteristic GSI-value at both damsites is within the range 85-95, which is very high.

6.3.3 Measurements of pore pressure

The measurements used are from the period March 2022 until June 2024. There is a total of 30 sensors when including water level and temperature. Unfortunately, there is a significant number of faulty measurements as well as periods without data. Obvious outliers and noise are removed, and empty timeslots are linearly interpolated with dots in the plot of the measurements in Figure 105. Obvious outliers should have been removed with a validation step before storage.

The plot on the next page, Figure 106, is separated into four subplots with identical scale for comparison between the subplots.

1. Common measurements: water level (WL) and atmospheric pressure (atm)
2. dam 1 [1]: dam 1 measurements that appears to have a strong influence from atm
3. dam 1 [2]: remaining measurements from dam 1
4. dam 2: all measurements from dam 2.

It visually clear that all pore pressure values are low and exhibit very low variation compared to the water level fluctuation in the magazine. The water level varies by approximately 13 meters, while the measured pore pressure values remain mostly stable, with variations limited to about 2 meters. This suggests that the sensors are not responsive to changes in the water level. There are several possible explanations for this lack of response: effective drainage, a non-permeable rock foundation, or unrepresentative measurements. Although the exact cause cannot be definitively determined, it is clear that there is no connection between the pore pressure values and the water level.

One hypothesis is that these measurements show water column in the bore holes, especially considering that all measurements are in the range of normal bore hole depth. Note, however, that there are negative values, suggesting that the data have already been adjusted. There is no available documentation on how these adjustments were made or how the values were calculated.

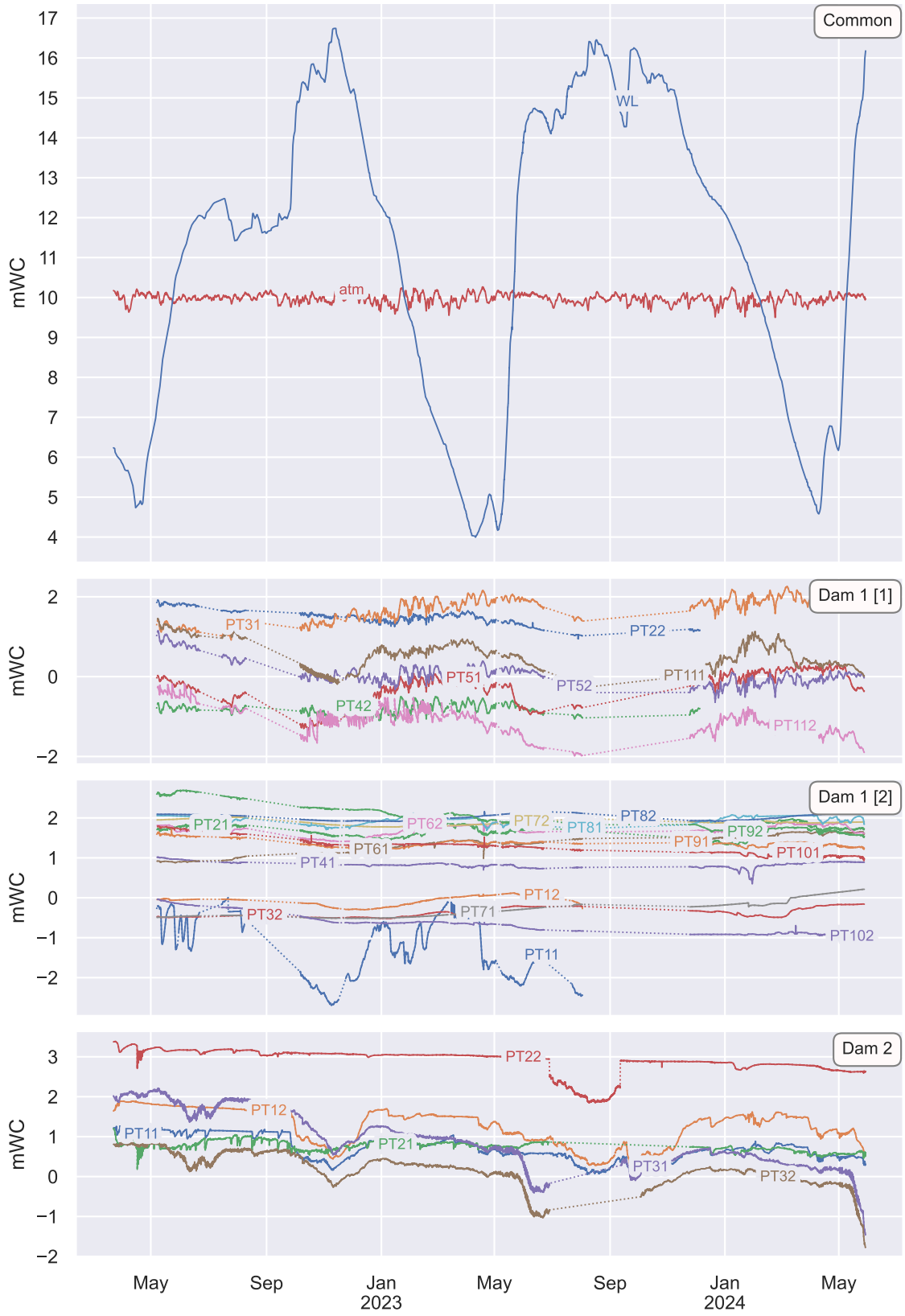

Figure 106: Line plot Dam C (1 and 2)

6.3.4 Assessment of results

As for almost all Scandinavian hard rocks the porosity of the amphibolite/gabbro and migmatite rocks are believed to be very low (< 1%) and the permeability of rock without fractures therefore is also very low (< 10^{-9} m/s). In practice all water flow and pressure build-up will take place in fractures, and if a piezometer borehole does not intersect water leading fractures, no water pressure will be measured.

According to (Norconsult, 2021), two piezometers at each buttress support were to be installed at both Dam1 and 2. Each piezometer borehole was described to be 1.5 m long (with the upper 0.5 m filled with expanding mortar), and to be drilled in direction perpendicularly to the dam axis and with an inclination of about 50° as shown in Drawing SO-B-207 and S2-B-404, respectively of the Norconsult document.

This corresponds to borehole direction/inclination of N273°E/50°W for Dam 1 and N305°E/50°NW for Dam 2, respectively. For the mapped fracture sets at Dam 1, as shown in Fig. 100, the borehole direction is favourable for intersecting foliation joints, but not for intersecting the predominant set of cross joints. For dam 2 the orientation of piezometer boreholes is favourable for intersecting cross joints, but not for intersecting foliation joints.

The lengths of the monitoring sections of piezometer boreholes have been only 1 m. This is very short for a situation where the typical fracture spacing is in the range of 0.6-2.0 m at dam 1 and 0.6-2 m and more at dam 2.

Thus, for the massive rock mass, with short piezometer drillholes and orientations as described in the Norconsult report, the probability of intersecting water bearing fractures was basically quite small (Norconsult, 2021). To increase the probability of intersecting water bearing joints, the direction of boreholes should be based more on data from joint mapping, and the lengths of piezometer drillholes should be increased beyond 1.5 m.

The data for both of these dams show small values typically less than 2 mWC and about half is negative values. The negative values indicate that something is wrong either with the calibration of the sensor, calibration regarding the installation depth or that something is wrong whit the sensor.

The low values may indicate that no sensor is intersecting rock joints.

It is important that the values from the instrumentation are validated and that calibration from installation is well documented.

6.4 Dam D

6.4.1 General overview of the dam

The dam was built in the 1965/66 with a maximum height of 14 m and a length of about 90 m. The original dam was built with 15 buttress sections and gravity sections against the abutments.

The dam was rehabilitated in 2020 and included the following:

- Gravity dam against the abutment: New concrete slab on the upstream side and dam crest
- Slab buttress dam: The area between every other buttress support in the original dam was filled with concrete, so that the buttress supports are about 5-6 m wide, while the centre spacing between the supports are 10 m. in total there are 7 new buttress supports.
- Upstream slab: New slab was cast on the upstream side of the original dam.
- Drainage gallery: Downstream the slab and upstream the buttress support, is drained (box drain). There is access to the opening through holes that are core-drilled through the old supports (hole of diameter 650 mm)
- Drainage curtain: Two drainage holes were drilled in front of each new buttress support (not in the hollow sections). Depth of holes equals to 50 % of the hydrostatic water pressure.
- Piezometers: There were 2 piezometers installed 1 m in the rock under each buttress support. In addition, 5 piezometers were placed on the interface between the rock and the new buttress support. In total 19 sensors.

There is no evidence of foundation grouting.

The dam has no visible leakage, but there are areas with accumulated water in part of the gallery, and some moist patches in the gallery.

Figure 107. Downstream side of the buttress dam, with gravity sections towards each abutment.

Figure 108. Upstream side with new concrete slab.

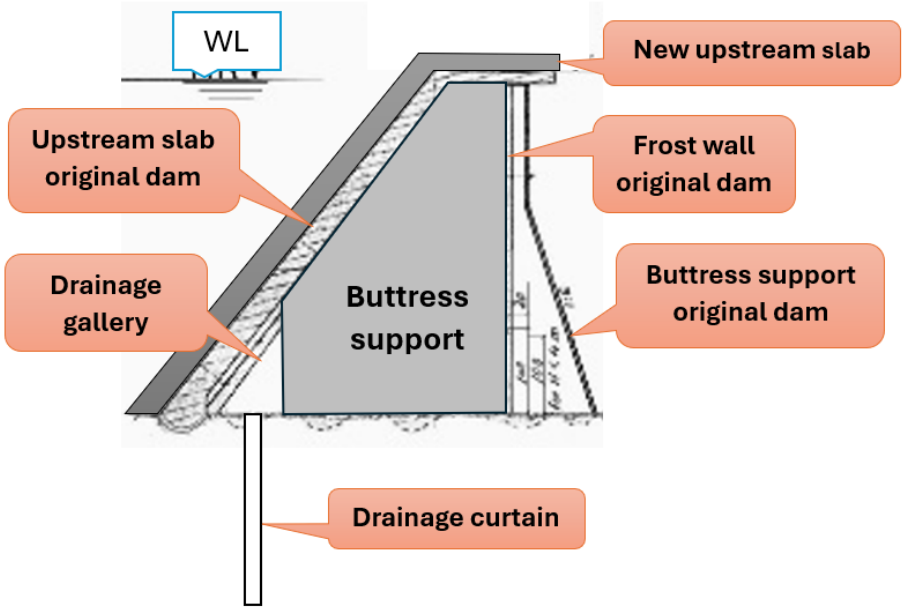

Figure 109. Section through the buttress with drains.

Figure 110. Drainage gallery in front of buttress.

Figure 111. Some of the drains have water seepage with mud-like material from borehole.

Figure 112. The highest section of the dam. No visible leakage, but seepage through the foundation makes the surface moist.

6.4.2 Description of the bedrock

This dam is located in Precambrian bedrock belonging to the South-Norwegian Precambrian region, which is dominated by gneisses. The area at the damsite is dominated by amphibolitic gneiss and felsic (light colored) volcanic rocks of ages around 1510-1560 my (NGU, 2024).

The site visit and engineering geological mapping was carried out on 6.6.2024. As basis for the mapping, geological and topographical maps were used (NGU, 2024), (Kartverket, 2024). Notes from engineering geological site visit were available, plus several other notes more aiming on description of piezometer installation design, dam rehabilitation and geological investigation of other, nearby areas (Norconsult, 2019).

Due to limited accessibility after filling of every second hollow section between supports with concrete, as recommended by Norconsult in the 2018 technical plan, and because outcrops for engineering geologic mapping were few inside the dam, the mapping was performed mainly on surface outcrops at the downstream side of the dam.

The bedrock at the dam site was found to be generally very massive and consisting of felsic volcanic rock (rhyolite) as indicated on the NGU geological map.

Signs of steeply oriented, planar structure/foliation, as illustrated in right part of Figure 113 and left part of Figure 114, were observed several places, although distinct jointing was not always observed to have developed along the foliation. Photos illustrating the rock conditions at the two dam sites are shown in Figure 113 and Figure 114, and further details on rock strength and fracturing are given below.

Figure 113: Left: overview of the dam as seen from south; Right: very massive bedrock with distinct banding near the northern end

Figure 114. Left: massive rhyolite with distinct planar structure/foliation; Right: water inflow with precipitation of mud-like material from borehole, probably originating from the bottom of the reservoir.

6.4.2.1 Rock strength

The Scmidt hammer stopped working the day before this site visit, and no Schmidt hammer monitoring was possible during the mapping.

However, the felsic volcanic rock showed all signs of having a very high mechanical strength. A UCS-range of 100-250 MPa is therefore used in the estimation based of RMR. This is believed to be on the safe side.

6.4.2.2 Fracture characteristics

Results from mapping of joint orientations based on stereographic projection (se chapter 4.3 for explanation) are shown in Figure 115. As can be seen, joints along the foliation/planar structure (with strike direction SSE/NNW and dip 70-90°NE, more rarely towards SW) were found to represent the predominant joint set at this dam site. This orientation is as expected based on the orientations of rock formations/layers shown on the NGU geological map and is also coinciding with Joint set S1 in Norconsult's report (Norconsult, 2019).

Cross joints, with strike direction NE-SW and steep dip mainly towards NW (more rarely towards SE, see Figure 115), were found to be quite distinct too, although less distinct than joints along the foliation. This joint set coincides well with Joint set S3 in Norconsult's report.

Sub-horizontal joints are scarce but have been observed occasionally and can be seen near the center of the stereo plot in Figure 115. This set coincides well with Joint set S2 in Norconsult's report.

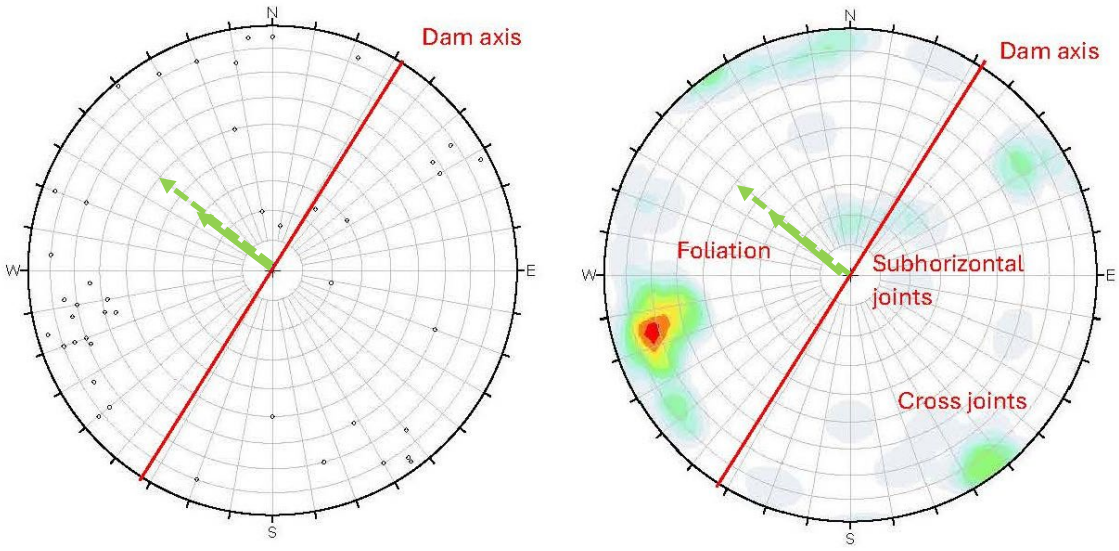

Figure 115. Distinct joints presented as pole plots (left) and contoured plot (right) with the colors representing pole concentrations of 10.8 -12 % (red), 9.6-10.8 % (pink), 8.4-9.6 % (yellow) and 3.6-8.4 % (dark green) respectively. Green arrows indicate vectors (directions and inclinations; N301°E/60°NW and N301°E/40°NW respectively, of piezometer drillholes. Number of measured joints: 44.

The degree of jointing was found to be generally low, with spacing between distinct joints of 1-2 m and more. Some, few places were found to have less joint spacing, down to 10-20 cm. Particularly this was the case at the deepest part of the cleft, where foliation joints were particularly distinct and hollow sections between supports were water-filled. The main conclusion based on the engineering geological mapping is however that the bedrock at the dam foundation must be characterized as mainly very massive.

No visible leakage was observed at the downstream side of the dam. Several of the hollow sections between buttress supports, particularly at the deepest part of the cleft were however quite wet, and a couple of them water filled. It was reported that since the renovation of the dam in 2019 the leakage has been decreasing. A possible reason for this might be that mud-like material as shown in Figure 111 and Figure 114 possibly combined with gouge material from fractures has had a sealing effect.

No faults or distinct weakness zones were observed at this damsite area. The deepest part of the cleft below the dam was however covered by soil and vegetation, and detailed study of this issue therefore difficult.

The main joint sets at the dam foundation are so steep that problems due to uplift pressure caused by these is regarded hardly to be possible. Foliation as well as cross joints may however in theory feed water down to sub-horizontal joints which have been observed at dam 1 and thus are important for the overall evaluation of potential risk of uplift.

6.4.2.3 Classification

Rock mass classification based on the RMR system, as described in Chapter 4.4, was done for selected, representative locations. The results are presented in Table 6-10 below. As can be seen, the ratings for both locations are very good.

Table 6-10. Estimation of RMR for selected locations at dam TA 1.

	N-end	**Betw. P8-9**
1 Rock strength (UCS)	10	12
2 RQD	20	20
3 Joint spacing	20	20
4 Joint condition		
- persistence	2	2
-separation	6	6
-roughness	5	5
-infilling	6	6
-weathering	6	6
5 Ground water	10	7
Rating adjustment	-2	-2
Rating	83	82
Class No.	I	I
Description	Very good	Very good

The Q- and GSI-systems, as explained in Chapter 4, are not considered suitable for evaluation of damsites and therefore have not been used systematically in this project. Some reconnaissance estimation of Q-value and GSI has however been done also here.

Based on this characteristic Q'-values of 20-30 have been estimated for the least massive sections and 50-100 for most massive sections, which for J_w and SRF equal to 1 corresponds to "Good" and "Very good" to "Extremely good", respectively. The characteristic GSI-value has been found to be within the region 75-90, which is high to very high.

6.4.3 Measurements of pore pressure

The measurements are manually recorded and consist of 17 datapoints per sensor from 2019 to today. Sampling rate is not consistent, with a higher number of measurements in 2020, as shown in the figure below. Each recording is marked with a plus (+). Data is not further explored as the number of measurements is insufficient. Current measurements implies that there is contact between the sensors and the atmosphere. Later work should start by checking if PT33 is deeper than the other boreholes.

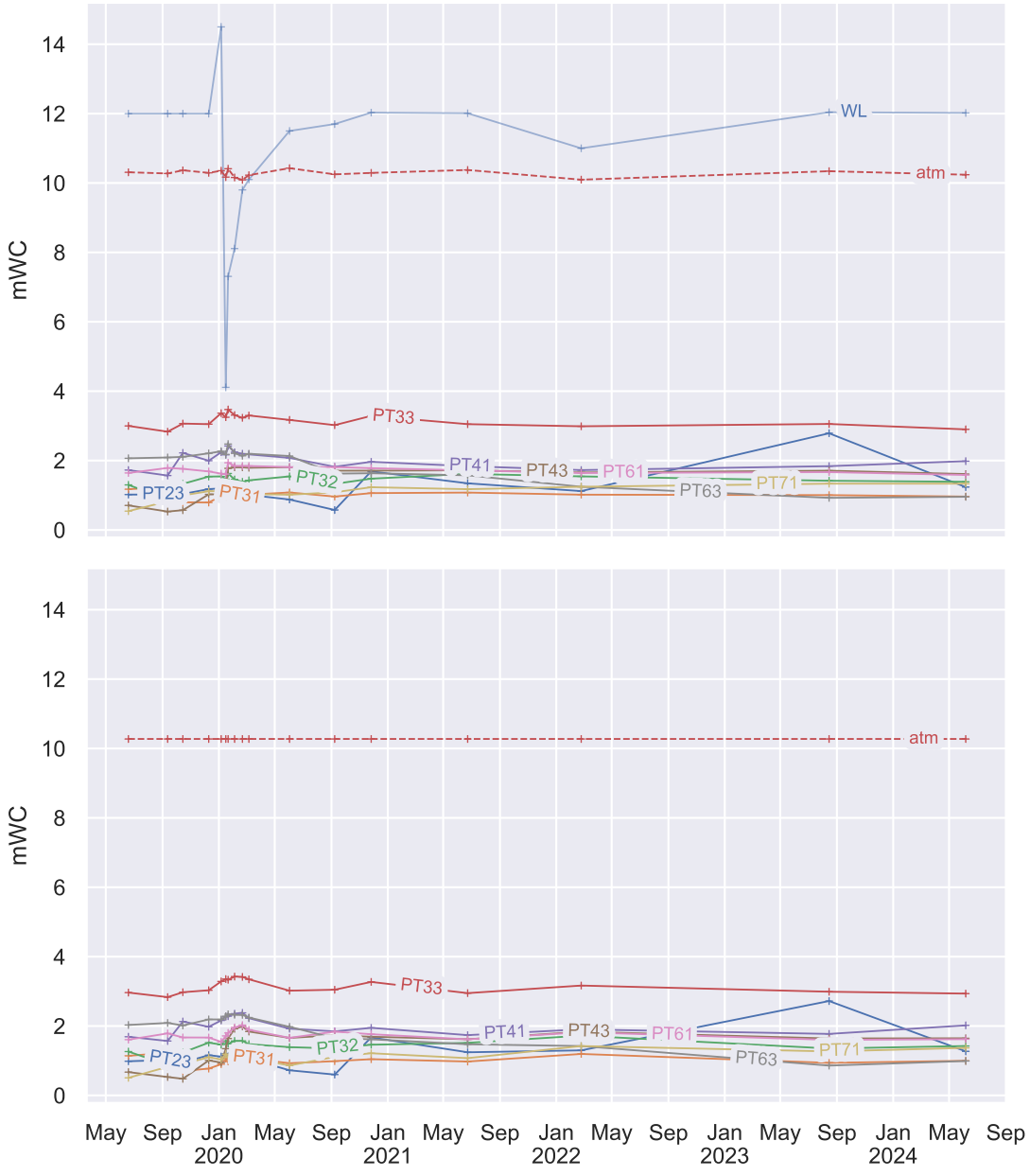

Figure 116: Line plot Dam D

6.4.4 Assessment of results

As for almost all Scandinavian hard rocks the porosity of the amphibolitic gneiss and felsic volcanic rocks is believed to be very low (< 1%) and the permeability of rock without fractures therefore is also very low (< 10^{-9} m/s). In practice all water flow and pressure build-up will take place in fractures, and if a piezometer borehole does not intersect water leading fractures, no water pressure will be measured.

Two piezometers have been installed at each buttress support at a depth of 1 m below the rock surface, and in addition 1 sensor at the transition from rock to concrete at the 5 highest buttress supports. The drilled length in rock according to Drawing no. 103 and 108 from the Consultant are about 1.5 m and the holes are drilled in upstream direction perpendicularly to the dam axis at inclination of 40-60°. This corresponds to borehole direction/inclination of N301°E/60°NW and N301°E/40°NW, respectively.

For the mapped fracture sets, as shown in Figure 115, the borehole directions are moderately favourable for intersecting many fractures, including sub-horizontal joints. The lengths of the monitoring sections in rock are however quite short; only 1 m like at dam C. This is very short for a situation where the typical fracture spacing is in the range 2 m, see Table 4-2 for estimated ratings of fracture spacings and Table 4-2 for conversion of ratings into spacings.

Thus, for the massive rock mass at Dam D, with the short lengths of piezometer drillholes, and not ideal direction of the drillholes, the probability of intersecting water bearing fractures was basically quite small. To increase the probability of intersecting water bearing joints, the lengths of piezometer drillholes should be increased beyond 1.5 m.

The data from manual collection of values has not much information. The small values measured indicate that no sensor is intersecting rock joints. Local storage or even an onsite camera filming an analog pressure gauge could mean that data could be collected for example once every year. No measured pore pressure is expected as the dam has a drainage curtain along the upstream side along the drainage curtain.

7 CONCLUSIONS

7.1 Pore pressure and design considerations

The assumptions for "Pore Pressure" in the Norwegian regulations, distinguish between the uplift pressures for the following calculations:

- **Dam stability:** Stability of the dam structure and the contact zone between concrete and rock foundation. Design considerations for gravity dams are given in the NVE guidelines for concrete dams (NVE, 2005) in the following chapters:
    - Gravity dams - chapter 2.2.1, "Internal pore pressure and drainage"
    - Buttress dams - chapter 2.6.1, under sub-chapter "Overturning where cracks will not cause increased pore pressure with uplift".
- **Foundation stability including the rock foundation;** Design considerations are given in the regulations, NVE (2005), chapter 3.7, "Foundation".

The assumptions for pore pressure in the regulations and guidelines are considered to be a good basis for design, and the regulations are in line with general international practice.

7.1.1 Dam stability and pore pressure

There are different safety requirements for gravity dams and buttress dams. The main differences concern assumptions for pore pressure distribution and safety limits for overturning as described here:

- **Gravity dams:** The safety against overturning is calculated by finding the point of action of the resultant force. The location of the resultant gives the compressive stress distribution along the foundation, and thereby the pore pressure distribution can be identified. In general, there is assumed to be full pore pressure in parts of the foundation with no compressive stress, while the pore pressure is linearly decreasing towards the downstream toe in the areas with compressive stress in the foundation (see table below).
- **Buttress dams:** Full pore pressure is assumed under the upstream slab and no pore pressure is assumed under the buttresses. The reason being that these dams are freely drained on the downstream side of the upstream slab, and dangerous pore pressure build-up cannot occur in the structure. The location of the resultant is therefore not critical for this dam type, and calculation of pore pressure distribution is not required. Safety against overturing is therefore defined by a safety factor. It is also assumed that this is the reason that a lower safety factor against sliding can be applied for this dam type, as the pore pressure is more predictable and thus provides less uncertainty in the calculations of stability.

As described in the above text, the likelihood of pore pressure build-up is the key factor to understand the safety requirements and the corresponding pore pressure distributions.

Undesired pore pressure and uplift affecting the structural stability can only develop if there is an open crack in the dam or in the concrete–rock contact zone, meaning that no bonding is present in the crack or along the interface between concrete and rock. In general, this will occur only if the pore pressure exceeds the bonding strength plus the weight of the overlying mass (rock mass and dam

weight). This may lead to hydraulic splitting (with bonding) and/or hydraulic jacking (without bonding). Since the tensile strength of a crack or of the contact zone in the foundation rock is weaker than that of the concrete structure itself, rock anchors (into the rock) or reinforcing steel (in construction joints) will reduce the risk of hydraulic jacking.

Table 7-1. Pore pressure distribution for different dam types.

Gravity dam:	**Drained Gravity dam.**	**Buttress dam:**
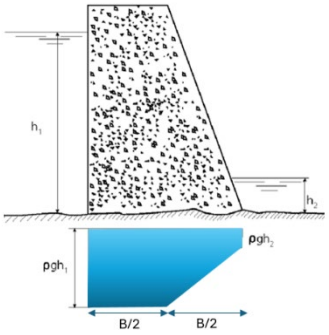	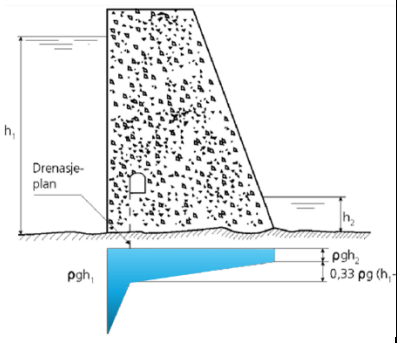	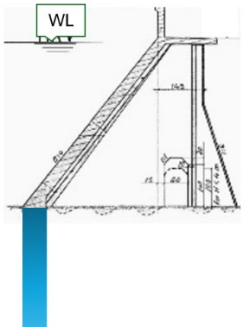
Linearly decreasing pore pressure is assumed in areas with compressive stress in the foundation, and full pore pressure in areas with no compressive stress. Example shows limit in ALS with compressive stress only in the downstream part.	Reduced pore pressure can be assumed when the dam is drained. However, full pore pressure should be considered in all parts of the cross-section where there are no calculated compressive stresses.	Stability requirements are given as a safety factor. As this method does not depend on the location of the resultant, no compressive stress under the upstream slab can occur, resulting in possible crack formation as for Gravity dams. Therefore, full pore pressure is assumed under the upstream slab.

7.1.2 Rock foundation and Pore pressure (Foundation stability)

The possibility of pore pressure build-up in the bedrock, should be assessed based on a geologic evaluation. This report has identified that the RMR system is the most suited for geological mapping of dam foundations.

The “joint water pressure” causing uplift in the foundation is the main concern when evaluating foundation stability. There is no “pore pressure” in sound Norwegian rock of good quality, however, in this report the term “pore pressure” is used as a general term and includes uplift pressure and joint water pressure.

Uplift can occur when joints are oriented parallel or sub-parallel to the surface, and the joints located close to the rock surface are those of most concern. This implies that increasing depth of the rock fracture reduce the adverse effects of uplift.

According to several studies, a drainage curtain in the foundation is the most efficient way to control the pore pressure. It is important to note that the drainage holes in a drain curtain will need to be checked and cleaned/flushed at regular intervals, as the holes can become clogged by fines and minerals from the bedrock. A well-designed grout curtain and other foundation treatments will also limit a possible pore pressure built-up.

Based on the experience from the cases in this report, measurement of pore pressure should only be used in special cases, when geological evaluation identifies significant uncertainty regarding the quality of the rock foundations. Given the potential errors associated with sensors, it is clear that structural safety should not be based on pore pressure measurements, if this can be avoided.

7.2 Engineering Geological Mapping

The bedrock at all five dam sites in this study consists of typical Scandinavian hard rock with porosity < 1 % and poor connection between pores. Therefore, potential water flow and leakage will follow discontinuities like joints and fractures and the hydraulic conductivity will be determined by the degree of fracturing and the character of rock joints. Instead of "pore pressure" the term "joint water pressure" should rather be used for rock mass.

Water flow in joints is rarely evenly distributed (as assumed in "parallel plate theory"), but rather concentrated in certain sections (flow channels). This means that monitoring of a borehole intersecting a fracture with water does not necessarily display any joint water pressure. It also means that estimating the resultant joint water pressure based on the monitored maximum value will give a gross over-estimation. On the other hand, if a piezometer borehole does not intersect a water leading sections of a fracture, no water pressure will be measured.

Based on literature reviews and experience from mapping and characterization of rock geological conditions for dam sites and other types of engineering projects, an investigation procedure for the five dam sites of this project was chosen based on the following steps:

1) Mapping of rock types and discontinuities like faults, joints and fractures, with subsequent plotting of discontinuities and analysis in stereographic projection.
2) Schmidt hammer testing for subsequent rock strength estimation.
3) Classification of rock mass quality based on the RMR-method (Rock Mass Rating).

This suggested procedure is believed to be a good option for dam foundations in general. Regarding classification of the rock mass, RMR is believed to be the best alternative for dam foundations based on the number of relevant parameters included and its special correction factor for foundations. RMR classification provides an objective characterization and may also be used as a guideline for what should be considered as "good bedrock" according to the Norwegian Dam safety Regulations ("Damsikkerhetsforskriften") Table 7-2-2 (Energidepartementet, 2009).

The stereographic projection technique is very useful for many purposes related to dam foundation considerations, such as evaluation related to stability/risk of sliding (cfr. The Malpasset case, see Figure 58) and finding optimum direction of boreholes, i.e. for grouting and piezometer-monitoring. The latter is illustrated in Figure 107, which provides a summary of the engineering geological conditions of the five damsites and shows the orientations of piezometer drillholes.

	A	B	C-1	C-2	D
Pole plot / Direction of piezometer BH	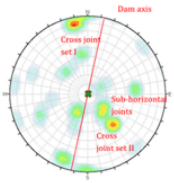	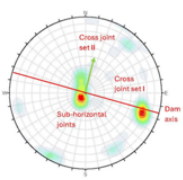	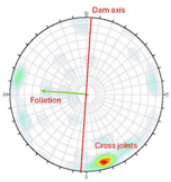	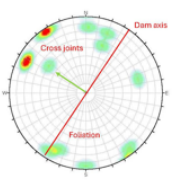	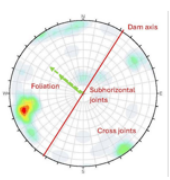
Rock type	Gneiss, granitic and migmatitic	Syenite	Amphibolite/ gabbro	Amphibolite/ gabbro	Rhyolite
R_L => ~UCS (MPa)	140-300	220-280	As for C-2 approx.	110-155	Approx.100-250
RMR	44-82	51-76	78-83	88-94	82-83
Designation	Fairly good to good/very good	Fairly good to good	Good til very good	Very good	Very good

Figure 117. Summary of engineering geological investigations. Green arrows indicate direction and inclinations of piezometer drillholes (90º/vertical for A, inclined in the direction of the arrow for the others – flatter the closer the arrowhead is to the periphery circle).

For the main joint sets illustrated in Figure 108, and directions of piezometer boreholes as reported for the five dam sites, it can be concluded that the orientations of the piezometer drillholes have been quite favourable (i.e. fairy perpendicular to a main joint set) for dam A, B and C2 and less favourable for C1 and D. This technique will be particularly valuable in connection with planning of new piezometer holes. The lengths of the monitoring sections of piezometer boreholes illustrated in Figure 108 have in most cases been only 0.5 m. This is very short when the typical fracture spacing for most of the dam sites is in the range of 0.6-2.0 m.

Thus, with short piezometer drillholes and orientations as shown in the figure above, the probability of intersecting water bearing fractures has been quite small, and it is not surprising that so many of the holes have been dry. To increase the probability of intersecting water bearing joints, the direction of boreholes should be based on data from joint mapping, and the lengths of piezometer drillholes should be increased beyond 2 m.

7.3 Instrumentation

When selecting sensors and planning their layout, the first step is to define the purpose of the measurements. This purpose may include:

- Monitoring pore pressure in weaker zones of the bedrock
- Assessing the effect of drainage holes
- Verifying that the pore pressure is within the design assumptions.

Each purpose may lead to a different sensor layout and installation order. However, there are some general guidelines to consider:

- Position sensors where peak values are expected, typically as far upstream and as close to the rock joints as possible.
- Engineering geologists should analyse joint patterns to identify potential water-conducting fractures and adjust the sensor layout accordingly. Joints that can cause uplift are generally oriented parallel or sub parallel to the foundation surface. The boreholes must intersect these fractures. Consider sensors at different depth if rock quality differs with depth.
- Ensure enough measurements to achieve the desired level of certainty. Avoid extrapolating data; instead, install more sensors and use interpolation.

7.3.1 Experience gained from this report

- The need for instrumentation with piezometers should be based on a geologic evaluation of the foundation. Random instrumentation of rock foundation is of little value.
- If piezometers are deemed necessary, their placement should be guided by geological mapping conducted by an engineering geologist to ensure the sensors are positioned in cracks that may cause unwanted uplift.
- All the dams evaluated in this report, are placed on good quality rock foundation. The permeability of intact rock is therefore very low. In practice, water flow and pressure build-up can only take place in fractures. If a borehole for piezometer installation is not intersecting any water leading fractures, no water pressure will be measured. Measurement of pore pressure does not increase the dam safety but can be used to verify that the dam's actual behaviour corresponds to the assumptions made during design. Given the potential for errors associated with sensors, it is clear that structural safety should not rely solely on instrumentation.

7.3.2 Sampling and data storage

Most guidelines for the instrumentation and monitoring of dams emphasize that instruments and the collection of measurement data alone do not improve dam safety. The Federal Energy Regulatory Commission (FERC, 1995), which regulates a large number of dams in the USA, points out in its guidelines for instrumentation and monitoring that instruments must be carefully selected, positioned, and installed. Data must be collected thoughtfully, carefully processed, analysed, and visualized, and this must be done within a reasonable timeframe to ensure dam safety.

A poorly planned or poorly executed monitoring program will generate large amounts of unnecessary data, causing the dam owner to waste time and money collecting and interpreting it. This can lead to confusion about the dam's actual behaviour and may result in the monitoring program being partially or entirely abandoned

Sampled data should always be stored at a time-synchronized consistent sampling rate across all sensors, and precautions should be taken to get gap-free timeseries. Time-synchronized sampling will reduce errors from non-stationary effects such as temperature fluctuations, changes in air pressure, and variations in water level. Gap-free timeseries with constant timesteps make postprocessing easier and opens up for more advanced methods of analysis, such as Fourier transforms and complex machine learning algorithms.

7.3.3 Experience from the cases in this report

Based on the measurements of the 87 piezometers, the main findings are:

- Drainage directly downstream the buttress slab eliminates pore pressure under the buttresses. For very wide buttresses, a gallery (or box drain) between the upstream slab and the buttress supports will give sufficient drainage.
    - No pore pressure was detected by the 71 piezometers installed in the dams with slender buttress supports or very wide buttress supports with an upstream gallery/box drain (dam B, C1, C2 and D).
    - "Very wide" buttress supports refer to cases C1, C2 and D that have about 6 m wide buttress supports with upstream drainage gallery/box drain.
- Most sensor values are correlated with hydrostatic pressure rather than the reservoir water level, indicating that they measure backwater or water depth in the drainage system or joints.
- Three of the analysed dams include measurements with negative values that should have been filtered out.
- Proper instrumentation of joint water pressure between the rock and concrete is achievable. However, it requires detailed geological mapping and a significant number of sensors to monitor pressure changes at and between the joints.

The decision to install piezometers in rock foundations should be based on an evaluation of the rock mass in the foundation and should only be installed if this evaluation conclude that pore pressure can be a potential issue regarding stability. If piezometers are deemed necessary, their placement should be guided by geological mapping conducted by an engineering geologist to ensure the sensors are positioned in cracks that may cause unwanted uplift.

Given the potential for errors associated with sensors, it is clear that structural safety should not rely solely on instrumentation. However, instrumentation can be highly valuable for assessing the long-term structural behaviour.

7.4 The Norwegian regulations

In general, monitoring of Norwegian dams has not been very extensive, and is often limited to monitoring for safe operation, i.e. water level monitoring. In general terms, monitoring for this can be partly explained by the fact that Norwegian dams, generally have been built with good safety margin, so that surveillance and monitoring has not been necessary. In addition, there is mainly good quality rock even at the ground surface in Norway, since glaciations have removed most weathered rock and loose material. The ground conditions are therefore often not comparable to the geology in other parts of the world.

According to the Norwegian Dam Safety Regulations (Energidepartementet, 2009), § 7-2, the following requirement applies for instrumentation of dams:

Table 7-2. Summary of table 7-2.2 from in the Norwegian dam safety regulations (Energidepartementet, 2009), sorted according to foundation properties.

Dam type	**Foundation**	*Dam class*	*Water level*	*Leakage*	*Deformations*	*Pore pressure*
Embankment dam	All types	2, 3, 4	x	x	x	
Concrete- or masonry dam	All types	3, 4	x	x	x	
		2	x	x		
All dam types	**Soil, clay, moraine or weak rock**	**2, 3, 4**	**-**	**-**	**-**	**x**

As shown in the above table, Pore pressure measurements are limited to dams with foundation on loose soil or poor-quality rock.

The assumptions for pore pressure in the Norwegian regulations and guidelines are considered to be a good basis for design, and the regulations are in line with general international practice. However, there is a need for better specifications of the design pore pressure for buttress dams.

We recommend that the terms defined in the regulations are to be used, i.e. light buttress dam and heavy buttress dam. Using terms not defined in the regulations will cause confusion, for example "strengthened buttress dams".

8 REFERENCES

Bandis, S. C.; Lumsden, A. C.; Barton, N., 1981. *Experimental studies of scale effects on the shear behavior of rock joints,* s.l.: Int. J. Rock Mech. Min. Sci. & Geomech. Abstr 18, 1–21..

Barton, 1988. *Predicting the behavior of underground openings in rock,* s.l.: s.n.

Barton, N., 1988. *Predicting the behavior of underground openings in rock,* s.l.: Norwegian Geotechnical Institute, Technical Report 172.

Barton, N. & Bandis, S., 1990. *Review of predictive capabilities of JRC-JCS model in engineering practice.* s.l.:In N. Barton and O. Stephansson (Eds.), Rock Joints, pp. 603–610. Balkema..

Bieniawski, Z.,R., 1989. *Engineering rock mass classifications,* s.l.: New York, Wiley..

Bieniawski, Z., 1984. *Rock mechanics design in mining and tunneling,* s.l.: Rotterdam: Balkema..

Carlsson, A. & Olsson, T., 1977. *Variations of hydraulic conductivity in some Swedish rock types,* s.l.: Proc. Int. Symp. Rockstore -77. 257-263..

Deere, D. & Miller, R., 1966. *Engineering classifications and index properties of intact rock,* s.l.: Technical report no. AFWL-TR 65-116, University of Illinois..

Dr.techn.Olav Olsen, 2024. *Dam A, Stabilitet basert på poretrykksmålinger,* s.l.: s.n.

Duffault, P., 2012. *What modern rock mechanics owe to the Malpasset arch dam failure. In: Harmonising Rock Engineering and the Environment,* s.l.: p.1889-1892– Qian & Zhou (eds), Taylor & Francis Group, London, ISBN 978-0-415-80444-8..

Duffaut, P., 2012. *What modern rock mechanics owe to the Malpasset arch dam failure,* s.l.: Taylor & Francis Group.

E. Fjær, R. H. P. H. A. R. R. R., 2008. Mechanics of hydraulic fracturing, Chapter 11. In: *Developments in Petroleum Science, ISBN 9780444502605,.* s.l.:Elsevier/ScienceDirect, pp. Pages 369-390,.

Energi Företagen, RIDAS, 2020 Oktober. *Tillämpningsvaågledning, Kapitel 9, Betongdammar.* Stockholm: s.n.

Energidepartementet, 2009. *Forskrift om sikkerhet ved vassdragsanlegg (Damsikkerhetsforskriften),* Oslo: Energidepartementet.

EPRI, 1992. *Uplift Pressures, ShearStrengths and Tensile Strengths for Stability Analysis of Concrete Gravity Dams, Vol. 1,* Denver, Colorado: Electic Power Reserch Institute.

FERC, 2016. *Engineering Guidelines for the evaluation of Hydropower Projects, Chapter 3 Gravity dams,* USA: Federal Energy Reulatory Commission, USA.

Freeze, R. A. & Cherry, J. A., 1979. *Groundwater,* s.l.: Englewood Cliffs, NJ: Prentice-Hall, Inc..

Goodman, R. E., 1993. *Engineering geology – Rock in in engineering construction,* s.l.: John Wiley &

Sons, 412 pp..

Grøneng, G. & Nilsen, B., 2009. *rocedure for determining input parameters for Barton-Bandis joint shear strength formulation,* s.l.: Rep. No. 28, NTNU, IGB, 22 pp. .

Hanssen, T. ,. H., 1988. *Rock properties,* s.l.: NJFF/NFF Publ. No. 5, p. 41-44..

Hoek, E., 2006. *Practical rock engineering,* s.l.: Book based on lecture notes Univ. of Toronto.

Hoek, E. & Bray, J., 1981. *Rock Slope Engineering,* s.l.: SPON Press Taylor and Francis Group.

Hoek, E. & Brown, E., 2019. *The Hoek-Brown failure criterion and GSI – 2018 edition,* s.l.: Journ. Rock Mech. and Getech.Eng., 11 (2019) 445-463..

Hoek, E. & Brown, E. T., 2019. *The Hoek-Brown failure criterion and GSI,* s.l.: Journ. Rock Mech. and Getech.Eng., 11 (2019) 445-463. .

IABSE, 1983. *The Itapu Dam, Design and Construction features,* s.l.: s.n.

ICOLD, 1994. *Technical Diconary for dams.* s.l.:ICOLD.

ICOLD, 2004. *Working Group on Uplift Pressures under Concrete Dams,* s.l.: ICOLD European Working group.

ISRM, 1979. *Suggested methods for determining the uniaxial compressive strength and deformability of rock material,* s.l.: s.n.

ISRM, 2009. *ISRM Suggested Method for Determination of the Schmidt Hammer Rebound Hardness,* s.l.: Testing and Monitoring: 2007-2014», Springer, 25-33..

ISRM, 2015. *ISRM Suggested Method for Determination of the Schmidt Hammer Rebpund Hardness; Revised Version,* s.l.: The ISRM Suggested Methods for Rock Characterization, Testing and Monitoring: 2007-2014», Springer, 25-33..

Kartverket, 2024. [Online]
Available at: https://www.norgeskart.no/

Kebab, H., Boumezbeur, A. & Rivard, P., 2020. *Rock mass properties and their suitability as a foundation for a rolled compacted concrete gravity dam: case study of Beni Haroun dam (Mila, NE Algeria),* s.l.: Bulletin of Engineering Geology and the Environment.

Konow, K. & Engseth, M., 2017. *Evaluering av eksisterende betong- og murdammer Rapport 1 – Anbefalinger,* s.l.: Rapport 12372 utarbeidet av Dr.techn. Olav Olsen for Energi Norge.

M. Abdi (KTH), D. N. (., 2022. *Numerical simulations of pore pressure on concrete buttress dams,* Stockholm: KTH.

NGI, 1994. *Retningslinjer for instrumentering av norske dammer. etterinstrumentering og tilstandsovervåking av eksistreende dammer,* Oslo: NGI.

NGI, 2015. *Using the Q-system- Rock mass classification and support design. Handbook, 54 pp..* s.l.:s.n.

NGU, 1975. *Geologisk kart over Norge, berggrunnskart Sauda 1:250.000,* s.l.: Norges geologiske undersøkels.

NGU, 2024. [Online]
Available at: https://www.ngu.no/geologiske-kart

Nilsen, B., 2016. *Rock slope stability analysis according to Eurocode 7, discussion of some dilemmas with particular focus on limit equilibrium analysis,* s.l.: Springer-Verlag.

Nilsen, B., 2019. *Dam A – stabilitet avfjellskråninger på nedstrøms side,* s.l.: s.n.

Nilsen, B. & Palmstrøm, 2000. *Engineering geology and rock engineering,* s.l.: NBG/NFF Handbook No. 2, 249 p..

Norconsult, 2018. *Dam D – Teknisk plan. 26 p. + appendix A and B,* s.l.: s.n.

Norconsult, 2019. *Dam B, rehabilitering av platedam, poretrykksmålere. Teg.B-312 og B313, 2023-01-30.,* s.l.: s.n.

Norconsult, 2019. *Dam D – Ingeniørgeologisk befaringsnotat,* s.l.: s.n.

Norconsult, 2020. *Dam B – Ingeniørgeololgisk befaring,* s.l.: s.n.

Norconsult, 2021. *Dam C1 og C2 - Forsterkning av platedammer, sluttrapport. Vedlegg I – Instrumentering og poretrykksmålere,* s.l.: s.n.

NVE/NGI, 2024. *Poretrykksmålinger på dammer, Ekstern rapport nr. 15/2024,* Oslo: NVE.

NVE, 2005. *Retningslinje for betongdammer, utgave 2, oktober 2005.* Oslo: NVE, Seksjon for damsikkerhet.

NVE, 2011. *Retningslinjer for murdammer, utgave 3, Desember 2011.* Oslo: NVEs seksjon for damsikkerhet.

P. Novak, A. M. C. N. a. R. N., 2007. *Hydraulic Stuctures, 4th Edition.* Oxon, UK: Taylor & Francis.

P. Obernhuber, F. P., 2009. *Arch Dam Analysis Using the Zillerground Dam as an Example,* Brasilia: ICOLD.

Quinones-Roso, C., 2010. *Lugeoen testing interpretation, revisited,* s.l.: Proc. USS Dams, Collaborotive management of integrated watersheds, p. 405-414..

R. S. Olsen, I. J. S., 2016. *Relearing how to look at piezometric data for seepage evaluation,* Denver: USSD.

R.B., P., September 2001. *Embankment Dams - Instrumentetion versus Moniroring,* s.l.: s.n.

Romana, M., 2003. *DMR (Dam Mass Rating). An adaptation of RMR geomechanics classification for use*

in dams foundations., s.l.: 10th ISRM Congress, p 977-980, 2003, 10th ISRM Congres..

Romana, M., 2011. *Use of DMR (Dam Mass Ratio), a new geomechanics classification, derived from RMR, in safety appraisals of old dams' foundations,* s.l.: Dam Maintenance and Rehabilitation II - Proceedings of the 2nd International Congress on Dam Maintenance and Rehabilitation, p 1127-1137.

Shafiel, A., Heidari, M. & Dusseault, M., 2007. *Rock mass characterization at the proposed Khorram-Roud dam site in Western Iran,* s.l.: Proceedings of the 1st Canada-US Rock Mechanics Symposium - Rock Mechanics Meeting Society's Challenges and Demands, Volume 2, Pages 1065-1073, 2007..

SNL, 2023. *Store norske leksikon; Demning.* s.l.:https://snl.no.

USACE/ERDC, 2002. *Assessment of Geology as it Pertains to Modeling Uplift in Jointed Rock: A Basis for Inclusion of Uncertainty in Flow Models,* s.l.: US Army Corps of Engineers, WilliamL. Murpy, Robert M. Edeling, John M. Andersen.

USACE, 1995. *Gravity Dam Design, Engineering manual,* Washington DC, USA: US Army Corps of Engineers, USACE.